博士論文

Selective Construction of C_3-Symmetric π-Conjugated Frameworks

（C_3 対称パイ共役系の選択的構築法の開発）

東京大学大学院理学系研究科

化学専攻

小島　達央

Selective Construction of C_3-Symmetric π-Conjugated Frameworks

Tatsuo Kojima

Abstract: The selective construction of the two kinds of extended π-conjugated frameworks, alternately substituted hexaphenylbenzene (HPB) frameworks and triphosphatruxene (TPT) frameworks, was described. The key selective steps were achieved in the late stage of the synthetic schemes in both the cases.

The selective alternate trilithiation of the HPB framework was achieved through a thermodynamically controlled halogen dance on the basis of the reversibility of the ArBr/ArLi exchange reaction. The detailed mechanism was experimentally elucidated. This reaction was found to be quite practical because of the scalability and the synthetic versatility of bromoarenes and organolithiums. The applicable scope of the substrate was expanded by the improved protocol with additional bromoarenes as lithiation mediators. These protocols can also afford the lower-symmetric HPB derivatives, which have been unavailable by any conventional methods. Quantitative analysis of the distribution of the lithiated species in the equilibrium mixture experimentally revealed the preferred arrangement of Li on the HPB framework. This preference was interpreted with the strong interaction between the phenyl groups on the HPB framework, highlighting the importance of the characteristic conformation of the HPB framework. The success of the selective alternate functionalization should be due to the combination of the lithiation reaction and the conformation of the HPB framework.

The sextuple aromatic nucleophilic substitution reaction achieved the efficient construction of the TPT framework, which is the first example of the π-conjugated framework containing more than two phosphorus centers. While this reaction proceeded in high *anti*-selectivity, vacuum sublimation completely converted the *anti*-isomer into the *syn*-isomer. This preference of the *syn*-iosmer was interesting because the *anti*-isomer was statistically favored and preferred in the solution phase. On the basis of these two complementary stereoselectivity, the selective preparation of the two stereoisomers of the TPT framework was realized.

Contents

Abbreviations and Symbols

Anal.	elemental analysis
Aq.	aqueous
Ar	aryl
ASAP	atmospheric pressure solid analysis probe
Br	broad
Bu	butyl
Calcd.	calculated
d	doublet
Dec.	decomposition
DFT	density functional theory
DMSO	dimethyl sulfoxide
eq	equivalent
h	hour(s)
HR	high-resolution
i-	iso-
J	coupling constant in Hz
Lit.	literature
m	multiplet
Me	methyl
min	minute(s)
mp	melting point
MS	mass spectrometry
m/z	mass-to-charge ratio
n	normal-

NMR	nuclear magnetic resonance
ORTEP	Oak Ridge thermal ellipsoid plot
Ph	phenyl
Pr	propyl
q	quartet
rt	room temperature
s	singlet
t	triplet
t	tertiary-
THF	tetrahydrofuran
TMS	trimethylsilyl

Chapter 1

General Introduction

1.1 Selective synthesis of large π-conjugated molecules

Sophisticated π-conjugated molecules are demanded more than ever by the recent expansion of the attractive fields where functionalized organic materials should play an important role. In such a scientific situation, one of the most important contributions that synthetic organic chemistry can make is bottom-up supply of pure π-conjugated compounds that are unavailable by other methods. To maximize the utility of π-conjugated molecules, the proper substituents should be introduced at the appropriate positions with the desired stereochemistry on the suitable π-conjugated framework on the basis of the elaborated molecular design. This difficult task has been accomplished splendidly by the progress of modern organic chemistry.

The author recognizes the development of new bond-forming reactions and the control of selectivity in chemical reactions as the two most important issues in the progress of modern organic chemistry. While the former is, needless to say, indispensable for the extension of molecular structures, the latter is also very important for the selective preparation of desired π-conjugated molecules. For example, substituted benzenes possess several potentially reactive but chemically different sites on their frameworks (Figure 1-1a). With the established insight of selectivity, we can now distinguish these sites in a rational way and functionalize the desired sites deliberately. Aromatic electrophilic substitution reactions proceed selectively at the predicted sites depending on the electronic perturbation of the substitutents (Figure 1-1b). Some reactions such as direct metalation proceed selectively at the *ortho*-positions of the substituent with a directing ability (Figure 1-1c). Very recently, selective *meta*-functionalization was even achieved with the elaborated directing groups.[1] A few reactions just depend on the steric hindrance around the reactive sites and proceed at the least hindered sites selectively (Figure 1-1d).[2] Now the appropriate consideration of the electronic, directing, and steric effects on potentially reactive sites can realize almost any selective functionalization of small π-conjugated frameworks.

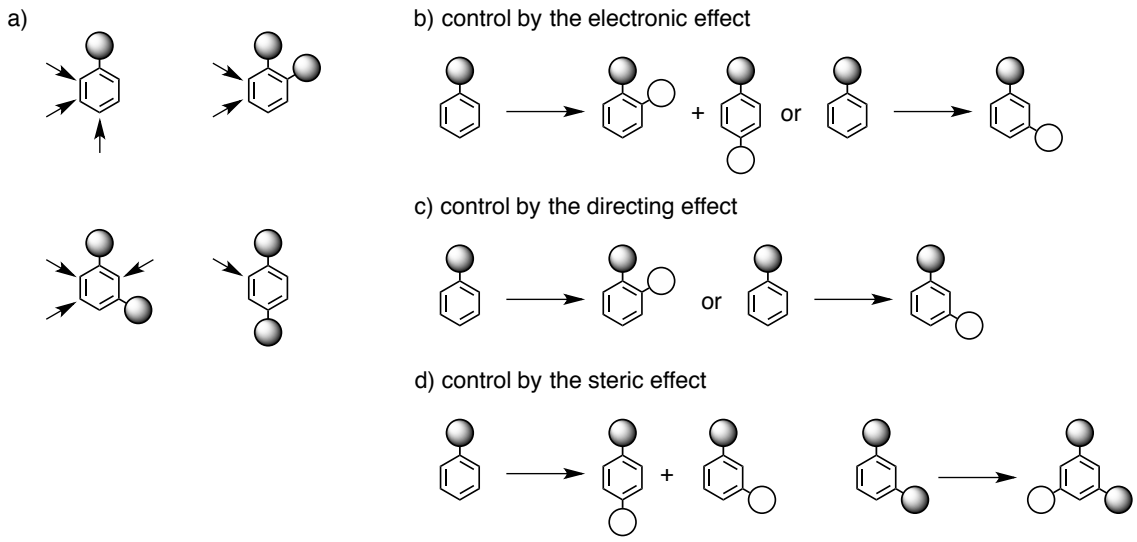

Figure 1.1 Selective functionalization of substituted benzenes: (a) chemically different sites of the substituted benzenes; (b) control by the electronic effect; (c) control by the directing effect; (b) control by the steric effect.

In contrast with small π-conjugated frameworks, selective functionalization intrinsically becomes difficult for extended π-conjugated frameworks (Figure 1-2). This is due to the small chemical difference of the potentially reactive sites owing to the weak electronic or steric perturbation from the other parts of the π-conjugated framework. If the potentially reactive sites behave independently, a reaction should afford the statistical mixture of the possible products. Therefore, selective functionalization of extended π-conjugated frameworks is generally recognized as difficult or even impossible, unless the target molecule is statistically much favored. Considering this synthetic difficulty, organic chemists have avoided the selective functionalization of extended π-conjugated frameworks and resolved the problem of the selectivity at the initial stage of synthetic schemes where the molecule is still small and able to be functionalized deliberately in an easy way. The selective functionalization of the small precursors is followed by the construction of the extended π-conjugated framework to achieve the synthesis of the target large π-conjugated molecule.

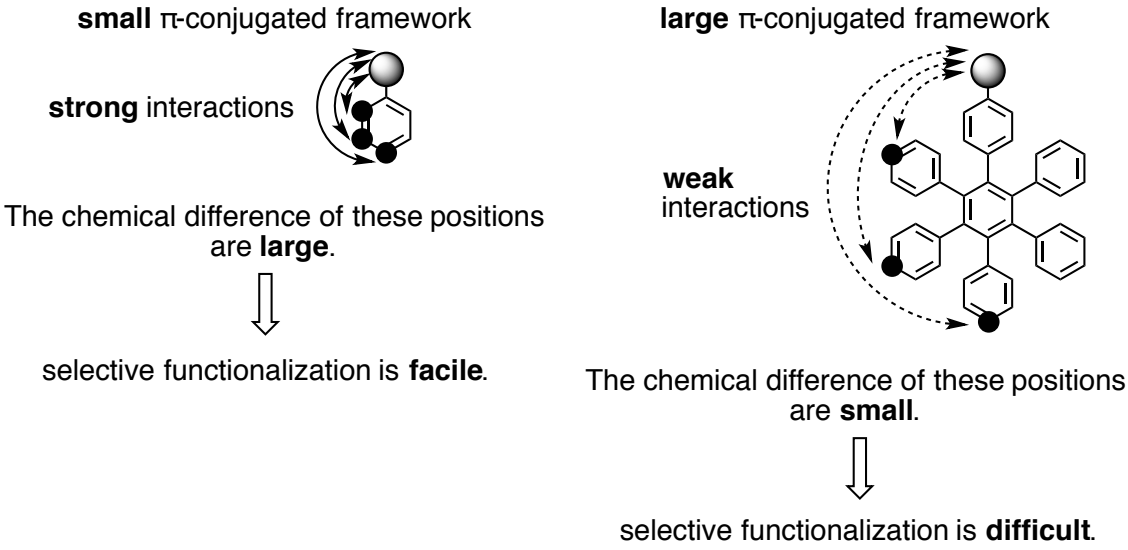

Figure 1.2 Schematic comparison of the selective functionalization of the substituted benzene and the extended π-conjugated framework.

From the viewpoint of the position of the key selective functionalization step in the synthetic schemes, synthetic schemes for extended π-conjugated molecules are classified into late-stage functionalization and prefuctionalization (Figure 1.3). In modern synthetic organic chemistry, the prefunctionalization approach can overcome most of the problems of the selectivity and has been effective for the preparation of extended π-conjugated molecules. The prefunctionalization approach seems much superior to the late-stage functionalization at this point. Comparison of these two synthetic approaches will be further discussed in the following Sections.

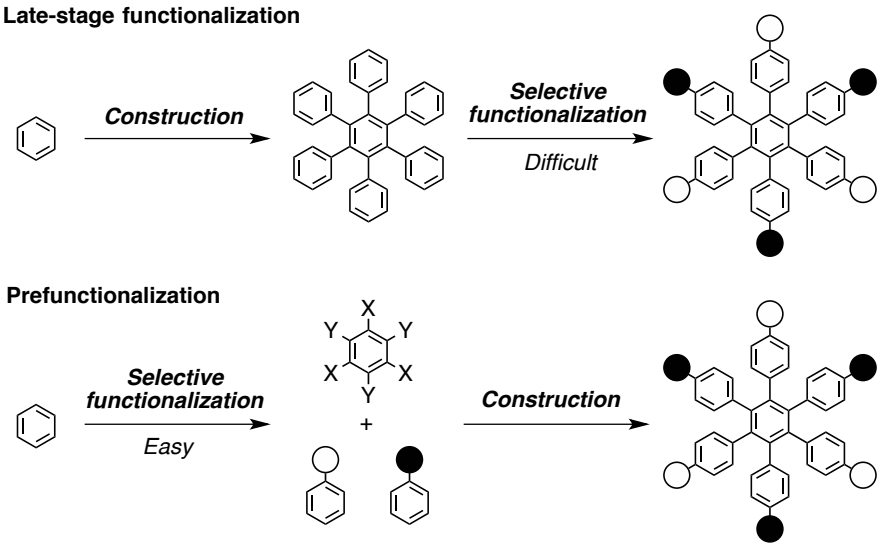

Figure 1.3 Comparison of the two synthetic approaches for the functionalization of extended π-conjugated frameworks.

1.2 Late-stage functionalization approach for large molecules

Despite its difficulty, the late-stage functionalization approach for the synthesis of large molecules is now actively pursued in the field of total synthesis of natural products because of its tremendous advantages. As one of the most influential works, Baran et al. recently reported the efficient two-phase synthesis of the five oxidized members of the eudesmane family of terpenes inspired by terpene biosynthesis (Scheme 1.1).[3] In their synthetic scheme, the carbon framework is constructed in the initial stage of the scheme (*cyclase phase*), and then the common carbon framework is efficiently functionalized with the stepwise site-selective C-H oxidation reactions to afford the five different derivatives (*oxidase phase*). This synthetic scheme is exactly a late-stage functionalization approach. The common synthetic intermediate where the target framework has already been constructed can lead to the molecular diversity efficiently. The functionalization at the late stage can also avoid the inessential synthetic steps such as protection and deprotection of the functional groups and makes the synthetic scheme very straightforward. These are all the unique advantages of the late-stage functionalization approach. Of course, the site-selective C-H oxidation at

the late stage of the synthetic scheme is essential and it should be the most difficult part of the scheme. However, this synthesis clearly demonstrates that the solution of the challenging problem of the selectivity at the late stage of synthetic schemes can lead to the successful achievement, which is inaccessible by other synthetic approaches.

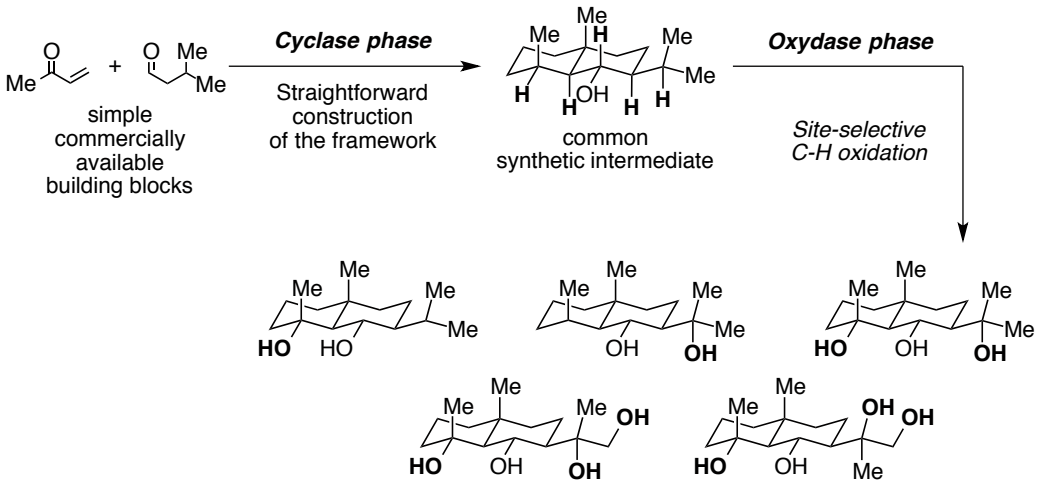

Scheme 1.1 Efficient two-phase synthesis of the five oxidized members of the eudesmane family of terpenes.

The above-described advantages of the late-stage functionalization approach hold true in the synthesis of large π-conjugated molecules. The molecular diversity is very important especially for the development of new organic materials. The smaller number of the inessential synthetic steps is obviously better. Furthermore, many unfunctionalized π-conjugated frameworks are readily available. They are preparable from inexpensive precursors in a few synthetic steps or even commercially available. They are the good starting material, which can cut short the synthetic scheme. However, the reported examples of the late-stage functionalization of extended π-conjugated frameworks are very limited. This should be due to the lack of the effective methodology to control the selectivity on large π-conjugated frameworks.

A few recent examples of the late-stage functionalization of extended π-conjugated frameworks are shown here. Tovar et al. reported the selective bromination of the two of the four almost chemically equivalent thiophene units in 1,2,4,5-tetrathienylbenzene derivative **1** with the proper choice of bromination

conditions (Scheme 1.2).[4] The detailed experimental study with the model compounds revealed that the observed difference of the reactivity is derived from the difference of the dihedral angles between the central benzene unit and the peripheral thiophene units owing to the existence of the *ortho*-Me groups.[5] It is worth noting that the thiophene units with the Me substituents are not protected so that they can be directly subjected to the following derivatization.

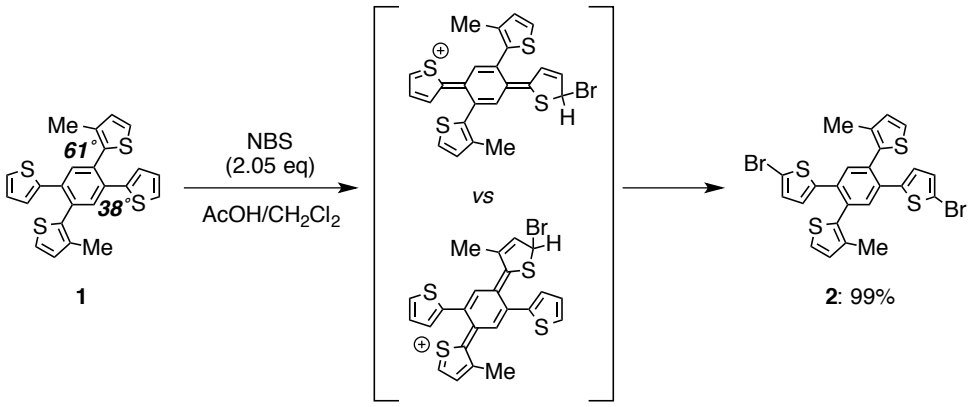

Scheme 1.2 Site-selective dibromination of derivative **1**. The calculated dihedral angles are listed in italics.

Huc et al. accidentally discovered the highly site-selective bromination of the helical quinoline oligoamides (Scheme 1.3).[6] The later theoretical study confirmed the importance of the helical conformation and they proposed that the through-space interaction between the quinoline units in the helical structure might control this unapparent site-selectivity.[7] Although these examples are just a discovery of the unapparent selectivity on the specific π-conjugated frameworks, they highlighted the possibility of the selective late-stage functionalization of extended π-conjugated frameworks and suggested the importance of the intrinsic conformation of π-conjugated frameworks for selective transformation.

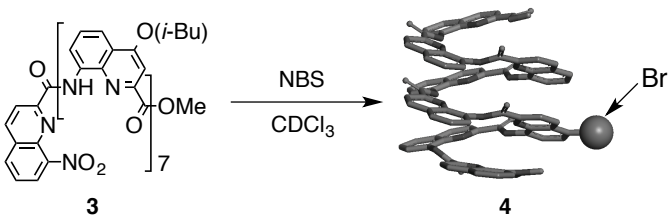

Scheme 1.3 Site-selective monobromination of quinoline oligoamide **3**. The hydrogen atoms and the *i*-Bu groups on the model of compound **4** are omitted for clarity.

1.3 C_3-symmetric hexaphenylbenzene and hexabenzocoronene

Hexaphenylbenzene (HPB) is a versatile precursor of hexabenzocoronene (HBC) and its extended analogues, *i.e.* partial fragments of graphene, which play an important role in a wide range of emerging fields (Figure 1-4).[8] The very strong aggregation ability of HBC has been often employed to construct well-defined nanostructures.[9,10] The partially oxidized HPB derivative **5** was recently adopted for the bottom-up fabrication of the chevron-type graphene nanoribbons on the gold surface (Scheme 1-4).[11] This success clearly highlights the potential of the HPB framework in the future nanotechnology. HPB itself has also been exploited as a rigid molecular scaffold in liquid crystal,[12] organic electronic materials,[13] chromophores,[14] ligands,[15] amphiphiles,[16] and molecular receptors.[17]

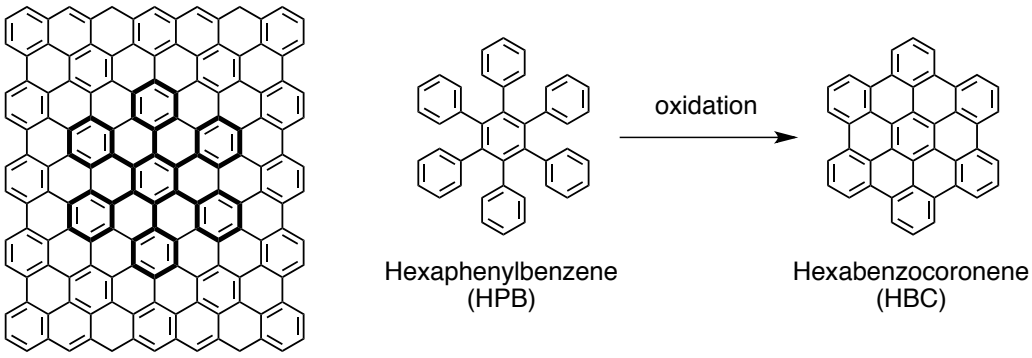

Figure 1.4 Structures of hexaphenylbenzene and hexabenzocoronene.

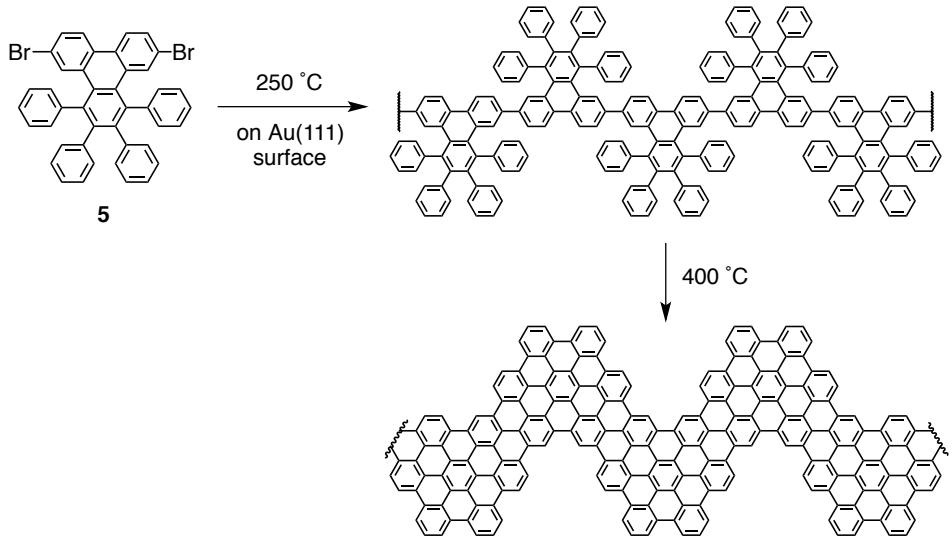

Scheme 1.4 Bottom-up fabrication of the shape-controlled graphene nanoribbon with HPB-based building block **5**.

To regulate the electronic and physical properties of HPB and HBC derivatives, the introduction of the proper substituents in the appropriate positions and arrangement is vitally required. Especially, HPB and HBC derivatives with C_3-symmetry, which possess two kinds of substituents arranged in an alternate pattern on the periphery, are established as an invaluable class (Figure 1-5).[11c, 15a, 16a, 16b,18] For example, HPB derivative **6** was reported to work both as a rare trivalent ligand which can form an octahedral M_6L_8-type molecular capsule with ten different transition metal ions and as a novel amphiphile which selectively constructs a cubic hexamer or a tetrahedral tetramer in aqueous methanol. HPB derivative **7** was applied to a redox chromophore utilizing the through-space charge transfer interactions between the substituents. HBC derivative **8** with alternateing hydrophobic and hydrophilic chains worked as a discotic nanographene material. In every case, the C_3-symmetric substitution pattern of HPB or HBC framework was crucial for the application.

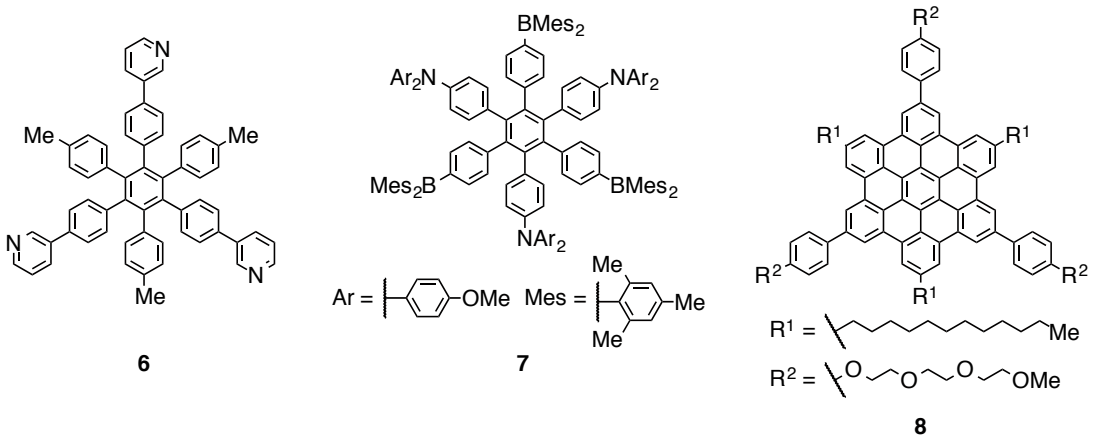

Figure 1-5 Examples of C_3-symmetric HPB and HBC derivatives.

Despite their importance, almost all C_3-symmetric HPB derivatives have been prepared so far by the inefficient synthetic protocol based on transition-metal-catalyzed trimerization of unsymmetrical diarylalkynes with two different substituents (Scheme 1-5).[19] As has been observed experimentally, this protocol inevitably affords a greater amount of the undesired "1,2,4-type" isomer than the desired "1,3,5-type" isomer in principle because the former one is statistically preferred. Furthermore, the isolation of the desired isomer is quite difficult because these isomers have similar chemical properties. This difficulty

has severely restricted the applicable functional groups. Another approach to prepare HPB derivatives is the reaction sequence of double dehydrative condensation and Diels-Alder reaction (Scheme 1-6).[19] This approach does not only require the three kinds of unsymmetrical precursors but also faces the problem of regioselectivity in both the synthetic steps. Owing to its inefficiency, this approach has never been adopted for the preparation of the alternately substituted C_3-symmetric HPB derivatives. Both of these two representative synthetic schemes correspond to the prefunctionalization approach because the precursors are functionalized before the construction of the HPB framework. Another intuitive synthetic scheme, which also corresponds to the prefunctionalization approach, is the sequential triple cross coupling reaction to the alternately functionalized benzene unit (Scheme 1-7). Although it could afford the target C_3-symmetric HPB derivative selectively in principle, this scheme has never been reported in the synthesis of HPB derivatives probably because of the difficulty of the cross coupling reactions under the sterically crowded environment.

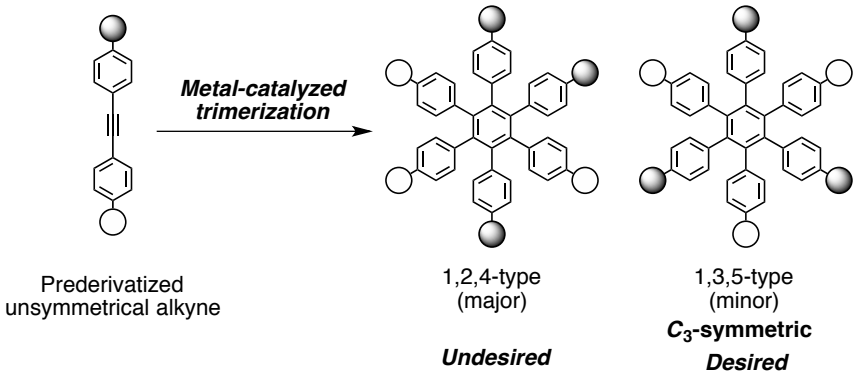

Scheme 1-5 Preparation of C_3-symmetric HPB derivatives based on trimerization of unsymmetrical diarylalkynes.

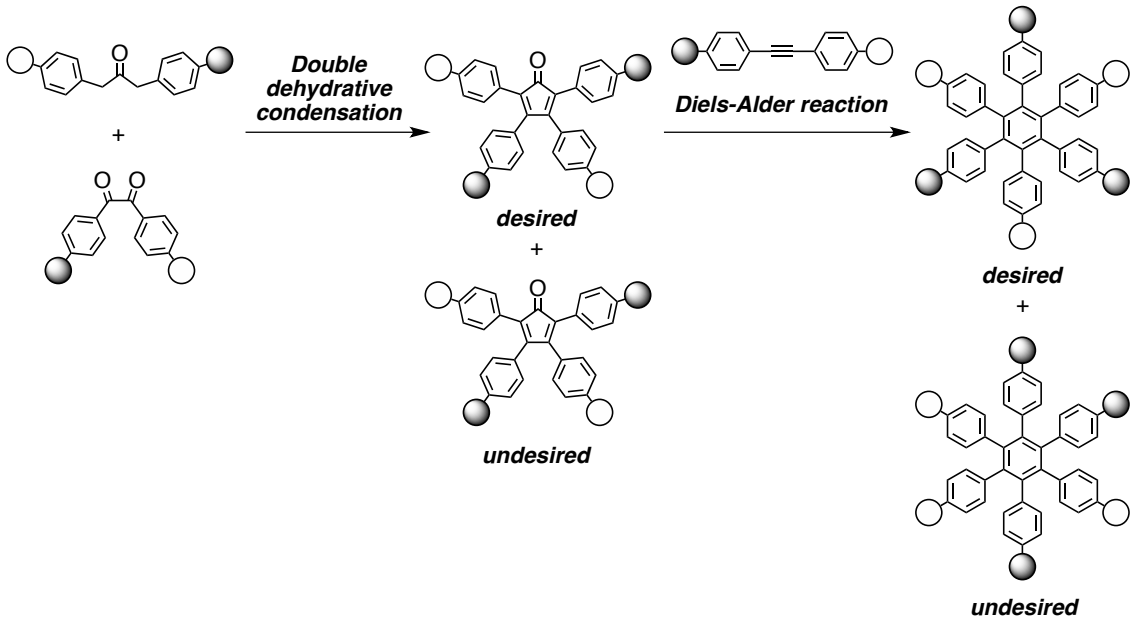

Scheme 1-6 Preparation of C_3-symmetric HPB derivatives based on the reaction sequence of double dehydrative condensation and Diels-Alder reaction.

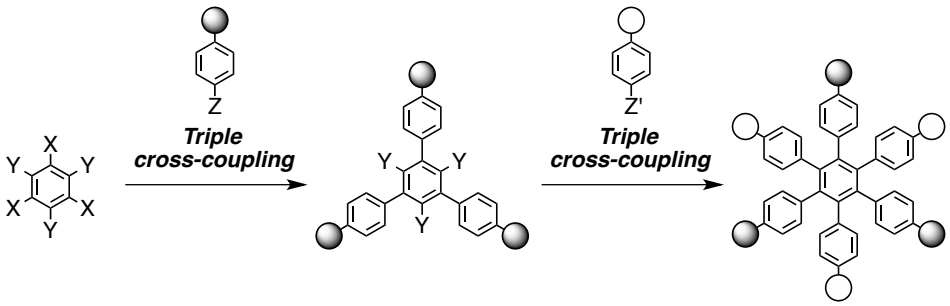

Scheme 1-7 Possible synthetic scheme for C_3-symmetric HPB derivatives based on the sequential triple cross coupling reactions.

Although it cannot afford C_3-symmetric HPB derivatives themselves, an alternative synthetic approach for C_3-symmetric HBC derivatives has been developed to compensate the lack of the efficient synthetic protocol for C_3-symmetric HPB derivatives. [20] This approach employs the 1,3,5-tris(2-biphenylyl)benzene system as the precursor of HBC instead of the HPB system (Scheme 1-8). It can selectively afford the desired C_3-symmetric HBC derivative but is not so efficient from the synthetic

viewpoint because it usually requires the several metal-catalyzed cross coupling reactions with the highly functionalized precursors.

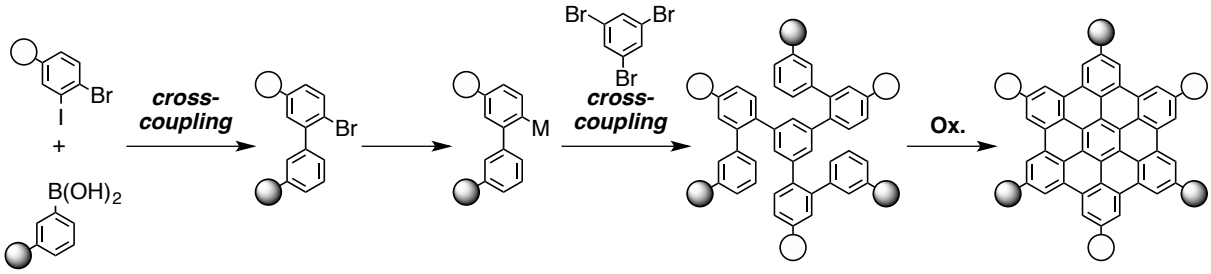

Scheme 1-8. Preparation of C_3-symmetric HBC derivatives from 1,3,5-tris(2-biphenylyl)benzene.

1.4 Preparation of phosphole-based extended π-conjugated molecules

Along with the kinds of substituents and their positions, the nature of a π-conjugated framework itself is even more crucial to define the property of π-conjugated molecules. Simple but the most powerful strategy to tune the nature of a π-conjugated framework is the replacement of some of the elements in the framework with another element. In this context, phosphorus, silicon, and boron have been investigated as new attractive components in the part of π-conjugated frameworks, in addition to the classical components such as carbon, nitrogen, oxygen, and sulfur.[21]

Among the new components of π-conjugated frameworks, phosphorus is thought to be unique because of its effective orbital interaction with π-systems, the facile derivatization of the phosphorus center, and its strong tendency of pyramidalization. Phosphorus has been utilized in various organic π-conjugated materials in the last decade.[22] Phosphorus atoms are most frequently incorporated in π-conjugated frameworks in the form of phosphole, the phosphorus analogue of cyclopentadiene. For example, phosphole-based π-conjugated molecules **9** and **10** were reported as attractive organic materials for organic light-emitting device (Figure 1-6).[23,24] Compound **11** was reported as an effective cathode buffer material in organic photovoltaics.[25]

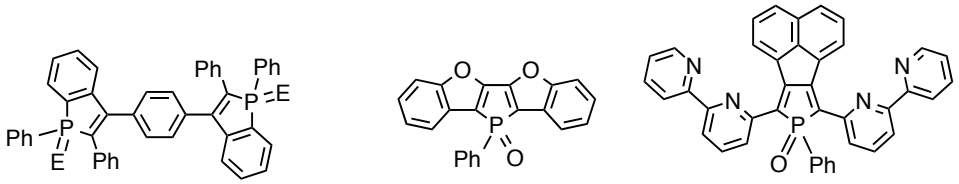

9 (E = O or S)
(mixture of diastereomers)

10

11

Figure 1.6 Phosphole-based π-conjugated molecules.

The success of phosphole-based organic materials has stimulated the molecular design to the extended π-conjugated frameworks bearing multiple phosphorus centers. Although the complex frameworks are not available with the conventional synthetic protocols, they have been successfully constructed by the progress of the new synthetic reactions. For example, phosphoryl-bridged stilbene derivative **14** was prepared using a new intramolecular cascade cyclization (Scheme 1-9).[26] The similar cyclization reaction with PBr_3 afforded a benzodiphosphole framework in moderate yield, where the bromine moieties were subjected to the following cross-coupling reactions. (Scheme 1-10).[27] The same benzodiphosphole framework was also constructed using a base-mediated cyclization reaction even in lower yield (Scheme 1-11).[28] The strained bis(phosphoryl)-bridged biphenyl framework was recently prepared utilizing a quadruple radical phosphanylation reaction (Scheme 1-12).[29] The same reaction was also applied to the construction of the ladder-type framework later (Scheme 1-13).[30] Interestingly, the selective precipitation of the *trans*-isomers before oxidation was observed in these examples.

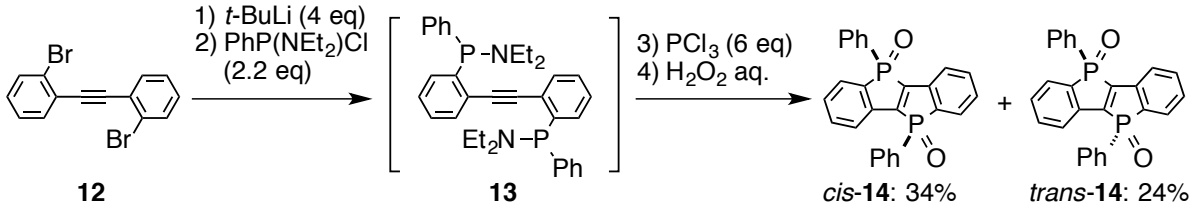

12

13

cis-**14**: 34%

trans-**14**: 24%

Scheme 1-9. Preparation of compound **14** using an intramolecular cascade cyclization.

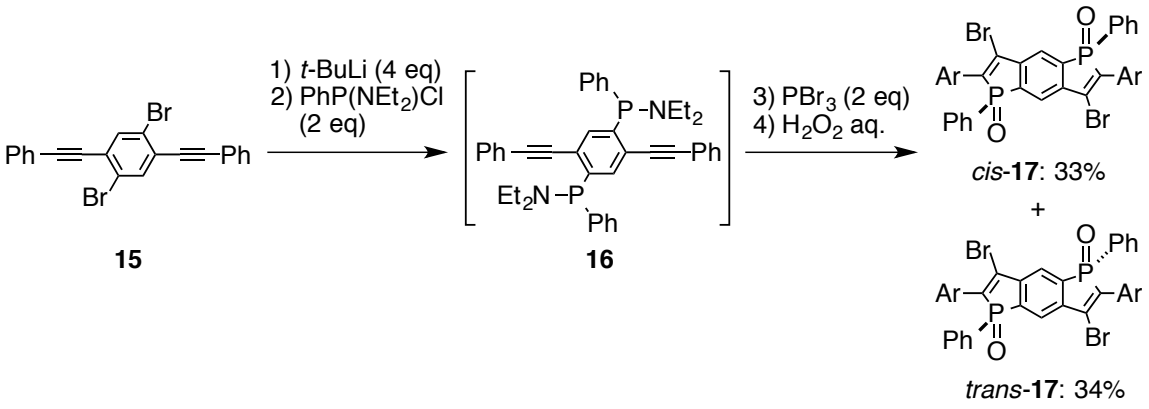

Scheme 1-10. Preparation of compound **17** using an intramolecular cyclization with PBr_3.

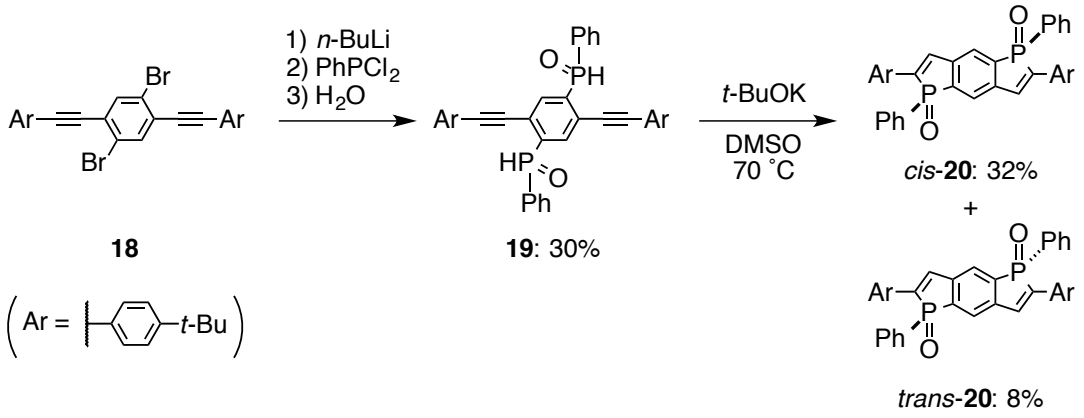

Scheme 1-11. Preparation of compound **20** using an base-mediated cyclization.

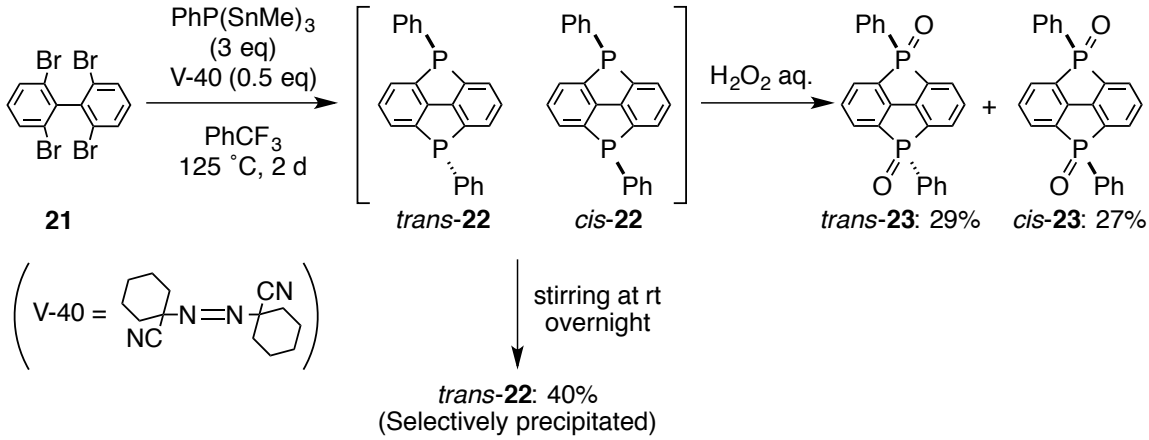

Scheme 1-12. Preparation of compound **23** using a quadruple radical phosphanylation and selective precipitation of *trans*-**22**.

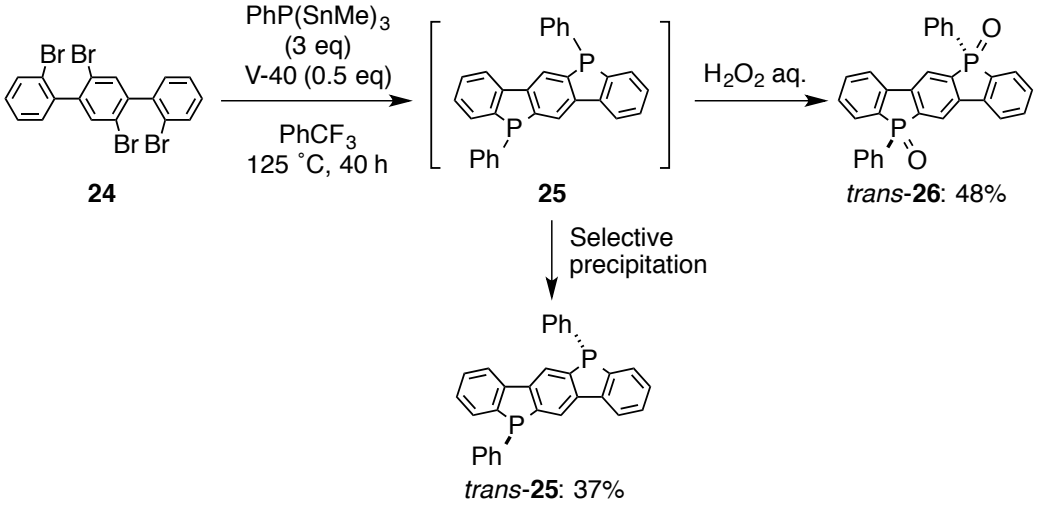

Scheme 1-13. Preparation of compound *trans*-**26** using a quadruple radical phosphanylation and selective precipitation of *trans*-**25**.

As shown in the above schemes, there exist some stereoisomers deriving from the relative stereochemistry of the pyramidal phosphorus centers in the π-conjugated frameworks bearing multiple phosphorus atoms. The possible stereoisomers have usually been obtained as a mixture and separated by silica-gel chromatography. In some cases, the *trans*-isomer was selectively precipitated before oxidation. However, the selective synthesis of the desired stereoisomer should be effective for the further development of the chemistry of phosphorus-containing π-conjugated systems, and the insight for the control of the stereochemistry of the phosphorus centers is demanded.

1.5 This work 1

As discussed in Section 1.3, the efficient synthetic protocol for C_3-symmetric HPB derivatives has been still missing in spite of their utility. Because the conventional protocols, which all correspond to the prefunctionalization approach, cannot avoid the problem of selectivity, a conceptually different approach is demanded. From such a viewpoint, the late-stage functionalization approach where the functionalization is performed after the construction of the HPB framework should be promising. However, it has not been

pursued because of the chemical intuition that it is impossible to functionalize the distant peripheral positions on the HPB framework in an alternate fashion selectively.

The synthesis of C_3-symmetric HPB derivatives should be innovatively improved if it is realized to selectively functionalize the three of the six chemically equivalent positions of the C_6-symmetrical HPB framework in an alternate manner (Scheme 1-14). On the basis of this synthetic analysis, the author has developed a late-stage derivatization approach for the synthesis of alternately functionalized C_3-symmetric HPB derivatives. His approach has also achieved the selective synthesis of HPB derivatives with the substitution pattern that is completely unavailable by any conventional approaches. The results described in this thesis demonstrate the possibility of the deliberate functionalization of the large HPB framework as the small benzene unit and the potential of the late-stage functionalization approach for the synthesis of extended π-conjugated molecules. The development of the new protocol utilizing a halogen dance reaction is discussed in Chapter 2. The improvement of the reaction conditions and the expansion of the scope of application are discussed in Chapter 3. The origin of the thermodynamic stability of the key alternately trilithiated species is discussed in Chapter 4.

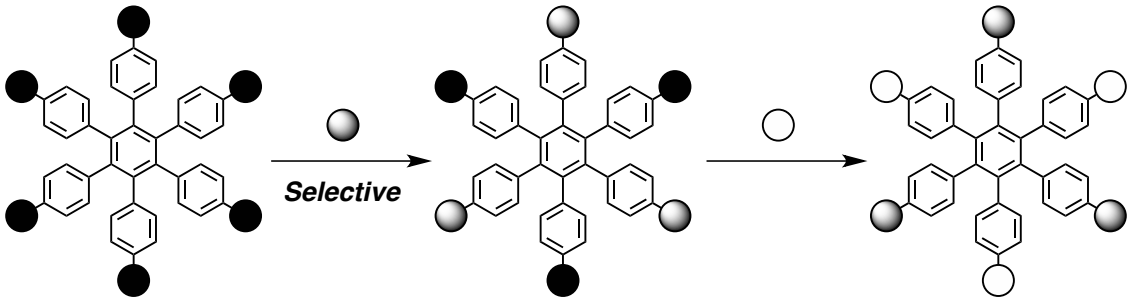

Scheme 1.14 Selective functionalization of the three of the six chemically equivalent positions of C_6-symmetrical HPB framework in an alternate manner.

1.6 This work 2

As discussed in Section 1.4, extended π-conjugated molecules bearing phosphorus centers are still limited despite the increasing demand as new organic materials. In particular, π-conjugated molecules

bearing more than two phosphorus centers have never been reported. This fact means that there are few C_3-symmetric π-conjugated frameworks incorporating phosphorus centers because C_3-symmetry demands at least three phosphorus centers except when the phosphorus atoms are only located on the C_3-axis. As the first example of a two-dimensionally extended π-conjugated framework bearing more than two phosphorus centers, the author designed the phosphorus analogue of truxene, triphosphatruxene (TPT) (Figure 1-7). The TPT framework possesses the two stereoisomers, *syn*-isomer and *anti*-isomer, deriving from the relative stereochemistry of the three pyramidal phosphorus centers. One of the two stereoisomers, *syn*-isomer, is C_3-symmetric, where the three substituents on the phosphorus atoms directed to the same face of the TPT framework. Selective preparation of one particular isomer is not only a challenging subject in synthetic chemistry of π-conjugated molecules, but also develop the new organic functional material. The author describes the first synthesis of TPT derivatives and the control of their stereochemistry in Chapter 5.

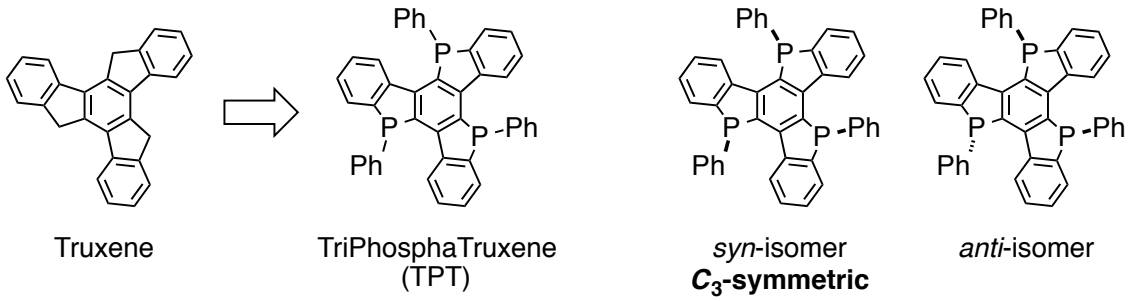

Figure 1.7 Triphosphatruxene (TPT) and its stereoisomers.

References

[1] Leow, D.; Li, G.; Mei, T.-S.; Yu, J.-Q. *Nature* **2012**, *486*, 518.

[2] Ishiyama, T.; Takagi, J.; Ishida, K.; Miyaura, N.; Anastasi, N. R.; Hartwig, J. F. *J. Am. Chem. Soc.* **2000**, *124*, 390.

[3] Chen, K.; Baran, P. S. *Nature* **2009**, *459*, 824.

[4] Guthrie, D. A.; Tovar, J. D. *Org. Lett.* **2008**, *10*, 4323.

[5] Guthrie, D. A.; Tovar, J. D. *Chem. Eur. J.* **2009**, *15*, 5176.

[6] Srinivas, K.; Kauffmann, B.; Dolain, C.; Léger, J.-M.; Ghosez, L.; Huc, I. *J. Am. Chem. Soc.* **2008**, *130*, 13210.

[7] Shravani, M.; Balaiah, S.; Srinivas, K.; Bhanuprakash, K.; Huc, I. *Chem. Phys. Chem.* **2012**, *13*, 3526.

[8] (a) Wu, J.; Pisula, W.; Müllen, K. *Chem. Rev.* **2007**, *107*, 718. (b) Chen, L.; Hernandez, Y.; Feng, X.; Müllen, K. *Angew. Chem., Int. Ed.* **2012**, *51*, 7640.

[9] (a) Hill, J. P.; Jin, W.; Kosaka, A.; Fukushima, T.; Ichihara, H.; Shimomura, T.; Ito, K.; Hashizume, T.; Ishii, N.; Aida, T. *Science* **2004**, *304*, 1481. (b) Yamamoto, Y.; Fukushima, T.; Suna, Y.; Ishii, N.; Saeki, A.; Seki, S.; Tagawa, S.; Taniguchi, M.; Kawai, T.; Aida, T. *Science* **2006**, *314*, 1761. (c) Zhang, W.; Jin, W.; Fukushima, T.; Saeki, A.; Aida, T. *Science* **2011**, *334*, 340.

[10] (a) Feng, X. L.; Pisula, W.; Takase, M.; Enkelmann, V.; Müllen, K. *Chem. Mater.* **2008**, *20*, 2872. (b) Feng, X. L.; Pisula, W.; Zhi, L.; Takase, M.; Müllen, K. *Angew. Chem., Int. Ed.* **2008**, *47*, 1703. (c) Feng, X. L.; Pisula, W.; Kudernac, T.; Wu, D.; Zhi, L.; Feyter, S. D.; Müllen, K. *J. Am. Chem. Soc.* **2009**, *131*, 4439.

[11] Cai, J.; Ruffieux, P.; Jaafar, R.; Bieri, M.; Braun, T.; Blankenburg, S.; Muoth, M.; Seitsonen, A. P.; Saleh, M.; Feng, X.; Müllen, K.; Fasel, R. *Nature* **2010**, *466*, 470.

[12] Geng, Y.; Fechtenkötter, A.; Müllen, K. *J. Mater. Chem.* **2001**, *11*, 1634.

[13] (a) Thomas, K. R. J.; Velusamy, M.; Lin, J. T.; Chuen, C. H.; Tao, Y.-T. *J. Mater. Chem.* **2005**, *15*, 4453. (b) Watanabe, S.; Kido, J. *Chem. Lett.* **2007**, *36*, 590. (c) Li, Z.; Ye, S.; Liu, Y.; Yu, G.; Wu, W.; Qin, J.; Li, Z. *J. Phys. Chem. B* **2010**, *114*, 9101.

[14] (a) Cho, H. S.; Rhee, H.; Song, J. K.; Min, C.-K.; Takase, M.; Aratani, N.; Cho, S.; Osuka, A.; Joo, T.; Kim, D. *J. Am. Chem. Soc.* **2003**, *125*, 5849. (b) Kodis, G.; Terazono, Y.; Liddell, P. A.; Andréasson, J.; Garg, V.; Hambourger, M.; Moore, T. A.; Moore, A. L.; Gust, D. *J. Am. Chem. Soc.* **2006**, *128*, 1818. (c) Terazono, Y.; Kodis, G.; Liddell, P. A.; Garg, V.; Moore, T. A.; Moore, A. L.; Gust, D. *J. Phys. Chem. B* **2009**, *113*, 7147. (d) Terazono, Y.; Kodis, G.; Bhushan, K.; Zaks, J.; Madden, C.; Moore, A. L.; Moore, T. A.; Fleming, G. R.; Gust, D. *J. Am. Chem. Soc.* **2011**, *133*, 2916.

[15] (a) Hiraoka, S.; Harano, K.; Shiro, M.; Ozawa, Y.; Yasuda, N.; Toriumi, K.; Shionoya, M. *Angew. Chem., Int. Ed.* **2006**, *45*, 6488. (b) Hiraoka, S.; Goda, M.; Shionoya, M. *J. Am. Chem. Soc.* **2009**, *131*, 4592. (c) Hoffmann, M.; Kärnbratt, J.; Chang, M.-H.; Herz, L. M.; Albinsson, B.; Anderson, H. L. *Angew. Chem., Int. Ed.* **2008**, *47*, 4993. (d) O'Sullivan, M. C.; Sprafke, J. K.; Kondratuk, D. V.; Rinfray, C.; Claridge, T. D. W.; Saywell, A.; Blunt, M. O.; O'Shea, J. N.; Beton, P. H.; Malfois, M.; Anderson, H. L. *Nature* **2011**, *469*, 72. (e) Zhao, Z.; Zheng, Y.-R.; Wang, M.; Pollock, J. B.; Stang, P. J. *Inorg. Chem.* **2010**, *49*, 8653. (f) Zheng, Y. R.; Zhao, Z.; Kim, H.; Wang, M.; Ghosh, K.; Pollock, J. B.; Chi, K.-W.; Stang, P. J. *Inorg. Chem.* **2010**, *49*, 10238. (g) Jia, W.-L.; Wang, R.-Y.; Song, D.; Ball, S. J.; McLean, A. B.; Wang, S. *Chem. Eur. J.* **2005**, *11*, 832. (h) Wang, J.-L.; Li, X.; Lu, X.; Hsieh, I-F.; Cao, Y.; Moorefield, C. N.; Wesdemiotis, C.; Cheng, S. Z. D.; Newkome, G. R. *J. Am. Chem. Soc.* **2011**, *133*, 11450.

[16] (a) Hiraoka, S.; Harano, K.; Shiro, M.; Shionoya, M. *J. Am. Chem. Soc.* **2008**, *130*, 14368. (b) Hiraoka, S.; Harano, K.; Nakamura, T.; Shiro, M.; Shionoya, M. *Angew. Chem., Int., Ed.* **2009**, *48*, 7006. (c) Hiraoka, S.; Nakamura, T.; Shiro, M.; Shionoya, M. *J. Am. Chem. Soc.* **2010**, *132*, 13223.

[17] (a) Shukla, R.; Lindeman, S. V.; Rathore, R. *J. Am. Chem. Soc.* **2006**, *128*, 5328. (b) Shukla, R.; Lindeman, S. V.; Rathore, R. *Chem. Commun.* **2007**, 3717. (c) Bhalla, V.; Vij, V.; Kumar, M.; Sharma, P. R.; Kaur, T. *Org. Lett.* **2012**, *14*, 1012. (d) Bhalla, V.; Vij, V.; Tejpal, R.; Singh, G.; Kumar, M. *Dalton Trans.* **2013**, *42*, 4456. (e) Maeda, H.; Shirai, T.; Uemura, S. *Chem. Commun.* **2013**, *49*, 5310.

[18] (a) Lambert, C.; Nöll, G. *Chem. Eur. J.* **2002**, *8*, 3467. (b) Traber, B.; Wolff, J. J.; Rominger, F.; Oeser, T.; Gleiter, R.; Goebel, M.; Wortmann, R. *Chem. Eur. J.* **2004**, *10*, 1227. (c) Xiao, W.; Feng, X.; Ruffieux,

P.; Gröning, O.; Müllen, K.; Fasel, R. *J. Am. Chem. Soc.* **2008**, *130*, 8910. (d) Zeng, Z.; Guan, Z.; Xu, Q.-H.; Wu, J. *Chem. Eur. J.* **2011**, *17*, 3837. (e) Lambert, C.; Ehbets, J.; Rausch, D.; Steeger, M. *J. Org. Chem.* **2012**, *77*, 6147. (f) Steeger, M.; Lambert, C. *Chem. Eur. J.* **2012**, *18*, 11937.

[19] Feng, X.; Pisula, W.; Müllen, K. *Pure. Appl. Chem.* **2009**, *81*, 2203.

[20] Wu, J.; Baumgarten, M; Debije, M. G.; Warman, J. M.; Müllen, K. *Angew. Chem., Int. Ed.* **2004**, *43*, 5311.

[21] Fukazawa, A.; Yamaguchi, S. *Chem. Asian J.* **2009**, *4*, 1386.

[22] (a) Baumgartner, T.; Réau, R. *Chem. Rev.* **2006**, *106*, 4681. (b) Hobbs, M. G.; Baumgartner, T. *Eur. J. Inorg. Chem.* **2007**, 3611. (c) Crassous, J.; Réau, R. *Dalton Trans.* **2008**, 6865. (d) Matano, Y.; Imahori, H. *Org. Biomol. Chem.* **2009**, *7*, 1258. (e) Ren, Y.; Baumgartner, T. *Dalton Trans.* **2012**, *41*, 7792.

[23] Tsuji, H.; Sato, K.; Sato, Y.; Nakamura, E. *J. Mater. Chem.* **2009**, *19*, 3364.

[24] Chen, H.; Delaunay, W.; Li, J.; Wang, Z.; Bouit, P.-A.; Tondelier, D.; Geffroy, B.; Mathey, E.; Duan, Z.; Réau, R.; Hissler, M. *Org. Lett.* **2013**, *15*, 330.

[25] Matano, Y.; Saito, A.; Suzuki, Y.; Miyajima, T.; Akiyama, S.; Otsubo, S.; Nakamoto, E.; Aramaki, S.; Imahori, H. *Chem. Asian J.* **2012**, *7*, 2305.

[26] Fukazawa, A.; Hara, M.; Okamoto, T.; Son, E.-C.; Xu, C.; Tamao, K.; Yamaguchi, S. *Org. Lett.* **2008**, *10*, 913.

[27] Fukazawa, A.; Ichihashi, Y.; Kosaka, Y.; Yamaguchi, S. *Chem. Asian J.* **2009**, *4*, 1729.

[28] Sanji, T.; Shiraishi, K.; Kashiwabara, T.; Tanaka, M. *Org. Lett.* **2008**, *10*, 2689.

[29] Bruch, A.; Fukazawa, A.; Yamaguchi, E.; Yamaguchi, S.; Studer, A. *Angew. Chem., Int. Ed.* **2011**, *50*, 12094.

[30] Hanifi, D.; Pun, A.; Liu, Y. *Chem. Asian J.* **2012**, *7*, 2615.

Chapter 2

Selective Alternate Trilithiation of the Hexaphenylbenzene Framework through a Thermodynamically Controlled Halogen Dance

2.1 Introduction

As discussed in Chapter 1, the efficient synthetic protocol for alternately functionalized HPB derivatives has been still missing in spite of their utility and a conceptually different approach has long been demanded. On the basis of the synthetic analysis, the author focused on the late-stage functionalization approach, where the selective derivatization of the three of the six chemically equivalent peripheral positions of the C_6-symmetrical HPB framework is performed instead of the conventional prefunctionalization approaches (Scheme 2.1). From thoroughly surveying the literature, the author found one novel example reported by Rathore et al.[1] a decade ago, which included an alternately substituted HPB derivative **28** that was accidentally produced in high yield through lithiation of C_6-symmetric hexakis(*p*-bromophenyl)benzene (**27**) by using 7.2 eq of *t*-BuLi followed by electrophilic trapping with benzophenone (Scheme 2.2). Although this reaction seemed promising for the selective synthesis of C_3-symmetric HPB derivatives, its mechanistic details and versatility have remained unexplored. This unexplored result inspired the author to develop a new methodology for the preparation of alternately functionalized C_3-symmetric HPB derivatives utilizing a Br/Li exchange reaction.

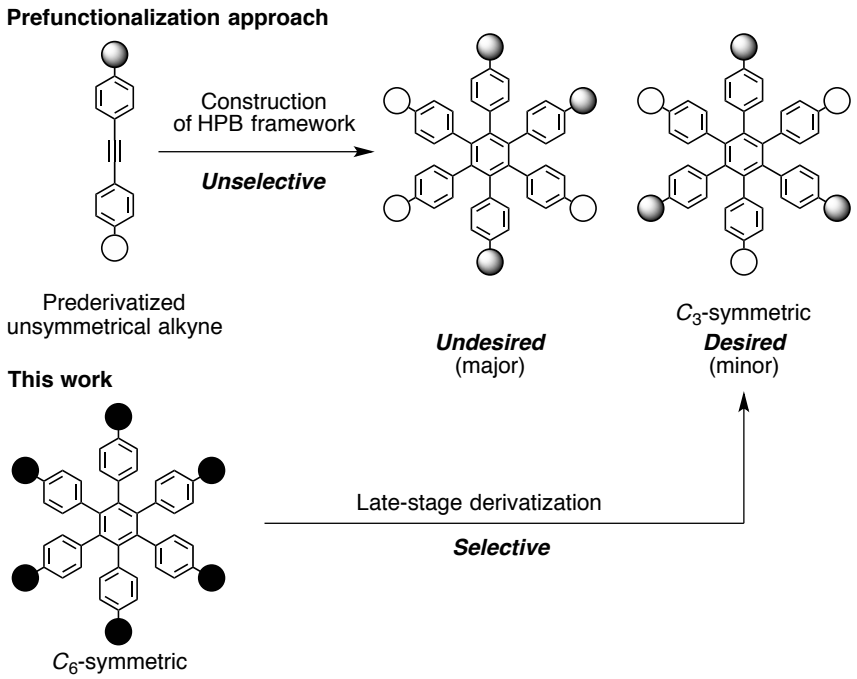

Scheme 2.1 Comparison of the prefunctionalization approach and the new approach studied in this thesis.

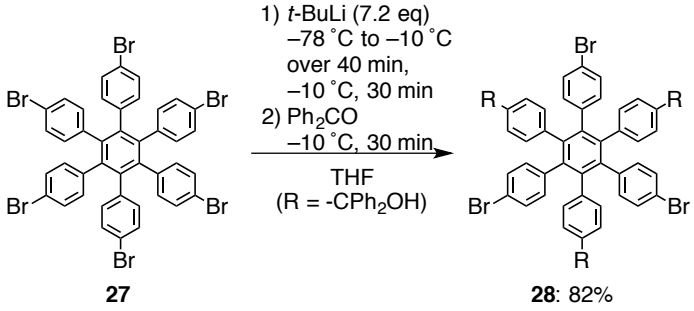

Scheme 2.2 Selective preparation of compound **28** by Rathore et al. with the unapparent selectivity.

In this chapter, the author discusses the selective alternate trilithiation of compound **27** and its detailed mechanism. The applicable scope of this new protocol is also discussed to obtain the low-symmetric HPB derivatives with the substitution pattern that is completely unavailable by any conventional protocols.

2.2 Selective alternate trilithiation of compound 27 and reaction monitor

Modifying Rathore's conditions, the author confirmed the selective alternate trilithiation of compound **27**. The author added 6.0 eq of *t*-BuLi into the suspension of **27** in THF at –98 °C, warmed it to rt to obtain a clear solution, and then quenched it with TMSCl at –98 °C. HPB derivative **30** was selectively obtained (^{1}H NMR yield: 84%) and isolated in 67% yield after recrystallization (Scheme 2.3). The structure of compound **30** was unambiguously characterized by ^{1}H and ^{13}C NMR based on its C_3-symmetry. This reproducible result indicated the selective generation of the C_3-symmetric alternately trilithiated species **29** before quenching. The crude product was expected as the mixture of the HPB derivatives where the number and the arrangement of the TMS groups were different from those of compound **30**. These HPB derivatives exhibited the almost same polarity and the isolation of compound **30** was only possible with recrystallization.

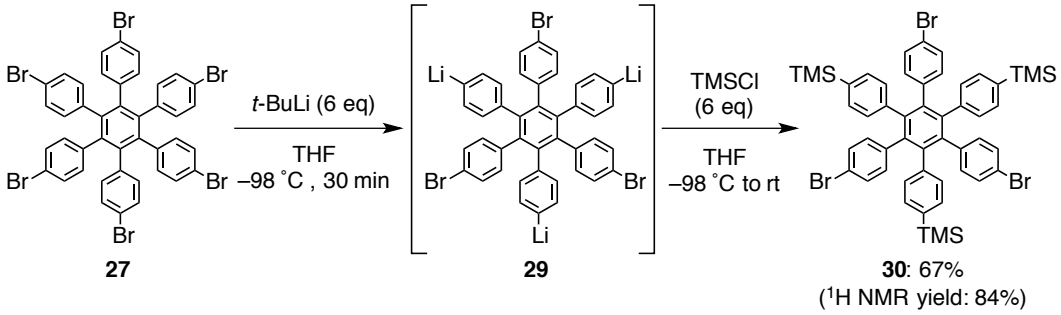

Scheme 2.3 Selective alternate trilithiation of compound **27**.

To clarify the reaction mechanism, the author monitored the composition of the reaction mixture by electrophilic trapping of the lithiated intermediates with TMSCl at –98 ˚C. The ^{1}H NMR spectra of the resulting crude mixture at various times are shown in Figure 2.1. The product obtained 2.5 min after removal of the cooling bath was a 1:1 mixture of starting material **27** and compound **31** derived from hexalithiated species **32** (Figure 2.1a). During the warming process, the ratio of **32** progressively decreased, and via a rather complex mixture (Figures 2.1b and c), finally the alternately trilithiated species **29** became the main component of the reaction mixture, which did not contain **32** at all (Figure 2.1d). This result indicates that alternately trilithiated species **29** is not a kinetic product but is produced from **27** and "overlithiated" species **32**.

This reaction was also found to be sensitive to the ratio of compound **27** and the amount of THF solvent. The use of a larger amount of THF resulted in the decrease of the target alternately trilithiated species **29** and the generation of a larger amount of overlithiated species, where the more than three Br moieties of compound **27** were lithiated. (Scheme 2.5, Figure 2.2).[2] It should be noted that some of compound **27** was precipitated before the addition of *t*-BuLi at –98 ˚C in all the conditions. This dependence on the ratio of compound **27** and the amount of THF solvent is an important finding for the mechanistic consideration of the alternate selectivity, which is discussed in the next section.

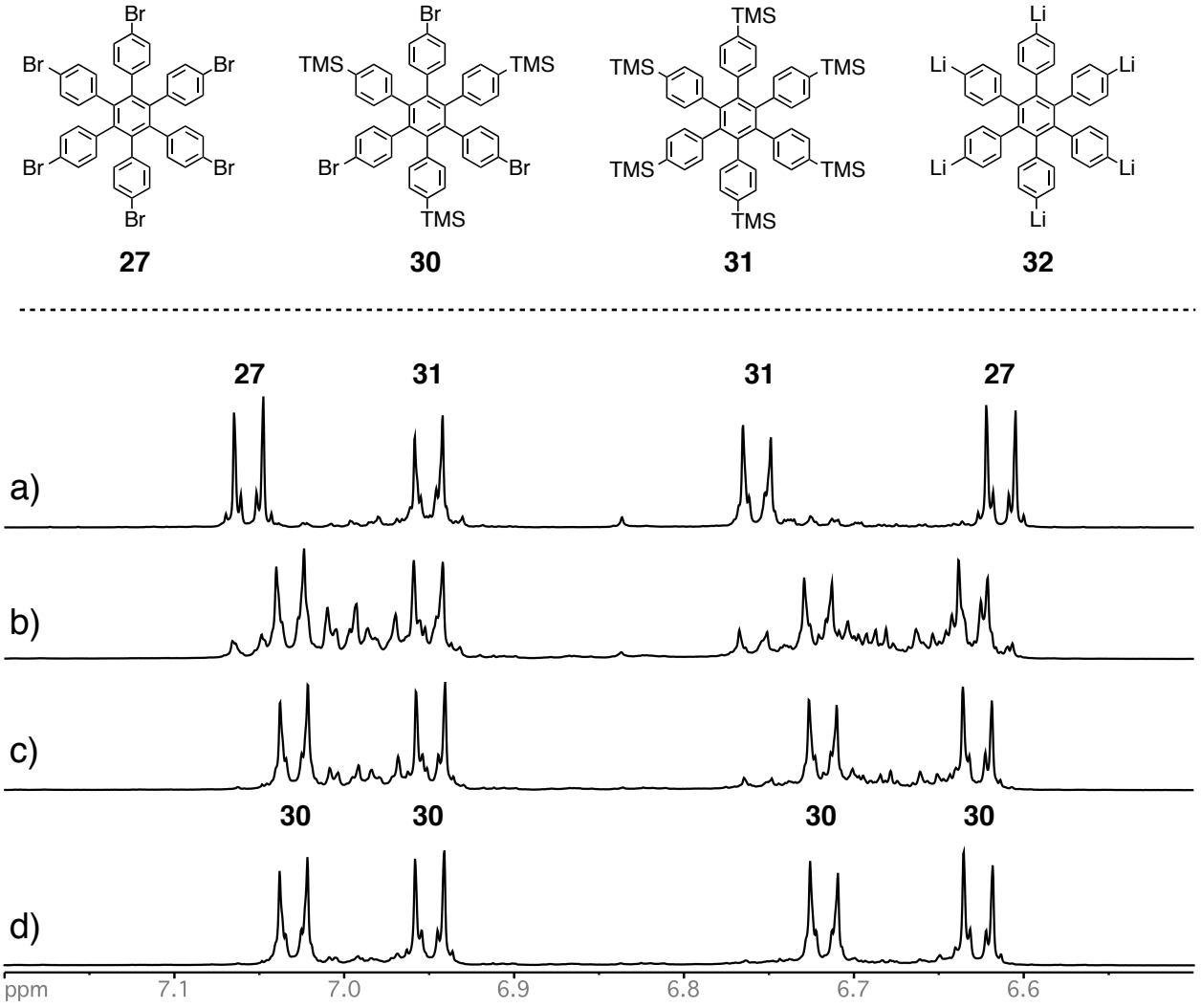

Figure 2.1 Partial ^{1}H NMR spectra (500 MHz, $CDCl_3$) of the crude mixture obtained by quenching with TMSCl at various times: a) 2.5 min, b) 5 min, c) 7.5 min, d) 30 min after removal of the cooling bath.

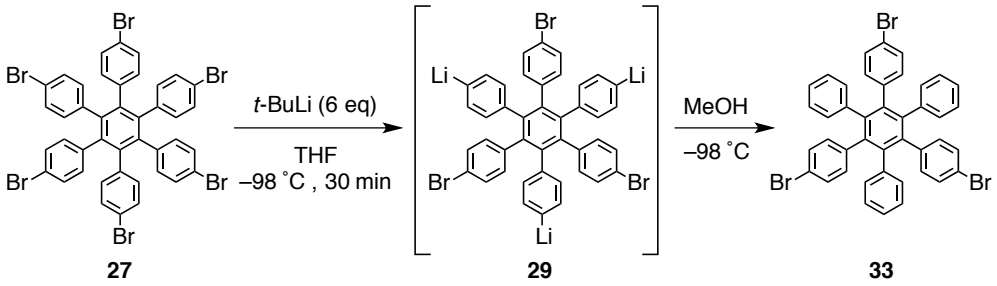

Scheme 2.5 Attempted selective alternate trilithiatin of compound **27** with various amount of THF.

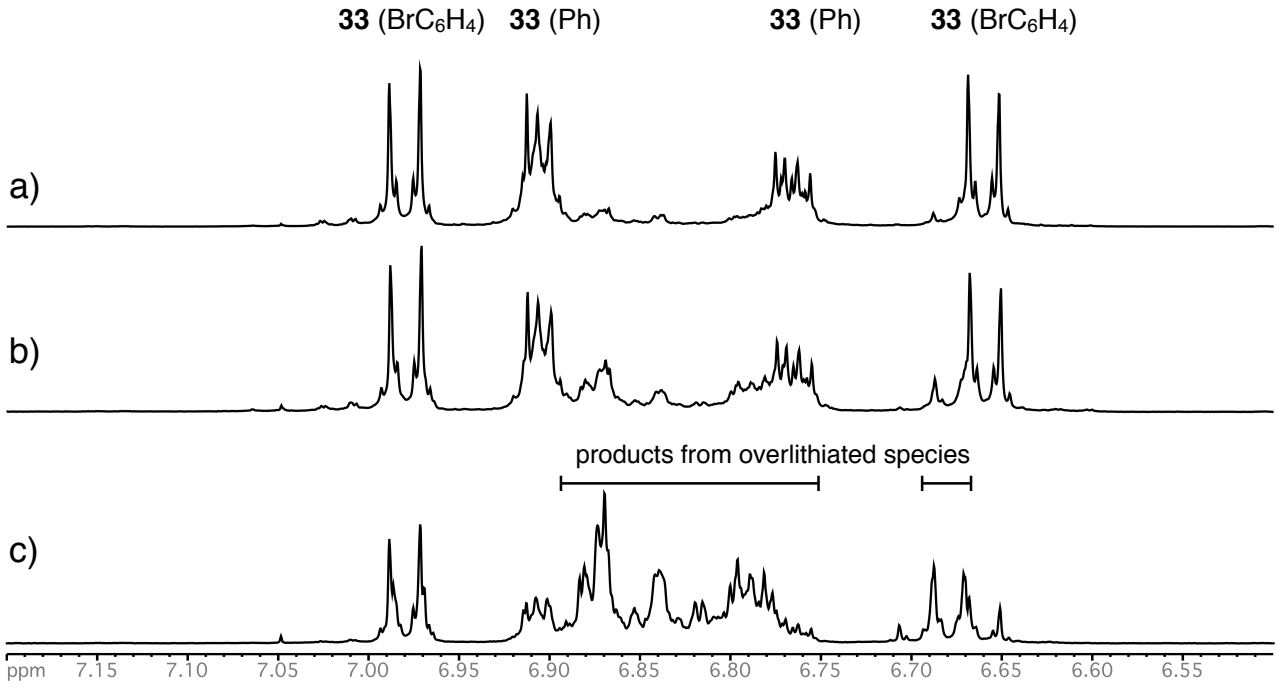

Figure 2.2 Partial ^{1}H NMR spectra (500 MHz, $CDCl_3$) of the crude mixture obtained with the various ratio of compound **27** and the amount of THF solvent (compound **27**/THF): a) 0.20 g/2 mL, b) 0.10 g/6 mL, c) 0.10 g/15 mL.

2.3 Mechanism of the selective alternate trilithiation

In Section 2.2, it was found that the key alternately trilithiated species **29** is not directly obtained from compound **27** as a kinetic product but that it is derived from the mixture of compound **27** and

hexalithiated species **32**. This result means that hexalithiated species **32** can return to trilithiated species **29**. Actually, the reversibility of the ArBr/ArLi exchange reaction in THF has been confirmed,[3] and the process leading to a thermodynamic equilibration is known as a halogen dance reaction (Scheme 2.6).[4] The halogen dance has been strategically exploited to prepare aryllithiums and heteroaryllithims that are difficult to obtain by other methods. Although the compounds that have been reported in the literatures concerning the halogen dance so far are limited to monocyclic aromatics and quinoline, it is natural to expect that the halogen dance should also occur on larger aromatic frameworks such as HPB.

Thus, the formation of **29** can be interpreted on the basis of the halogen dance on the HPB frameworks (Scheme 2.7). The selective alternate trilithiation reaction consists of two reaction phases: a lithiation phase and a halogen dance phase (Scheme 2.8). At the initial stage of the warming process, hexalithiated species **32** selectively generates and the reaction between ArBr and *t*-BuLi is completed (lithiation phase). The halogen dance between **27**, **32**, and the various partially lithiated species then takes place to afford an equilibrium mixture which contains **29** as a major component (halogen dance phase). As far as the author knows, this is the first report demonstrating that the halogen dance is applicable for the selective derivatization of polyaromatic hydrocarbons.

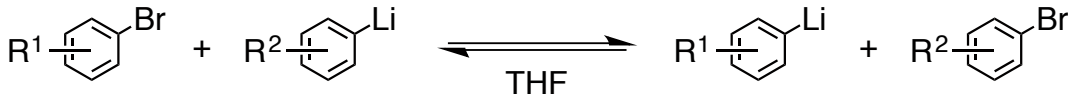

Scheme 2.6 Thermodynamically controlled halogen dance between ArBr and ArLi on the basis of the reversibility of the ArBr/ArLi exchange reaction.

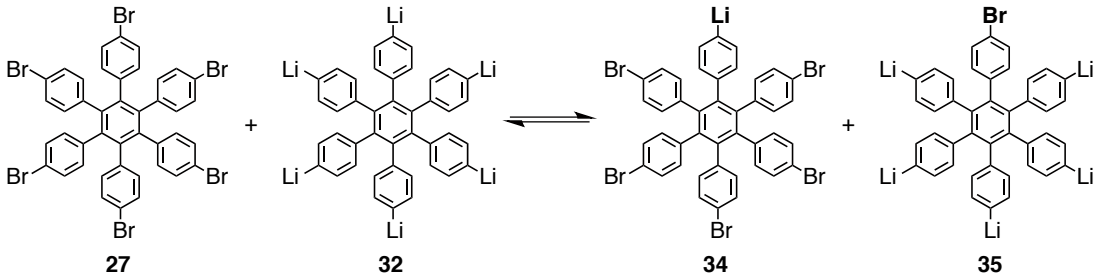

Scheme 2.7 Example of the halogen dance between the HPB frameworks.

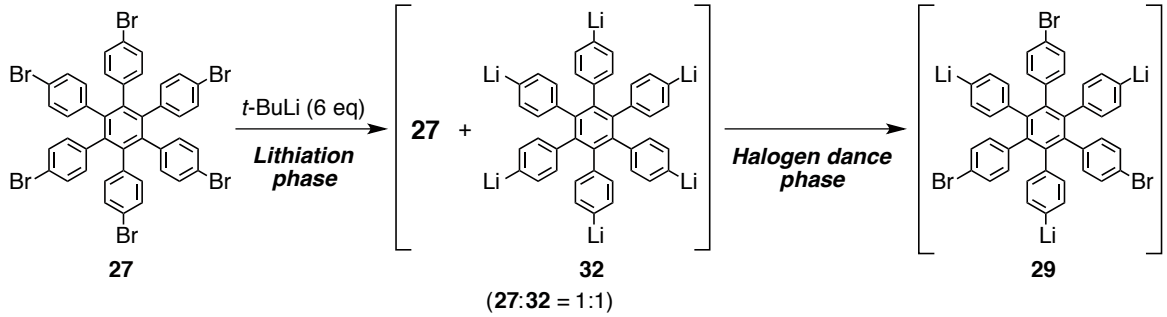

Scheme 2.8 Mechanism of the selective alternate trilithiation of the HPB framework through a thermodynamically controlled halogen dance.

To exactly understand the process of the selective alternate trilithiation, the further discussion is necessary because the selective formation of hexalithiated species **32** without any other partially lithiated species in the lithiation phase and the dependence of the products on the ratio of compound **27** and the amount of THF solvent in Section 2.2 are not apparent. The author analyzed that this reaction consists of four independent processes: (1) the Br/Li exchange reaction between ArBr and *t*-BuLi, (2) the elimination reaction between *t*-BuBr and *t*-BuLi, (3) the dissolution of precipitated compound **27**, and (4) the halogen dance between **29**, **32**, and partially lithiated HPB derivatives (Figure 2.3). At first, the selective formation of **32** without any other partially lithiated species was attributed to the slower dissolution rate of precipitated **27** than the rate of the Br/Li exchange reaction on the dissolved partially lithiated species with *t*-BuLi because there is no special reason for the acceleration of the Br/Li exchange reaction of the partially lithiated HPB species. Next, hexalithiation of exactly half of compound **27** is based on the kinetics that the rate of the elimination reaction of *t*-BuBr with *t*-BuLi is faster than the dissolution rate of compound **27**. Otherwise, more than half of compound **27** could be hexalithiated because the reaction rate of the Br/Li exchange between ArBr and *t*-BuLi is usually faster than that of the subsequent elimination reaction.[5] In such a situation, the equivalents of Li on the HPB framework after the lithiation phase should be more than three, and the amount of trilithiated species should be decreased at the equilibration after the halogen dance phase. Lithiation of the HPB framework of exactly three equivalents is prerequisite for the system to reach the equilibration where alternately trilithiated species **29** is the main component. This interpretation can also

explain the dependence of the selectivity on the amount of used THF solvent. If the amount of THF is increased, the dissolution of precipitated compound **27** is promoted and the excessive Br/Li exchange reaction between compound **27** and *t*-BuLi starts to compete with the elimination reaction between *t*-BuBr and *t*-BuLi, Therefore, the most important kinetics for the selective alternate trilithiation of compound **27** is that the elimination reaction of *t*-BuBr with *t*-BuLi is faster than the dissolution of compound **27**. The dissolution of the precipitated starting material vitally affects the alternate selectivity.[6]

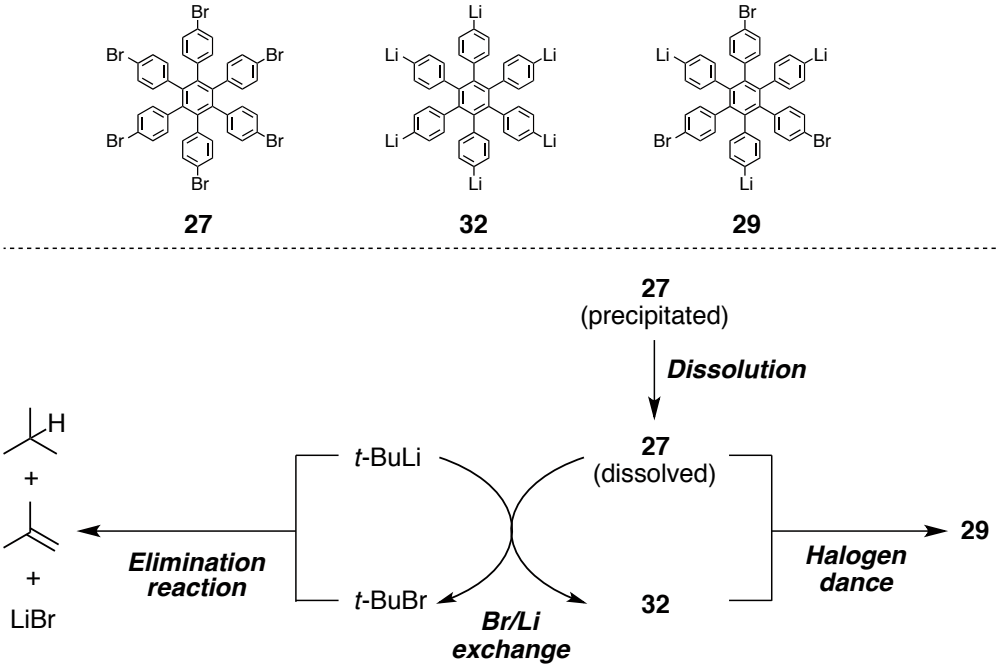

Figure 2.3 Detailed mechanism for the selective alternate trilithiation of compound **27**.

2.4 Application of the selective alternate trilithiation of the HPB framework

The selective late-stage derivatization through the halogen dance of hexabrominated HPB derivative **27**, which is easily prepared from the inexpensive starting materials only with filtration purification in a large scale (Scheme 2.9),[7] is quite practicable to obtain alternately functionalized HPB derivatives. For instance, selective alternate introduction of the three TMS groups was accomplished in 75% yield after recrystallization at the 10-g scale (Scheme 2.10). Large-scale sequential trilithiation also succeeded in producing HPB derivative **40** with the Me and TMS groups arranged in an alternate pattern,

which was difficult to obtain through the conventional trimerization approach because of the tedious separation of the two possible isomers (1,2,4-type isomer and 1,3,5-type isomer). The synthetic versatility of organolithiums and bromoarenes can effectually expand the availability of HPB derivatives.

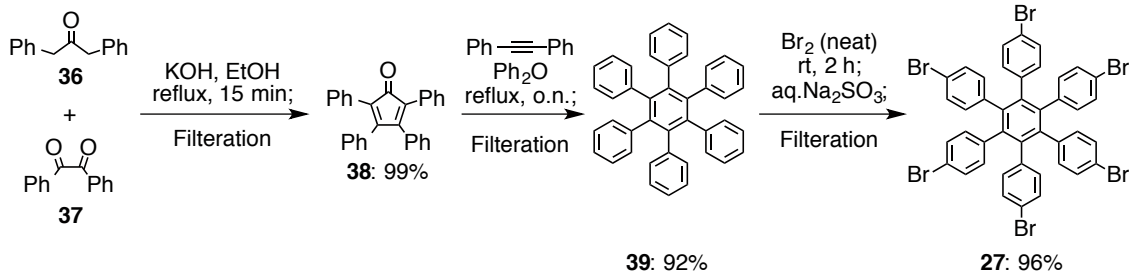

Scheme 2.9 Efficient and large-scale preparation of compound **27**.

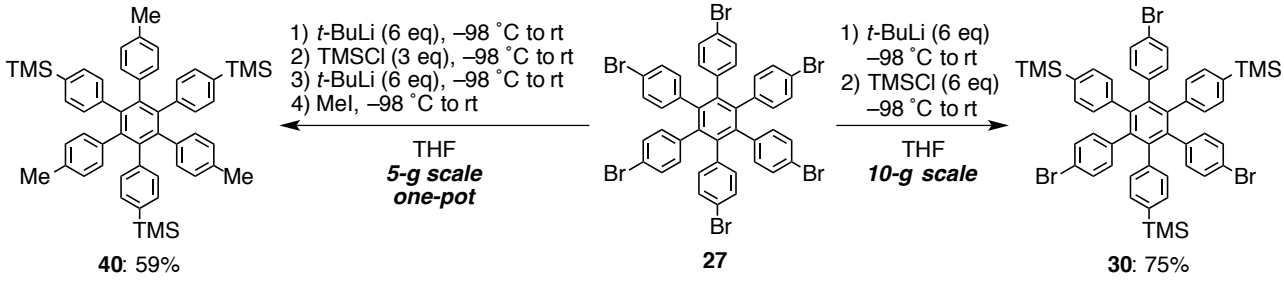

Scheme 2.10 Application of the selective alternate trilithiation of compound **27**.

2.5 Selective alternate trilithiation of the low-symmetric HPB frameworks

To expand the versatility of the selective alternate trilithiation to the brominated HPB derivatives that can afford a novel substitution pattern, the author subjected brominated HPB derivatives **41**-**45** possessing one substituent (CF_3, Cl, H, Me, or OMe) and five Br substituents, which are readily available through Diels-Alder reaction without the problem of regioselectivity,[8] to the condition of trilithiation for compound **27** (Scheme 2.11, Figure 2.4). It was found that the newly introduced substituents of **41**-**45** strongly affect the result of trilithiation of HPB framework although they and Br moieties are distributed on the different phenyl groups. The high alternate selectivity was observed only for **41** and **42**, which contain an electron-withdrawing group (R = CF_3, Cl). On the other hand, trilithiation of **43**, **44**, and **45** bearing a

hydrogen or an electron-donating group (R = Me, OMe) gave a complex mixture. In addition to the distinctive difference of the crude products, the difference of the time for the dissolution of the precipitated starting material was observed. Compounds **43**, **44**, and **45**, which afforded the complex mixture, took longer time for the suspension of the precipitated starting material to dissolve. This is the important observation to improve the selective alternate trilithiation protocol in Chapter 3.

The electrophilic trapping of the alternately trilithiated species derived from compounds **41** and **42** with TMSCl gave the products bearing the three TMS groups arranged in an alternate manner in 57% and 45% isolated yield, respectively. The C_{2v}-symmetric structures of compounds **41** and **42** were clearly confirmed by ^{1}H and ^{13}C NMR spectroscopy. This is the first selective synthesis of the low-symmetric HPB derivatives with this type of substitution pattern. The late-stage desymmetrization approach utilizing the halogen dance was demonstrated to be effective for the preparation not only of C_3-symmetric HPB derivatives but also of lower-symmetric HPB derivatives that are almost impossible to synthesize and isolate with the conventional prederivatization approaches.

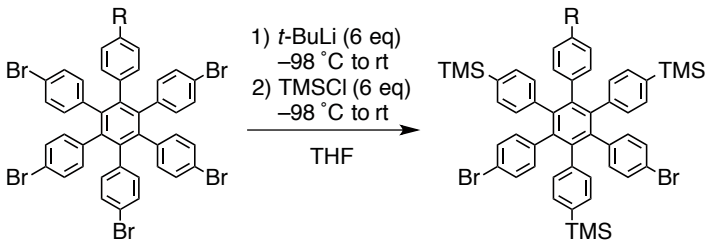

41 (R = CF_3)
42 (R = Cl)
43 (R = H)
44 (R = Me)
45 (R = OMe)

46 (R = CF_3): 57%
47 (R = Cl): 45%
48 (R = H): n.d.
49 (R = Me): n.d.
50 (R = OMe): n.d.

Scheme 2.11 Attempted selective trilithiation of compounds **41**-**45**.

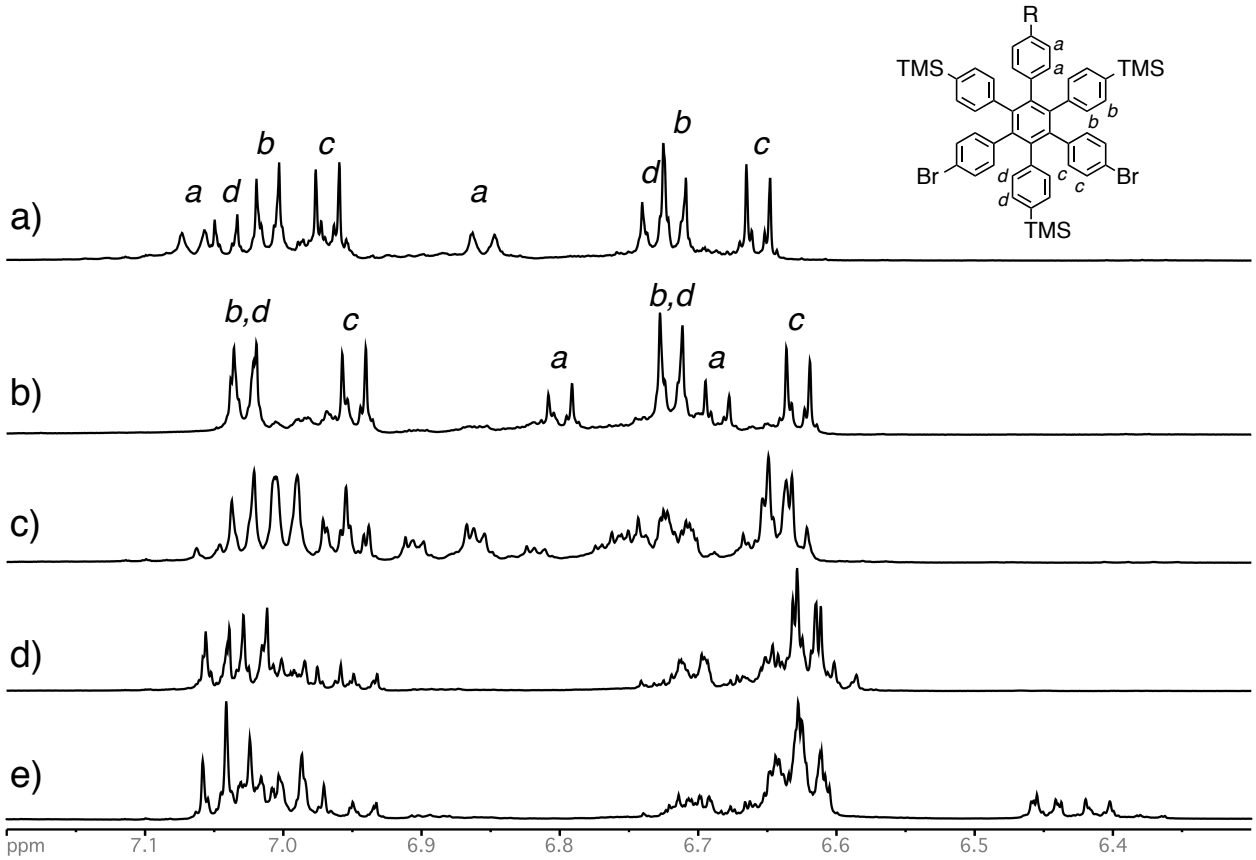

Figure 2.4 Partial ^{1}H NMR spectra (500 MHz, $CDCl_3$) of the crude mixture obtained by attempted trilithiation of (a) **41**, (b) **42**, (c) **43**, (d) **44**, and (e) **45**.

2.6 Conclusion

The selective alternate trilithiation of the hexabrominated HPB framework and its detailed mechanism were described as the late-stage derivatization approach for the preparation of C_3-symmetric HPB derivatives. It was revealed that the alternate selectivity is based on the thermodynamically controlled halogen dance and the exquisite balance of the kinetics of several independent processes, which contain the dissolution of the starting material. The applicability of this protocol for the efficient and large-scale synthesis of alternately functionalized C_3-symmetric HPB derivatives was also demonstrated. The selective preparation of the low-symmetric HPB derivatives, which had been unavailable with any conventional methods, was also achieved although the limitation of the substrates existed. On the basis of the detailed analysis of the reaction mechanism in this Chapter, the improvement of the selective alternate trilithiation protocol to expand the applicable scope of the substrates is discussed in the next Chapter.

Experimental Section

General procedures for Chapters 2, 3, and 4

^{1}H NMR and ^{13}C NMR were recorded with tetramethylsilane as the internal standard using a Bruker AV-500 (500 MHz) spectrometer. Chemical data for protons are reported in parts per million (ppm, δ scale) downfield from tetramethylsilane, and referenced internally to tetramethylsilane as a standard in $CDCl_3$ and to the residual proton in the solvent ($CDCl_3$: δ7.26). Chemical data for carbon are reported in parts per million (ppm, δ scale) downfield from tetramethylsilane, and are referenced to the carbon resonance of the NMR solvent ($CDCl_3$: δ77.16). HRMS were obtained using a Waters Xevo G2 Tof mass spectrometer. Melting points of solid materials were determined using a SCINICS SMP-300 instrument. Column chromatography was performed using SiO_2 [Merck, silica gel 60 for column chromatography (230-400 mesh ASTM)]. Unless otherwise noted, all solvents and reagents were obtained from commercial suppliers (TCI Co., Ltd., WAKO Pure Chemical Industries Ltd., KANTO Chemical Co., Ltd., and Sigma-Aldrich Co.) and were used as received. Compound **27**,[6] diarylalkyne **51**,[9] **52**,[10] **53**,[11] and tetracyclone **54**[12] were prepared according to the literature.

Synthesis of compound 30 (Scheme 2.3)

To the suspension of compound **27** (0.200 g, 0.198 mmol) in THF (2 mL) was added the freshly titrated pentane solution of *t*-BuLi (1.68 M, 0.708 mL, 1.19 mmol) at –98 ˚C. After removal of the cooling bath, the reaction mixture was stirred for 30 min, and then quenched by the addition of TMSCl (0.151 mL, 1.19 mmol) at –98 ˚C. After the addition of water and $CHCl_3$, the organic layer was separated, dried over $MgSO_4$, and filtered. Then the solvent was removed in vacuo and recrystallization from $CHCl_3$/EtOH afforded compound **30** (0.132 g, 67%) as a colorless solid.

m.p. >300 ˚C; ^{1}H NMR (500 MHz, $CDCl_3$, 293 K): δ 7.03 (d, J = 8.5 Hz, 6H), 6.95 (d, J = 8.5 Hz, 6H), 6.72 (d, J = 8.5 Hz, 6H), 6.63 (d, J = 8.5 Hz, 6H), 0.14 (s, 27H); ^{13}C NMR (126 MHz, $CDCl_3$, 293 K): δ 140.65, 140.29, 139.41, 139.39, 137.67, 133.04, 132.02, 130.64, 129.89, 119.61, –1.05; HRMS (ASAP): Calcd for $[M]^+$ $C_{51}H_{51}{}^{79}Br_3Si_3$ 984.0849, found 984.0836.

Large-scale synthesis of compound 30 (Scheme 2.10)

To the suspension of compound **27** (10.0 g, 9.92 mmol) in THF (100 mL) was added the pentane solution of *t*-BuLi (1.6 M, 37.2 mL, 60 mmol) at –98 ˚C. After removal of the cooling bath, the reaction mixture was stirred for 1 h. Then the reaction was quenched by the addition of TMSCl (7.6 mL, 60 mmol) at –98 ˚C. After the addition of aq. NH_4Cl and $CHCl_3$, the organic layer was separated, dried over $MgSO_4$, and filtered. Then the solvent was removed in vacuo and recrystallization from $CHCl_3$/EtOH afforded compound **30** (7.33 g, 75%) as a colorless solid.

Large-scale synthesis of compound 40 (Scheme 2.10)

To the suspension of compound **27** (5.00 g, 4.96 mmol) in THF (50 mL) was added the pentane solution of *t*-BuLi (1.6 M, 18.6 mL, 30 mmol) at –98 ˚C. After removal of the cooling bath, the reaction mixture was stirred for 1 h. Then to the solution was added TMSCl (1.9 mL, 15 mmol) at –98 ˚C. After removal of the cooling bath, the reaction mixture was stirred for 1 h. Then to the solution was added the pentane solution of *t*-BuLi (1.6 M, 18.6 mL, 30 mmol) at –98 ˚C. After removal of the cooling bath, the reaction mixture was stirred for 30 min. Then the reaction was quenched by the addition of MeI (1.9 mL, 30 mmol) at –98 ˚C. After the addition of aq. NH_4Cl and $CHCl_3$, the organic layer was separated, dried over $MgSO_4$, and filtered. Then the solvent was removed in vacuo and recrystallization from $CHCl_3$/EtOH afforded compound **40** (2.36 g, 59%) as a colorless solid.

m.p. 298 ˚C (dec); ^{1}H NMR (500 MHz, $CDCl_3$, 293 K): δ 6.97 (d, J = 8.0 Hz, 6H), 6.76 (d, J = 8.0 Hz, 6H), 6.63 (d, J = 8.0 Hz, 6H), 6.60 (d, J = 8.0 Hz, 6H), 2.08 (s, 9H), 0.10 (s, 27H); ^{13}C NMR (126 MHz, $CDCl_3$, 293 K): δ 141.57, 140.52, 140.31, 137.78, 136.30, 134.21, 131.50, 131.47, 130.95, 127.24, 21.08, –1.02; HRMS (ASAP): Calcd for $[M]^+$ $C_{54}H_{60}Si_3$ 792.4003, found 792.4014.

Preparation of unsymmetrical diarylalkyne 57 (Scheme 2.12)

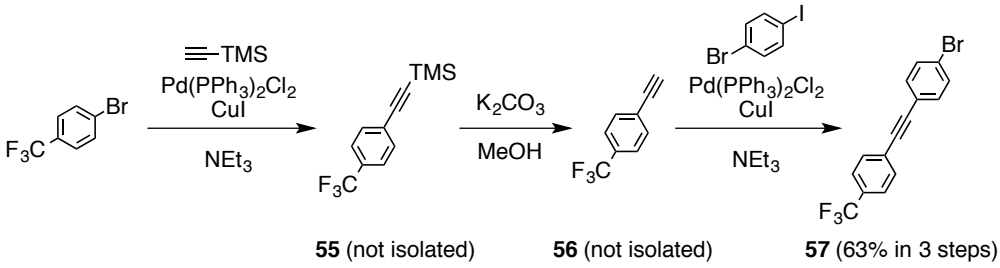

Scheme 2.12 Preparation of unsymmetrical diarylalkyne **57**.

To the solution of *p*-bromobenzotrifluoride (1.00 mL, 7.24 mmol), $Pd(PPh_3)_2Cl_2$ (51 mg, 73 μmol), CuI (14 mg, 73 μmol) in degassed NEt_3 (6 mL) was added trimethylsilylacetylene (1.13 mL, 7.97 mmol) at rt. Then the solution was stirred for 3 h at 70 °C, diluted with Et_2O, and washed with water and 5 M aq. HCl. Then the organic layer was filtered through Celite®. The filtrate was washed with water and 10% aq. NH_3, dried over $MgSO_4$, filtered, and concentrated in vacuo to afford brown oil. To the obtained oil was added K_2CO_3 (1.0 g, 7.2 mmol) and degassed MeOH (15 mL). The mixture was stirred for 1 h at rt, diluted with CH_2Cl_2, and washed with water. The organic layer was dried over $MgSO_4$, filtered, and concentrated to afford brown oil (1.30 g). The solution of the obtained oil in THF (5 mL) was added dropwise to the solution of *p*-bromoiodobenzene (1.70 g, 6.00 mmol), $Pd(PPh_3)_2Cl_2$ (42 mg, 60 μmol), CuI (11 mg, 60 μmol) in degassed NEt_3 (2 mL). The mixture was stirred for 3 h at rt, diluted with CH_2Cl_2, and washed with 5 M aq. HCl, water, and 10% aq. NH_3. The organic layer was dried over $MgSO_4$, and filtered. Then the solvent was removed in vacuo and recrystalization from CH_2Cl_2 afforded compound **57** (1.18 g, 50%) as a colorless solid. Silica-gel column chromatography (hexane) of the mother liquor afforded the additional amount of compound **57** (0.30 g, 13%) as a colorless solid (Total yield: 1.48 g, 63% in 3 steps).

m.p. 133-134 °C; ^{1}H NMR (500 MHz, $CDCl_3$, 293 K): δ 7.62 (s, 4H), 7,51 (d, J = 8.5 Hz, 2H), 7.41 (d, J = 8.5 Hz, 2H); ^{13}C {^{1}H} NMR (126 MHz, $CDCl_3$, 293 K): δ 133.28, 131.95, 131.90, 130.31 (q, J = 33 Hz), 126.90, 125.48 (q, J = 4 Hz), 124.03 (q, J = 273 Hz), 123.32, 121.66, 90.76, 89.17; HRMS (ASAP): Calcd for $[M]^+$ $C_{15}H_8BrF_3$ 323.9761, found 323.9731.

Preparation of unsymmetrical diarylalkyne 60 (Scheme 2.13)

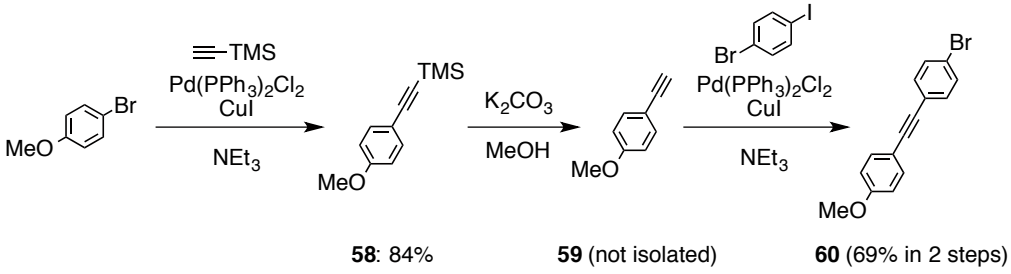

Scheme 2.13 Preparation of unsymmetrical diarylalkyne **60**.

To the solution of *p*-iodoanisole (1.50 g, 6.41 mmol), $Pd(PPh_3)_2Cl_2$ (45 mg, 64 μmol), CuI (11 mg, 64 μmol) in degassed piperidine (6 mL) was added trimethylsilylacetylene (1.02 mL, 7.05 mmol) at rt. Then the solution was stirred for 2 h at 70 ˚C After removal of piperidine in vacuo, the residue was dissolved in Et_2O and washed with water, 5 M aq. HCl, and 10% aq. NH_3. The organic layer was dried over $MgSO_4$ and filtered. Then the solvent was removed in vacuo and Silica-gel column chromatography ($CHCl_3$/Hexane = 1/3) afforded *p*-(trimethylsilylethynyl)anisole **58** (1.08 g, 84%) as yellow oil. To the obtained oil was added K_2CO_3 (0.89 g, 6.4 mmol) and degassed MeOH (8 mL). The mixture was stirred for 1 h at rt, diluted with CH_2Cl_2, and washed with water. The organic layer was dried over $MgSO_4$, filtered, and concentrated to afford yellow oil (0.73 g). The solution of the obtained oil in THF (2 mL) was added dropwise to the solution of *p*-bromoiodobenzene (1.48 g, 5.23 mmol), $Pd(PPh_3)_2Cl_2$ (37 mg, 52 μmol), CuI (10 mg, 52 μmol) in degassed NEt_3 (5 mL). The mixture was stirred for 1.5 h at rt. After removal of the solvent in vacuo, the residue was dissolved in CH_2Cl_2 and washed with water, 5 M aq. HCl, and 10% aq. NH_3. The organic layer was dried over $MgSO_4$ and filtered. Then the solvent was removed in vacuo and recrystalization from CH_2Cl_2 afforded compound **60** (1.18 g, 69% in 2 steps) as a colorless solid.

The spectroscopic data of **60** were in agreement with those reported in the literature.[13]

Preparation of brominated HPB derivative 42 (Scheme 2.14)

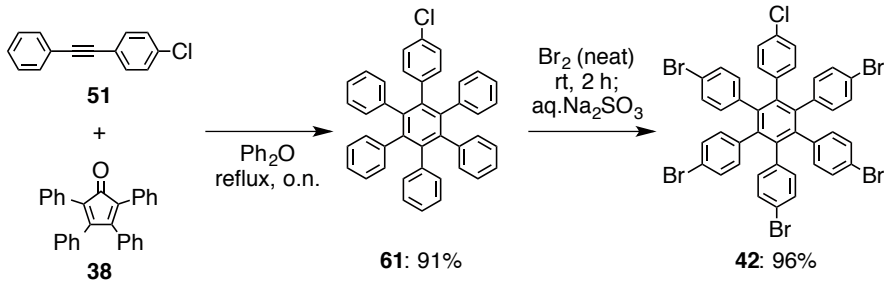

Scheme 2.14 Preparation of brominated HPB derivative **42**.

The mixture of diarylalkyne **51** (1.12 g, 5.27 mmol) and tetracyclone (2.02 g, 5.27 mmol) in Ph_2O (4.5 mL) was refluxed for 3 h. After cooling to rt, the mixture was poured into EtOH (20 mL) at 0 ˚C. The resulting precipitation was filtered and washed with EtOH to afford compound **61** (2.74 g, 91%) as a colorless solid.

m.p. >300 ˚C; ^{1}H NMR (500 MHz, $CDCl_3$, 293 K): δ 6.90-6.80 (m, 27H), 6.76 (d, J = 9.0 Hz, 2H); ^{13}C NMR (126 MHz, $CDCl_3$, 293 K): δ 140.82, 140.63, 140.60, 140.57, 140.46, 140.42, 139.37, 139.14, 132.80, 131.49, 131.47, 131.29, 127.00, 126.94, 126.75, 125.56, 125.41 (17 signals; Three signals were not observed because of overlapping.); HRMS (ASAP): Calcd for $[M+H]^+$ $C_{42}H_{30}Cl$ 569.2036, found 569.2020.

After dropwise addition of bromine (6.0 mL, 0.12 mol) into compound **61** (2.70 g, 4.74 mmol) at 0 ˚C, the mixture was vigorously stirred for 2 h at rt, and then poured into ice-cooled aqueous solution of Na_2SO_3. After stirring overnight, the resulting precipitation was filtered and washed with water, acetone, and CH_2Cl_2 to afford compound **42** (4.39 g, 96%) as a colorless solid.

m.p. >300 ˚C; ^{1}H NMR (500 MHz, $CDCl_3$, 293 K): δ 7.07-7.04 (m, 10H), 6.90 (d, J = 8.5 Hz, 2H), 6.67 (d, J = 8.5 Hz, 2H), 6.63-6.59 (m, 10H); ^{13}C NMR (126 MHz, $CDCl_3$, 293 K): δ 139.78, 139.74, 139.69, 138.59, 138.57, 138.08, 132.70, 132.36, 132.24, 130.59, 130.57, 127.66, 120.48, 120.46 (14 signals; Six signals were not observed because of overlapping.); HRMS (ASAP): Calcd for $[M]^+$ $C_{42}H_{24}{}^{79}Br_5Cl$ 957.7484, found 957.7502.

Preparation of brominated HPB derivatives 41, 43, 44, and 45 (Scheme 2.15)

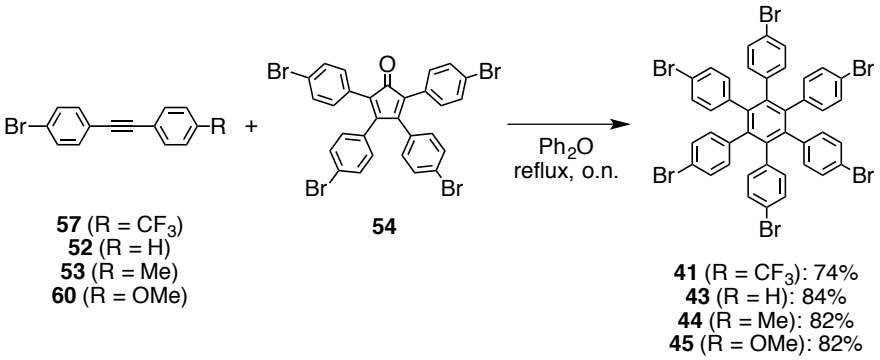

57 (R = CF_3)
52 (R = H)
53 (R = Me)
60 (R = OMe)

54

41 (R = CF_3): 74%
43 (R = H): 84%
44 (R = Me): 82%
45 (R = OMe): 82%

Scheme 2.15 Preparation of the brominated HPB derivatives.

General procedure

The mixture of corresponding diarylalkyne and tetracyclone **54** in Ph_2O was refluxed for 18-24 h. After cooling to rt, the resulting precipitation was filtered and thoroughly washed with Et_2O to afford the target HPB derivative.

HPB derivative 41

The reaction of diarylalkyne **57** (0.409 g, 1.26 mmol) and tetracyclone **54** (0.800 g, 1.14 mmol) in Ph_2O (2 mL) afforded compound **41** as a colorless solid (0.847 g, 74%).

m.p. >300 °C; ^{1}H NMR (500 MHz, $CDCl_3$, 293 K): δ 7.19 (broad d, J = 8.0 Hz, 2H), 7.08-7.05 (m, 6H), 7.04 (d, J = 8.5 Hz, 4H), 6.87 (broad d, J = 8.0 Hz, 2H), 6.64-6.59 (m, 10H); ^{13}C {^{1}H} NMR (126 MHz, $CDCl_3$, 293 K): δ 143.51 (q, J = 1 Hz), 139.99, 139.78, 139.64, 139.57, 138.45, 138.42, 138.32, 132.67, 132.64, 131.42, 130.63, 130.60, 128.35 (q, J = 33Hz), 124.31 (q, J = 4 Hz), 124.06 (q, J = 273 Hz), 120.60, 120.55 (18 signals; Three singlet signals was not observed because of overlapping.); HRMS (ASAP): Calcd for $[M]^+$ $C_{43}H_{24}{}^{79}Br_5F_3$ 991.7747, found 991.7733.

HPB derivative 43

The reaction of diarylalkyne **52** (1.01 g, 3.93 mmol) and tetracyclone **54** (2.50 g, 3.57 mmol) in Ph_2O (5 mL) afforded compound **43** as a colorless solid (2.77 g, 84%).

m.p. >300 ˚C; ^{1}H NMR (500 MHz, $CDCl_3$, 293 K): δ 7.07-7.04 (m, 6H), 7.01 (d, *J* = 8.5 Hz, 4H), 6.92-6.88 (m, 3H), 6.74-6.70 (m, 2H), 6.65-6.60 (m, 10H); ^{13}C NMR (126 MHz, $CDCl_3$, 293 K): δ 141.09, 139.80, 139.49, 139.47, 139.29, 138.89, 138.77, 138.73, 132.81, 132.79, 131.12, 130.54, 130.32, 127.33, 126.15, 120.37, 120.17 (17 signals; Three signals were not observed because of overlapping.); HRMS (AP): Calcd for $[M]^+$ $C_{42}H_{25}{}^{79}Br_3{}^{81}Br_2$ 927.7873, found 927.7861.

HPB derivative 44

The reaction of diarylalkyne **53** (0.895 g, 3.30 mmol) and tetracyclone **54** (2.10 g, 3.00 mmol) in Ph_2O (4.5 mL) afforded compound **44** as a colorless solid (2.33 g, 82%).

m.p. >300 ˚C; ^{1}H NMR (500 MHz, $CDCl_3$, 293 K): δ 7.06-7.03 (m, 6H), 7.02 (d, *J* = 8.5 Hz, 4H), 6.70 (d, *J* = 8.0 Hz, 2H), 6.64-6.60 (m, 10H), 6.59 (d, *J* = 8.0 Hz, 2H), 2.14 (s, 3H); ^{13}C NMR (126 MHz, $CDCl_3$, 293 K): δ 141.10, 139.90, 139.44, 139.10, 139.05, 138.87, 138.80, 136.34, 135.61, 132.83, 132.81, 132.79, 130.95, 130.52, 130.50, 130.30, 128.08, 120.33, 120.31, 120.09, 21.25; HRMS (AP): Calcd for $[M]^+$ $C_{43}H_{27}{}^{79}Br_2{}^{81}Br_3$ 943.7952, found 943.7944.

HPB derivative 45

The reaction of diarylalkyne **60** (0.345 g, 1.20 mmol) and tetracyclone **54** (0.700 g, 1.00 mmol) in Ph_2O (1.5 mL) afforded compound **45** as a pale yellow solid (0.784 g, 82%).

m.p. >300 ˚C; ^{1}H NMR (500 MHz, $CDCl_3$, 293 K): δ 7.07-7.02 (m, 10H), 6.64-6.60 (m, 12H), 6.45 (d, *J* = 9.0 Hz, 2H), 3.66 (s, 3H); ^{13}C NMR (126 MHz, $CDCl_3$, 293 K): δ 157.65, 140.74, 140.07, 139.46, 139.12, 139.08, 138.87, 138.80, 132.84, 132.80, 132.79, 132.19, 131.76, 130.51, 130.38, 120.34, 120.32, 120.09, 112.83, 55.13 (20 signals; One signal was not observed because of overlapping.); HRMS (ASAP): Calcd for $[M+H]^+$ $C_{42}H_{28}{}^{79}Br_3{}^{81}Br_2$ 958.8057, found 958.8044.

Attempted alternate trilithiation of compounds 41-45 (Scheme 2.11)

To the suspension of brominated HPB derivative (0.150-0.300 g) in THF (HPB derivative 0.1 g/THF 1 mL) was added the freshly titrated pentane solution of *t*-BuLi (6 eq) at –98 ˚C. After removal of the cooling bath, the reaction mixture was stirred for 30 min. Then the reaction was quenched by the addition of TMSCl (6 eq) at –98 ˚C. After the addition of aq. NH_4Cl and $CHCl_3$, the organic layer was analyzed with ^1H NMR measurements. In the case of compound **41** and **42**, the organic layer was separated, dried over $MgSO_4$, and filtered. Then the solvent was removed in vacuo and recrystallization from $CHCl_3$/EtOH afforded compound **46** or **47** (For **46**, 57%; For **47**, 45%) as a colorless solid.

46: m.p. 285-288 ˚C; ^1H NMR (500 MHz, $CDCl_3$, 293 K): δ 7.06 (broad d, *J* = 8.0 Hz, 2H), 7.04 (d, *J* = 8.0 Hz, 2H), 7.01 (d, *J* = 8.5 Hz, 4H), 6.97 (d, *J* = 8.5 Hz, 4H), 6.85 (broad d, *J* = 8.0 Hz, 2H), 6.74-6.70 (m, 6H), 6.65 (d, *J* = 8.5 Hz, 4H), 0.14 (s, 9H), 0.11 (s, 18H); $^{13}C\{^1H\}$ NMR (126 MHz, $CDCl_3$, 293 K): δ 144.42 (q, *J* = 2 Hz), 140.94, 140.58, 140.20, 140.07, 139.53, 139.35, 139.27, 137.87, 137.76, 133.03, 132.06, 132.02, 131.62, 130.62, 130.58, 129.97, 127.44 (q, *J* = 33Hz), 124.29 (q, *J* = 273 Hz), 123.57 (q, *J* = 4 Hz), 119.72, –1.05, –1.15; HRMS (ASAP): Calcd for $[M]^+$ $C_{52}H_{51}{}^{79}Br_2F_3Si_3$ 974.1617, found 974.1622.

47: m.p. >300 ˚C; ^1H NMR (500 MHz, $CDCl_3$, 293 K): δ 7.05-7.01 (m, 6H), 6.95 (d, *J* = 8.5 Hz, 4H), 6.80 (d, *J* = 8.5 Hz, 2H), 6.73-6.70 (m, 6H), 6.68 (d, *J* = 8.5 Hz, 2H), 6.63 (d, *J* = 8.5 Hz, 4H), 0.14 (s, 9H), 0.13 (s, 18H); ^{13}C NMR (126 MHz, $CDCl_3$, 293 K): δ 140.72, 140.63, 140.32, 140.31, 139.43, 139.39, 138.92, 137.66, 137.64, 133.04, 132.69, 132.01, 131.35, 130.64, 129.89, 126.96, 119.60, –1.05 (18 signals; Four signals were not observed because of overlapping.); HRMS (ASAP): Calcd for $[M]^+$ $C_{51}H_{51}{}^{79}Br_2ClSi_3$ 940.1354, found 940.1346.

References

[1] R. Rathore, C. L. Burns, I. A. Guzei, *J. Org. Chem.* **2004**, *69*, 1524.

[2] The ^{1}H NMR spectra of the partially brominated HPB derivatives are shown in Chapter 4.

[3] Winkler, H. J. S.; Winkler, H. *J. Am. Chem. Soc.* **1966**, *88*, 964.

[4] (a) Bunnett, J. *Acc. Chem. Res.* **1972**, *5*, 139. (b) Schnürch, M.; Spina, M.; Khan, A. F.; Mihovilovic, M. D.; Stanetty, P. *Chem. Soc. Rev.* **2007**, *36*, 1046. (c) Schlosser, M. *Angew. Chem., Int. Ed.* **2005**, *44*, 376.

[5] For example, see: Waldmann, C.; Schober, O.; Haufe, G.; Kopka, K. *Org. Lett.* **2013**, *15*, 2954.

[6] A solubility-controlled overlithiation followed by the halogen dance was once proposed on monolithiation of 2,6-dibromopyridine. See: Cai, D.; Hughes, D. L.; Verhoeven, T. R. *Tetrahedron Lett.* **1996**, *37*, 2537.

[7] (a) Johnson, J. R.; Grummitt, O. *Org. Synth. Coll. 3*, 806; **1943**, *23*, 92. (b) Fieser, L. F. *Org. Synth. Coll. 5*, 604; **1966**, *46*, 44. (c) Rathore, R.; Burns, C. L. *Org. Synth.* **2005**, *82*, 30.

[8] See Experimental Section.

[9] Belger, C.; Plietker, B. *Chem. Commun*. **2012**, *48*, 5419.

[10] Karastatiris, P.; Mikroyannidis, J. A.; Spiliopoulos, I. K. *Macromolecules* **2004**, *37*, 7867.

[11] Liang, B.; Dai, M.; Chen, J.; Yang, Z. *J. Org. Chem.* **2005**, *70*, 391.

[12] Vives, G.; Rapenne, G. *Tetrahedron* **2008**, *64*, 11462.

[13] Shao, G.; Orita, A.; Nishijima, K.; Ishimaru, K.; Takezaki, M.; Wakamatsu, K.; Gleiter, R.; Otera, J. *Chem. Asian J.* **2007**, *2*, 489.

Chapter 3

Selective Alternate Trilithiation of the Hexaphenylbenzene Framework with Additional Bromoarenes as a Lithiation Mediator

3.1 Introduction

In the previous Chapter, the author has developed a new synthetic protocol for the selective alternate trilithiation of the HPB framework through a thermodynamically controlled halogen dance. This protocol did not only achieve the selective and efficient preparation of alternately functionalized C_3-symmetric HPB derivatives, but also afforded the lower-symmetric HPB derivatives with the precursors where the one Br substituent of compound **27** was replaced by another substituent. However, the selectivity significantly depended on the kinds of newly introduced substituent and the applicable scope was restricted. In this Chapter, the author describes an improved protocol for the selective alternate derivatization of a broader range of HPB derivative with additional bromoarenes as a lithiation mediator on the basis of the consideration of the effects of lithiating reagents.

3.2 Effects of lithiating reagents for the selective alternate trilithiation

In the detailed analysis of the reaction mechanism of the selective alternate trilithiation of the HPB framework in the previous Chapter, it was revealed that the success is based on the exquisite balance of the kinetics of several independent processes. Especially, the slow dissolution of the precipitated starting material was essential. If the dissolution is faster than or competes with the elimination reaction between *t*-BuBr and *t*-BuLi, the system should be "overlithiated" and the alternately trilithiated species could not be obtained as the main product. On the other hand, if the dissolution of the starting material is too slow, a new independent process, the decomposition of *t*-BuLi in THF, should be involved in the overall reaction during the warming process owing to the intrinsic reactivity of *t*-BuLi with THF (Scheme 3.1).[1,2] Then the lithiation of the three equivalents of the HPB frameworks cannot be completed in the lithiation phase and the system reaches an undesired equilibrium, where the averaged equivalent of Li on the HPB framework is less than three. Actually, in the previous Chapter, the slower dissolution of the precipitated starting material was observed when the reaction did not selectively afford the target alternately functionalized HPB derivative. The simplest approach to resolve this problem is just the use of a larger amount of THF solvent.

Unfortunately, this approach was not so effective for the selective alternate trilithiation of compound **44** (Scheme 3.2, Figure 3.1). The excessive dilution could have the negative effect on the subsequent halogen dance between the HPB frameworks. Another approach is the use of a larger amount of *t*-BuLi in consideration of its decomposition. However, this approach requires the elaborated optimization of the equivalent of *t*-BuLi because the lithiation of exactly three equivalents of the HPB frameworks is crucial. The optimization for each substrate is not practical. On the basis of the above discussion, the use of lithiating reagents that is more stable in THF than *t*-BuLi is most promising to achieve the selective alternate trilithiation of hardly soluble HPB derivatives such as compound **44**.

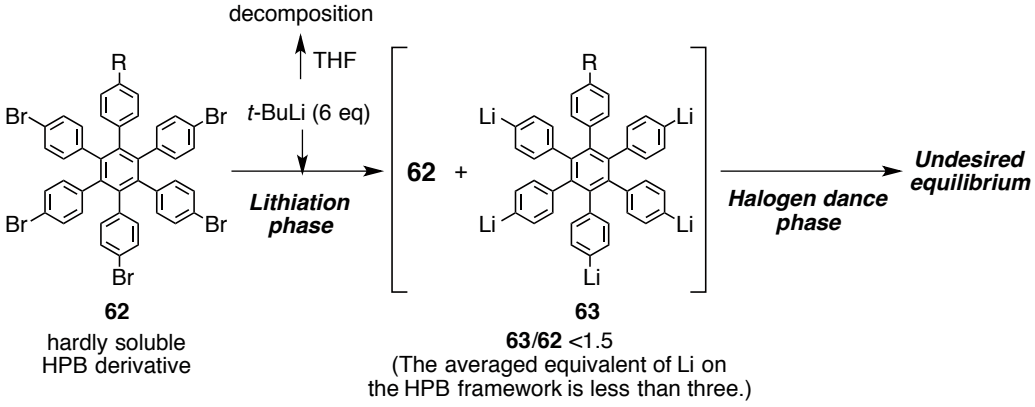

Scheme 3.1 Schematic representation of the problem of the alternate trilithiation of a hardly soluble HPB derivative.

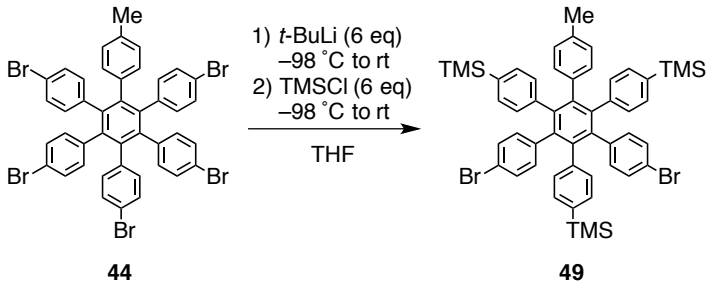

Scheme 3.2 Attempted alternate trilithiation of compound **44** with a larger amount of THF.

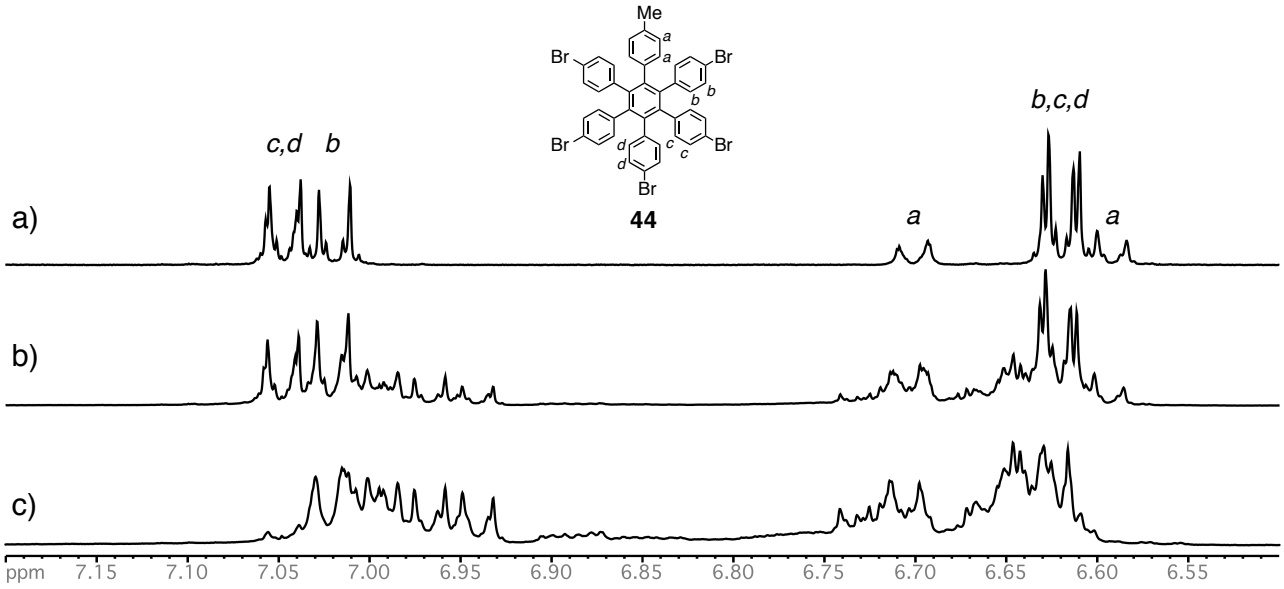

Figure 3.1 a) Partial ^{1}H NMR spectra (500 MHz, $CDCl_3$) of compound **44**. Partial ^{1}H NMR spectra (500 MHz, $CDCl_3$) of the crude mixture obtained in the attempted alternate trilithiation of compound **44** with the different ratio of compound **44** and the amount of THF solvent (compound **44**/THF): b) 0.20 g/2 mL, c) 0.10 g/5 mL.

One of the possible candidates for the alternative lithiating reagent among general reagents was *n*-BuLi. It is well recognized that *n*-BuLi possesses an ability to completely lithiate bromoarenes through the Br/Li exchange reaction on the basis of the thermodynamic instability of alkyllithiums compared with aryllithiums. Furthermore, *n*-BuLi is more stable in THF than *t*-BuLi.[1] However, the attempted alternate trilithiation of compound **27** with 3 eq of *n*-BuLi was hampered by the inevitable substitution reaction between the resulting organolithiums and *n*-BuBr during the warming process, which is necessary to complete the dissolution of the starting material and the halogen dance.

Another potential alternative reagent to *t*-BuLi, PhLi, resulted in the much lower selectivity when 3 eq of PhLi was used for the trilithiation of compound **27** (Scheme 3.3, Figure 3.2). The similar crude product was obtained even in the prolonged reaction time and this crude product should be derived from the equilibrium mixture. This result is quite rational in consideration of the difference of the stability between PhLi and the lithiophenyl group on the HPB framework. There should not be so a large energetic difference

because both of them are aryllithiums. Therefore, the distribution of Li was not biased onto the HPB framework and the equivalent of Li on the HPB framework was less than three at the equilibration (Scheme 3.4). Although the use of a larger amount of PhLi could shift the equilibrium and load a larger equivalent of Li on the HPB framework, the elaborated optimization of the equivalent of PhLi is neither a practical nor a general way.

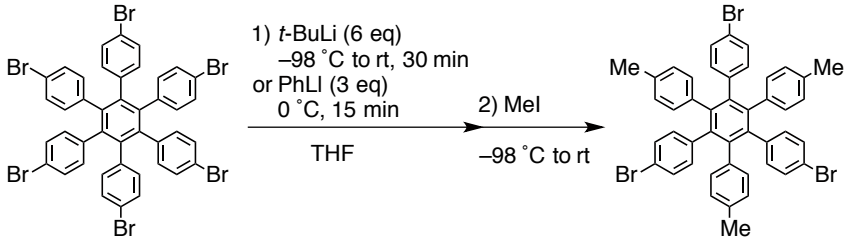

Scheme 3.3 Comparison of the effects of the lithiating reagents for the alternate trilthiation of compound **27**.

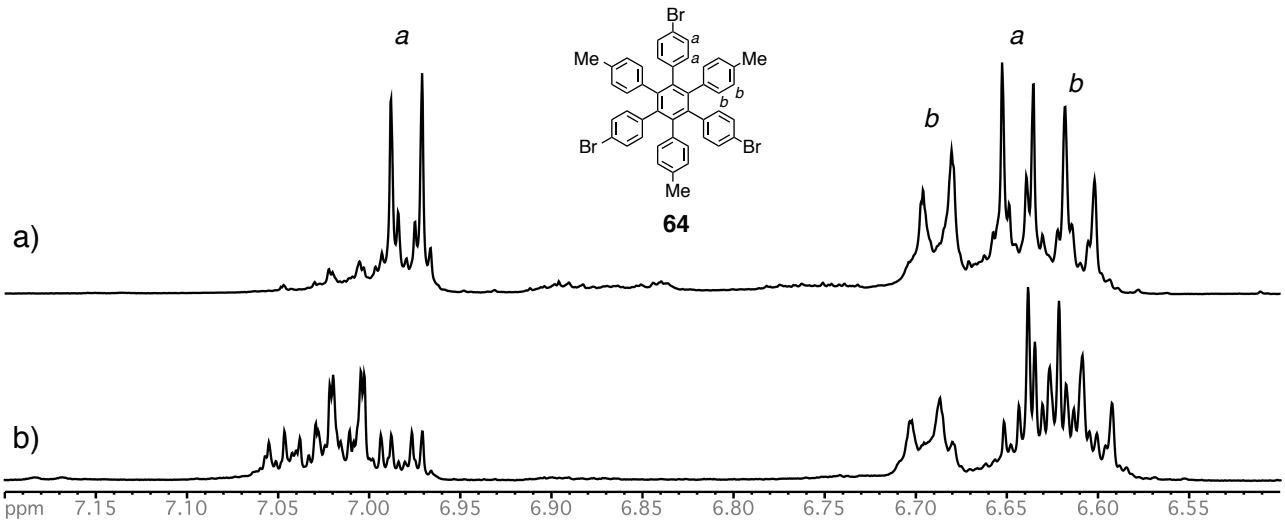

Figure 3.2 Partial ^{1}H NMR spectra (500 MHz, $CDCl_3$) of the crude mixture obtained in the attempted alternate trilithiation of compound **27** with a) *t*-BuLi (6 eq), b) PhLi (3 eq).

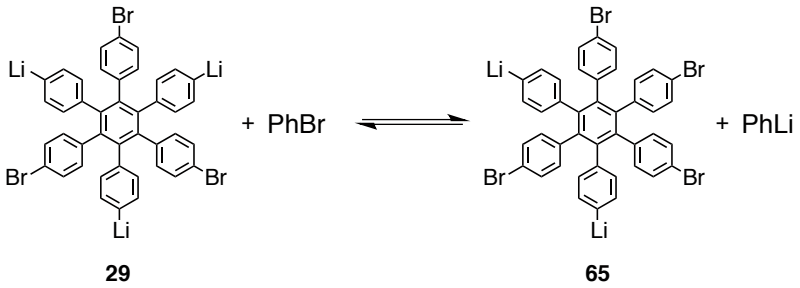

29 **65**

Scheme 3.4 Schematic representation of one of the possible equilibrium schemes between the partially lithiated HPB derivative such as **29** and PhLi.

The results with *n*-BuLi and PhLi indicated the necessity of new organolithiums as the lithiating reagent satisfying the following conditions: (1) the new organolithium should be much more stable in THF than *t*-BuLi. (2) The new organolithium should be thermodynamically much less stable than the lithiophenyl group on the HPB framework. (3) The byproduct of the Br/Li exchange (organobromine compounds) should be inert in the reaction mixture.

3.3 Substituent effects on the thermodynamic stability of aryllithiums

On the basis of the first and the third criteria of the new lithiating reagents in the previous Section, aryllithiums seem better than alkyllithiums because aryllithiums are generally more stable in ethereal solvents than alkyllithiums and because the resulting bromoarenes after the Br/Li exchange are less reactive in the presence of aryllithiums than bromoalkanes such as *t*-BuBr and *n*-BuBr. However, PhLi itself was too stable in the ArBr/ArLi exchange equilibration to completely lithiate the bromophenyl groups on the HPB framework as shown in the previous Section. Thermodynamically much less stable aryllithiums are attractive candidates for the new lithiating reagents.

A facile but versatile way to tune the thermodynamic stability of aryllithiums is the introduction of some substituents. The substituent effects on the thermodynamic stability of aryllithium were recently pursued by Schlosser et al. from the viewpoint of the electronic influence.[3] They mixed the different kinds

of aryllithiums and bromoarenes and monitored the composition of the mixture (Scheme 3.5). They proposed that the proximal σ-polarization and the distal σ/π polarization are the key operative factors to determine the stability of aryllithiums (Figure 3.3). In the former, the increased electron density in the σ-framework of the lithiated carbon is reduced by the polarization through the σ-bonds. In the latter, the increased electron density in the σ-framework is reduced by the polarization of the π-cloud. It was experimentally confirmed that the electron-withdrawing substituents such as F, Cl, CF_3, and OCF_3 at any position can thermodynamically stabilize the aryllithium in THF. On the other hand, OMe substituent stabilizes the aryllithium when it is located at the *ortho*-position to the Li moiety, but destabilizes the aryllithium when at the *para*-position. This difference is easily acceptable in the qualitative consideration of the high electronegativity and the electron-donating nature of oxygen. These reported substituent effects implied that the strong electron-donating groups should significantly destabilize aryllithiums. Although the effects of the electron-donating substituents have not been investigated directly, the good correlation has been confirmed between the thermodynamic substituent effects on aryllithiums and the kinetic substituent effects on bromoarenes in the almost irreversible Mg/Br exchange reaction with *i*-PrMgCl·LiCl reported by Mayr et al. (Scheme 3.6).[4] The more stable the substituent makes aryllithiums, the more reactive the substituent makes bromoarenes. Mayr et al. experimentally investigated a much broader range of substituent including electron-donating groups and confirmed that electron-donating groups certainly make bromoarenes less reactive. This observation also suggested the thermodynamic destabilization effects of electron-donating groups on aryllthiums.

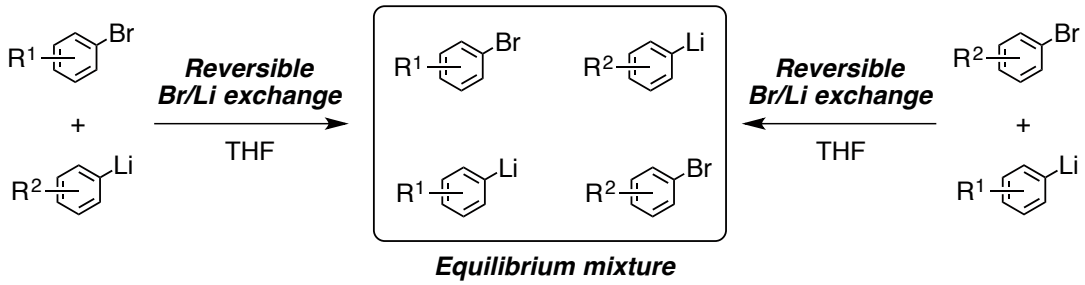

Scheme 3.5 Experimental study of the substituent effects on the thermodynamic stability of aryllithiums by Schlosser et al.

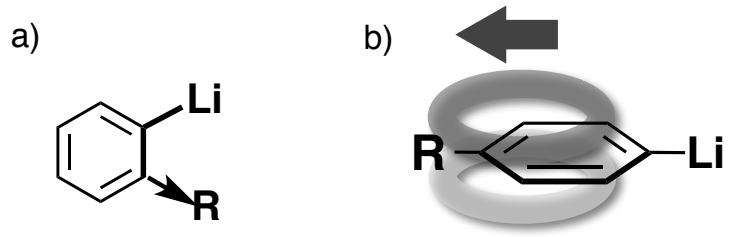

Figure 3.3 Two stabilizing effects of the substituent on the Li moiety of aryllithiums: a) σ-polarization, b) σ/π polarization.

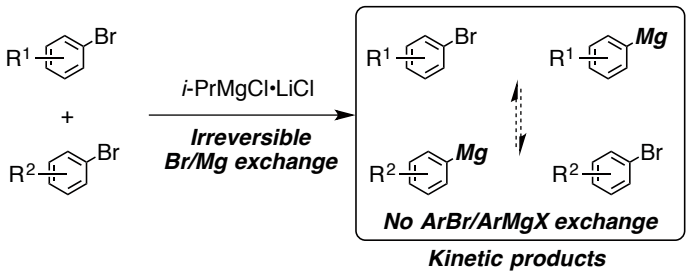

Scheme 3.6 Experimental study of the substituent effects on the kinetic reactivity of bromoarenes by Mayr et al.

3.4 Selective alternate trilithiation of the HPB framework with additional bromoarenes as a lithiation mediator

The author chose two organolithiums, mesityllithium (MesLi) and *p*-(dimethylamino)phenyllithium (MapLi), as the candidates for the new lithiating reagents. The discussion in the previous Section suggested that the corporation of the three moderately electron-donating Me groups or the strongly electron-donating *p*-NMe_2 group should diminish the thermodynamic stability of the aryllithium. The thermodynamic stability of MesLi should also be diminished by the ineffective solvation of THF because of the steric hindrance of the two *ortho*-Me groups. The resulting byproducts after the Br/Li exchange reaction, bromomesitylene (MesBr) and *p*-bromo-*N,N*-dimethylaniline (MapBr), are expected to be inert in the reaction mixture except the Br/Li exchange reaction. While the thermodynamic instability of MesLi and MapLi in the equilibration among aryllithiums was once implied sixty years ago,[5] they have

never been employed as the lithiating reagent in the Br/Li exchange reactions. In fact, MesLi has been even featured as the useful organolithium base that does not react with bromoarenes through the Br/Li exchange reaction (Scheme 3.7).[6] The author ascribed the reported inertness of MesLi in the Br/Li exchange reaction to the low reaction temperature (–78 ˚C). Recently, MesLi has been utilized for the I/Li exchange reaction of the iodoarenes bearing a nucleophilic functional group.[7] The representative example with the substrate bearing the highly nucleophilic α-keto ester moiety is shown below (Scheme 3.8). However, the driving force for the selective generation of the new functionalized aryllithiums has never been discussed in spite of the I/Li exchange reaction between the aryllithium and the iodoarene. MapLi has never been employed as a lithiating reagent as far as the author knows.

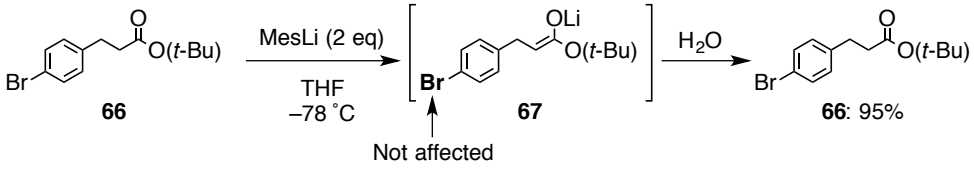

Scheme 3.7 Reported example of the inertness of MesLi in the Br/Li exchange reaction.

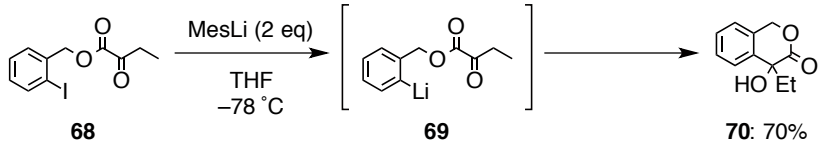

Scheme 3.8 Example of the I/Li exchange reaction between MesLi and iodoarene **68**.

The author checked the effectiveness of the new lithiating reagents for the selective alternate trilithiation of the HPB framework. The author added 6.0 eq of *t*-BuLi into the suspension of compound **27** in THF at –98 ˚C in the presence of 2.8 eq of MesBr or MapBr (Scheme 3.9). Whereas most of compound **27** is precipitated under these conditions, MesBr or MapBr possesses a sufficient solubility and is expected to be able to react with *t*-BuLi almost selectively. This expectation was confirmed by the rapid quenching of the reaction in the presence of MesBr (Figure 3.4). While the initial lithiation phase had been completed in the absence of MesBr in 2.5 min, most of compound **27** remained unlithiated in the presence of MesBr. This difference is due to the selective consumption of *t*-BuLi by MesBr. The *in situ* preparation of MesLi or

MapLi is quite practical because of avoiding the tedious handling of reactive organolithiums. Slightly less than 3 eq of MesBr and MapBr were employed in consideration of the trace amount of dissolved compound **27**, which were able to be directly lithiated by *t*-BuLi. After quenching with TMSCl and work-up, both the reactions afforded the crude mixture of compound **30** and the used bromoarene (MesBr or MapBr) as the main components.[8] In the case of MapBr, removal of the residual MapBr is possible just by acid washing. Compound **30** was isolated after recrystallization in 66% and 63% yields, which were almost identical with that without the additional bromoarenes (67%). This result indicates that all the three equivalents of Li in the system are distributed selectively on the HPB framework at the equilibration after the halogen dance. It also confirms experimentally the thermodynamic instability of MesLi or MapLi, with which the reaction can reach the desired equilibrium mixture that contained alternately trilithiated species **29** as the main component in contrast with that with PhLi as the lithiating reagent. The importance of the kinds of additional bromoarenes was demonstrated in the control experiments in the presence of bromobenzene or *p*-bromobenzotrifluoride (Figure 3.5).

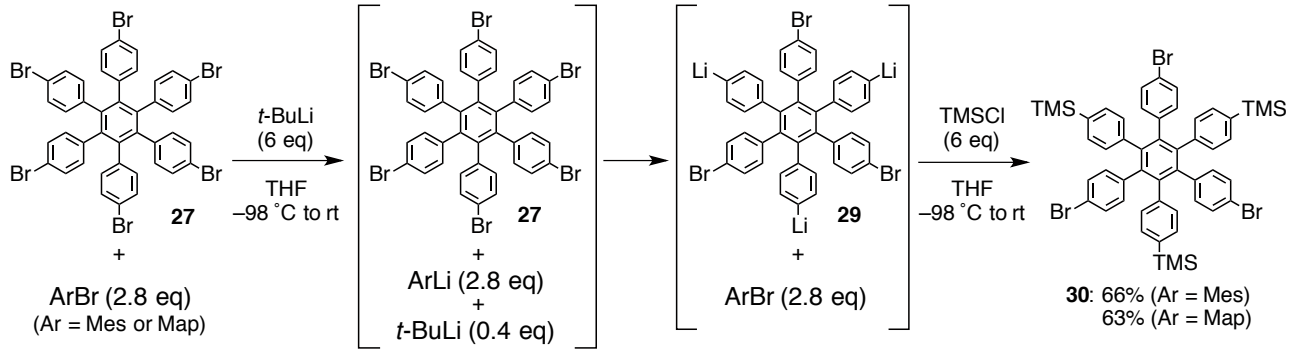

Scheme 3.9 Selective alternate trilithiation of compound **27** in the presence of MesBr or MapBr.

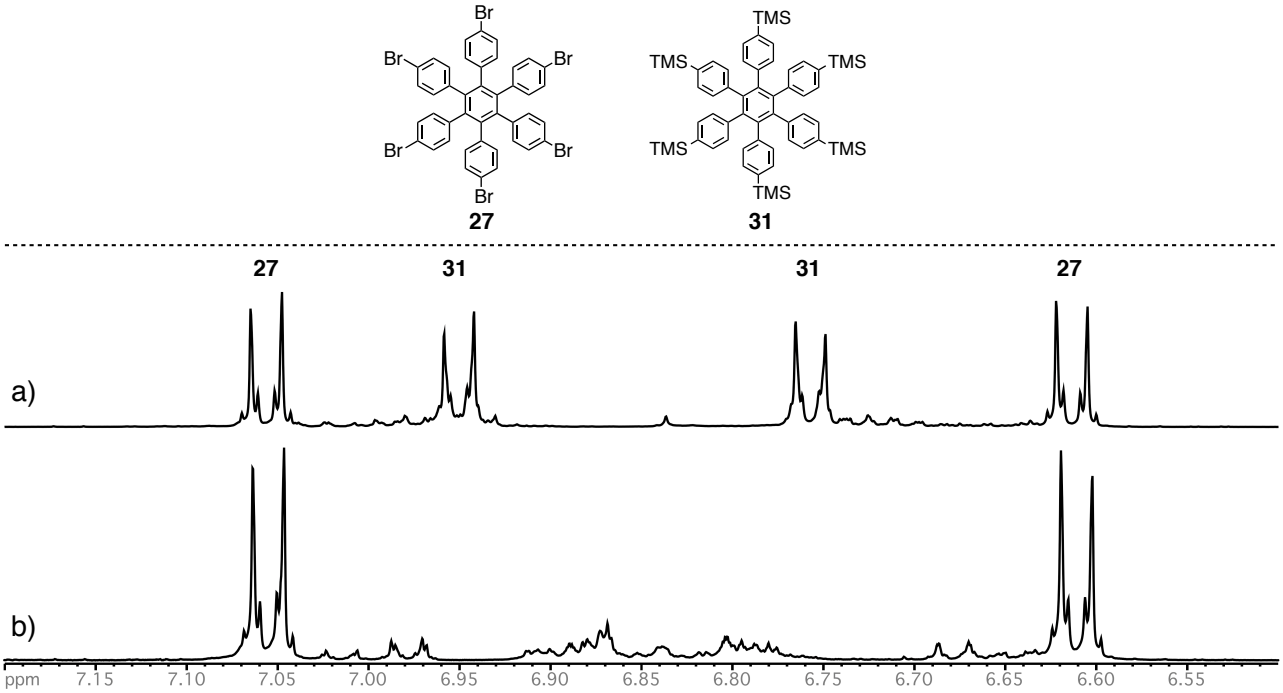

Figure 3.4 Partial ^{1}H NMR spectra (500 MHz, $CDCl_3$) of the crude mixture obtained by quenching with TMSCl 2.5 min after removal of the cooling bath a) in the absence of MesBr, b) in the presence of MesBr.

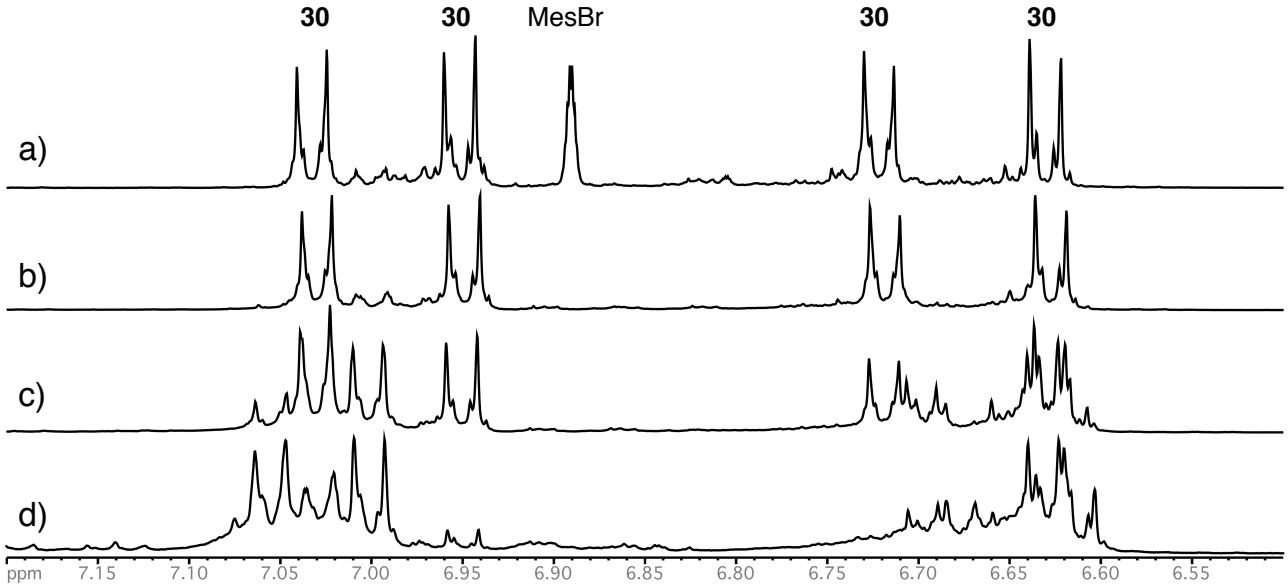

Figure 3.5 Partial ^{1}H NMR spectra (500 MHz, $CDCl_3$) of the crude mixture obtained with various kinds of additional bromoarenes: a) MesBr, b) MapBr, c) PhBr, d) *p*-$CF_3C_6H_4Br$.

The different reaction processes in the selective alternate trilithiation of the HPB framework in the presence of an additional bromoarene (MesBr or MapBr) is summarized in Figure 3.6. The additional bromoarene relays the strong lithiating ability of *t*-BuLi before its decomposition in THF and can be regarded as a lithiation mediator. Avoiding the decomposition of *t*-BuLi in THF, this mediator juggles the two different Br/Li exchange reactions: the Br/Li exchange reaction with *t*-BuLi at the low temperature and the Br/Li exchange reaction with compound **27** at the relatively high temperature.

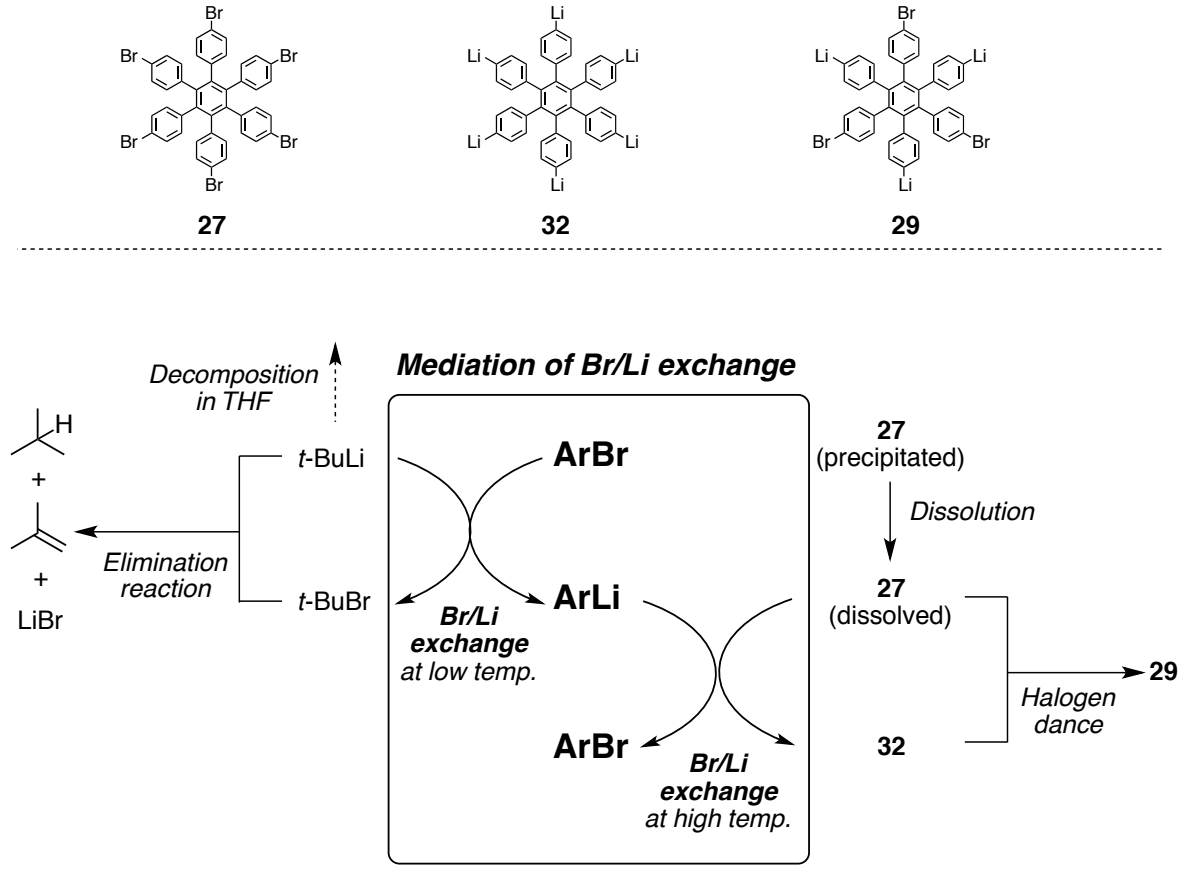

Figure 3.6 Different reaction processes in the selective alternate trilithiation in the presence of an additional bromoarene (Ar = Mes or Map).

3.5 Selective alternate trilithiation of the low-symmetric HPB framework in the presence of MesBr

On the basis of the success of the selective alternate trilithiation of compound **27** in the presence of an additional bromoarene as a lithiation mediator, the author subjected compounds **43**, **44**, and **45**, of which the attempted alternate trilithiation failed in the previous Chapter, to the new conditions (Scheme 3.10). All the reactions exhibited the high alternate selectivity, and the alternately functionalized products were isolated in 54%, 67%, and 60% yields after recrystallization. Three new C_{2v}-symmetric HPB derivatives **48**, **49**, and **50** were characterized by ^{1}H and ^{13}C NMR based on their symmetry. The effects of the presence of MesBr are demonstrated by the comparison of the ^{1}H NMR spectra of the crude product in Figure 3.7. The success is due to the mediation of the lithiating ability of *t*-BuLi by MesBr to compensate the quite slow dissolution of compounds **43**, **44**, and **45**. It should be again emphasized that the selective alternate trilithiation of compound **44** succeeded neither when the reaction was performed with a larger amount of THF solvent nor when the reaction was performed at –43 ˚C for more than 3 h followed by the warming process. The use of MesBr as a lithiation mediator was essential.

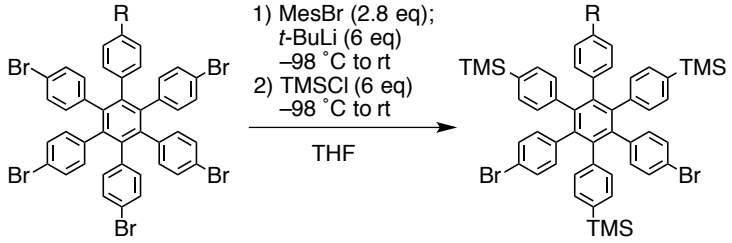

43 (R = H)
44 (R = Me)
45 (R = OMe)

48 (R = H): 54%
49 (R = Me): 67%
50 (R = OMe): 60%

Scheme 3.10 Selective alternate trilithiation of compounds **43**, **44**, and **45** in the presence of MesBr as a lithiation mediator.

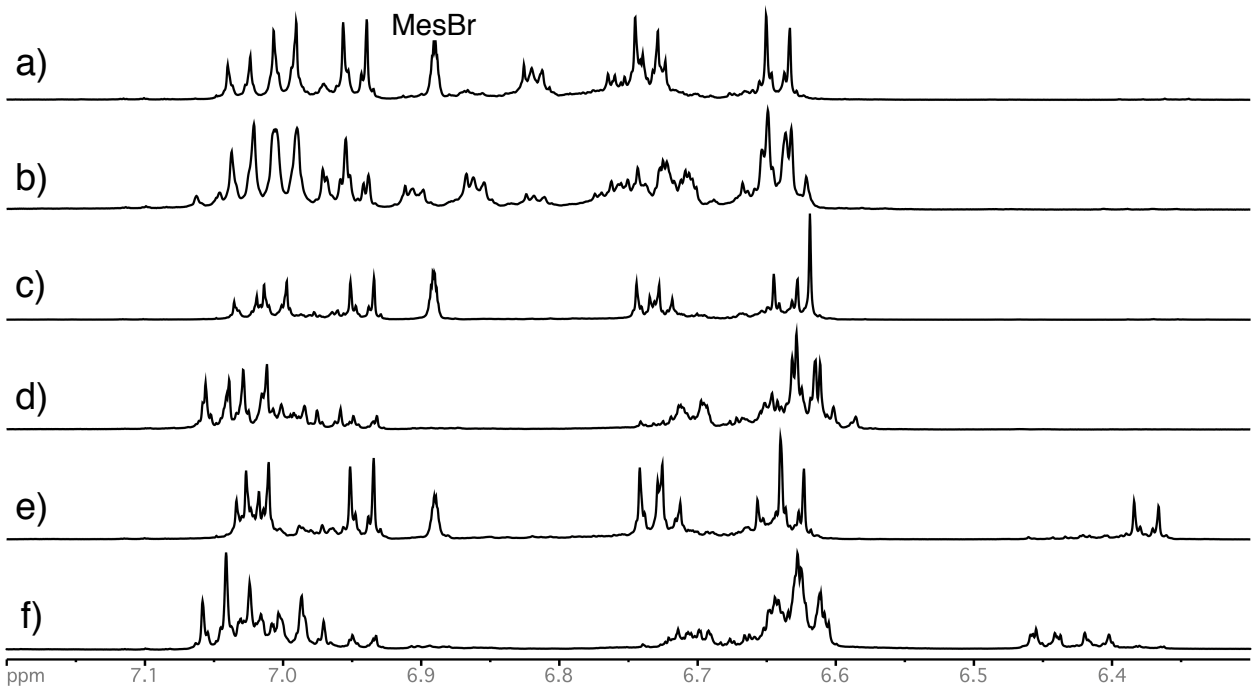

Figure 3.7 Partial ^{1}H NMR spectra of the crude mixture of the attempted alternate trilithiation of compounds **43**, **44**, and **45**: a) **43** in the presence of MesBr, b) **43** in the absence of MesBr, c) **44** in the presence of MesBr, d) **44** in the absence of MesBr, e) **45** in the presence of MesBr, f) **45** in the absence of MesBr.

3.6 Conclusion

In this Chapter, the author developed the improved method for the selective alternate trilithiation of HPB derivatives utilizing additional bromoarenes as lithiation mediators. With this new protocol, the author succeeded in the expansion of the applicable scope of the selective alternate derivatization of the HPB frameworks. The problem of the solubility is quite general in the derivatization of polyhalogenated π-conjugated frameworks,[9] and this new lithiation protocol with a lithiation mediator is promising for the derivatization of the broad range of hardly soluble π-conjugated molecules.

Experimental Section

Comparison of the effect of the lithiating reagents for alternate trilithiation of compound 27

To the suspension of compound **27** (0.200 g, 0.198 mmol) in THF (2 mL) was added the hexane solution of *n*-BuLi (1.65 M, 0.360 mL, 0.594 mmol) at –98 ˚C, the pentane solution of *t*-BuLi (1.68 M, 0.708 mL, 1.19 mmol) at –98 ˚C, or the diethyl ether and cyclohexane solution of PhLi (1.07 M, 0.556 mL, 0.594 mmol) at 0 ˚C. After removal of the cooling bath (for *n*-BuLi and *t*-BuLi), the reaction mixture was stirred for various times, and then quenched by the addition of MeI (0.20 mL) at –98 ˚C. After the addition of water and $CHCl_3$, the organic layer was monitored by ^1H NMR spectroscopy.

Selective alternate trilithiation of compound 27 in the presence of MesBr

To the suspension of compound **27** (0.200 g, 0.198 mmol) and MesBr (84 μL, 0.55 mmol) in THF (2 mL) was added the freshly titrated pentane solution of *t*-BuLi (1.68 M, 0.708 mL, 1.19 mmol) at –98 ˚C. After removal of the cooling bath, the reaction mixture was stirred for 30 min, and then quenched by the addition of TMSCl (0.151 mL, 1.19 mmol) at –98 ˚C. After the addition of water and $CHCl_3$, the organic layer was separated, dried over $MgSO_4$, and filtered. Then the solvent was removed in vacuo and recrystallization from $CHCl_3$/EtOH afforded compound **30** (0.129 g, 66%) as a colorless solid.

Selective alternate trilithiation of compound 27 in the presence of MapBr

To the suspension of compound **27** (0.200 g, 0.198 mmol) and MapBr (0.111 g, 0.555 mmol) in THF (2 mL) was added the freshly titrated pentane solution of *t*-BuLi (1.68 M, 0.708 mL, 1.19 mmol) at –98 ˚C. After removal of the cooling bath, the reaction mixture was stirred for 30 min, and then quenched by the addition of TMSCl (0.151 mL, 1.19 mmol) at –98 ˚C. After the addition of water and $CHCl_3$, the organic layer was separated, washed twice with aq.HCl (1 M), dried over $MgSO_4$, and filtered. Then the solvent was removed in vacuo and recrystallization from $CHCl_3$/EtOH afforded compound **30** (0.124 g, 63%) as a colorless solid.

Preparation of HPB derivatives 48, 49, and 50

To the suspension of brominated HPB derivative **43**, **44**, or **45** (0.150 g) and MesBr (2.8 eq) in THF (1.5 mL) was added the freshly titrated pentane solution of *t*-BuLi (1.68 M, 6 eq) at –98 ˚C. After removal of the cooling bath, the reaction mixture was stirred for 30-40 min. Then the reaction was quenched by the addition of TMSCl (6 eq) at –98 ˚C. After the addition of aq. NH_4Cl and $CHCl_3$, the organic layer was separated, dried over $MgSO_4$, and filtered. Then the solvent was removed in vacuo and recrystallization from $CHCl_3$/EtOH afforded compound **48**, **49**, or **50** (**48**: 80 mg, 54%, **49**: 98 mg, 67%, **50**: 88 mg, 60%) as a colorless solid.

48: m.p. 296-299 ˚C; ^{1}H NMR (500 MHz, $CDCl_3$, 293 K): δ 7.03 (d, *J* = 8.2 Hz, 2H), 7.00 (d, *J* = 8.2 Hz, 4H), 6.95 (d, *J* = 8.6 Hz, 4H), 6.84-6.80 (m, 3H), 6.77-6.74 (m, 2H), 6.73 (d, *J* = 8.2 Hz, 4H), 6.73 (d, *J* = 8.2 Hz, 2H), 6.64 (d, *J* = 8.6 Hz, 4H), 0.14 (s, 9H), 0.11 (s, 18H); ^{13}C{^{1}H} NMR (126 MHz, $CDCl_3$, 293 K): δ 140.75, 140.70, 140.64, 140.49, 140.29, 140.26, 139.65, 139.24, 137.52, 137.21, 133.13, 131.99, 131.81, 131.45, 130.73, 129.84, 126.69, 125.31, 119.50, –1.03, –1.06 (21 signals; One signal in an aromatic region was not observed because of overlapping.); HRMS (ASAP): Calcd for $[M]^+$ $C_{51}H_{52}{}^{79}Br_2Si_3$ 906.1744, found 906.1756.

49: m.p. >300 ˚C; ^{1}H NMR (500 MHz, $CDCl_3$, 293 K): δ 7.02 (d, *J* = 8.2 Hz, 2H), 7.00 (d, *J* = 8.2 Hz, 4H), 6.94 (d, *J* = 8.6 Hz, 4H), 6.73 (d, *J* = 8.2 Hz, 4H), 6.72 (d, *J* = 8.2 Hz, 2H), 6.63 (d, *J* = 8.6 Hz, 4H), 6.62 (s, 4H), 2.08 (s, 3H) 0.14 (s, 9H), 0.12 (s, 18H); ^{13}C{^{1}H} NMR (126 MHz, $CDCl_3$, 293 K): δ 140.85, 140.80, 140.71, 140.54, 140.08, 139.72, 139.19, 137.46, 137.16, 137.07, 134.57, 133.13, 131.97, 131.78, 131.29, 130.74, 129.81, 127.38, 119.45, 21.08, –1.04 (21 signals; One signal in an aromatic region and one signal from TMS group were not observed because of overlapping.); HRMS (ASAP): Calcd for $[M]^+$ $C_{52}H_{54}{}^{79}Br_2Si_3$ 920.1900, found 920.1909.

50: m.p. 286-289 ˚C; ^{1}H NMR (500 MHz, $CDCl_3$, 293 K): δ 7.02 (d, *J* = 8.2 Hz, 2H), 7.02 (d, *J* = 8.2 Hz, 4H), 6.94 (d, *J* = 8.5 Hz, 4H), 6.73 (d, *J* = 8.2 Hz, 4H), 6.72 (d, *J* = 8.2 Hz, 2H), 6.65 (d, *J* = 8.9 Hz, 2H), 6.63 (d, *J* = 8.5 Hz, 4H), 6.37 (d, *J* = 8.9 Hz, 2H), 3.60 (s, 3H), 0.14 (s, 9H), 0.12 (s, 18H); ^{13}C{^{1}H} NMR (126 MHz, $CDCl_3$, 293 K): δ 157.22, 140.98, 140.83, 140.53, 140.28, 140.12, 139.72, 139.24, 137.48,

137.11, 133.13, 132.72, 132.50, 131.98, 131.87, 130.78, 130.74, 129.82, 119.47, 112.31, 55.15, –1.03 (22 signals; One signal from TMS group was not observed because of overlapping.); HRMS (ASAP): Calcd for $[M]^+$ $C_{52}H_{54}{}^{79}Br_2Si_3O$ 936.1849, found 936.1843.

References and Notes

[1] The half-lives of *t*-BuLi in THF was reported as 338 min at –40 ˚C and as 42 min at –20 ˚C. See: Stanetty, P.; Mihovilovic, M. D. *J. Org. Chem.* **1997**, *62*, 1514.

[2] The author has confirmed that the reaction mixture reaches 0 ˚C in 5 min after removal of the cooling bath when the reaction is performed in 2 mL of THF in a standard two-neck flask.

[3] Gorecka-Kobylinska, J.; Schlosser, M. *J. Org. Chem.* **2009**, *74*, 222.

[4] (a) Shi, L.; Chu, Y.; Knochel, P.; Mayr, H. *Angew. Chem., Int. Ed.* **2008**, *47*, 202. (b) Shi, L.; Chu, Y.; Knochel, P.; Mayr, H. *J. Org. Chem.* **2009**, *74*, 2760.

[5] (a) Rosenberg, S. D. *J. Am. Chem. Soc.* **1954**, *76*, 4389. (b) Gilman, H.; Summers, L. *J. Am. Chem. Soc.* **1950**, *72*, 2767.

[6] Yamamoto, Y.; Maeda, K.; Tomimoto, K.; Mase, T. *Synlett* **2002**, 561.

[7] (a) Kondo, Y.; Asai, M.; Miura, T.; Uchiyama, M.; Sakamoto, T. *Org. Lett.* **2001**, *3*, 13. (b) Lage, S.; Villaluenga, I.; Sotomayor, N.; Lete, E. *Synlett* **2008**, 3188. (c) García-Calvo, O.; Coya, E.; Lage, S.; Coldham, I.; Sotomayor, N.; Lete, E. *Eur. J. Org. Chem.* **2013**, 1460. (d) Kim, H.; Nagaki, A.; Yoshida, J. *Nat. Commun.* **2011**, *2*, 264.

[8] The recovery of MesBr or MapBr was not quantitatively determined owing to their volatility during the work-up process.

[9] For example, see: Wu, J.; Watson, M. D.; Müllen, K. *Angew. Chem., Int. Ed.* **2003**, *42*, 5329.

Chapter 4

Investigation of the Origin of the Thermodynamic Stability of the Alternately Trilithiated Hexaphenylbenzene Species

4.1 Introduction

In Chapters 2 and 3, the author developed the new synthetic protocols for the selective alternate trilithiation of the HPB framework. It was revealed that the halogen dance selectively affords the alternately trilithiated HPB species under thermodynamic control if exactly three equivalents of Li are loaded on the HPB framework. However, the reason why the alternately trilithiated species is the main component in the equilibrium mixture is not apparent. Because the alternately trilithiated species **29** deriving from compound **27** is statistically unfavorable compared with 1,2,4-type trilithiated species **70** (Figure 4.1), the preference of the 1,3,5-type alternately trilithiated species **29** at the equilibration should be attributed to the energetic stability of the 1,3,5-type trilithiated species **29** or from the energetic instability of the 1,2,4-type trilithiated species **70**. The large energetic difference depending on the arrangement of the same numbers of Br and Li is unapparent since each Br substituent and Li substituent is distributed on the different phenyl groups on the HPB framework. In this Chapter, the author experimentally investigates the distribution of the lithiated species in the equilibrium mixture and discusses the stability of the alternately trilithiated species in detail.

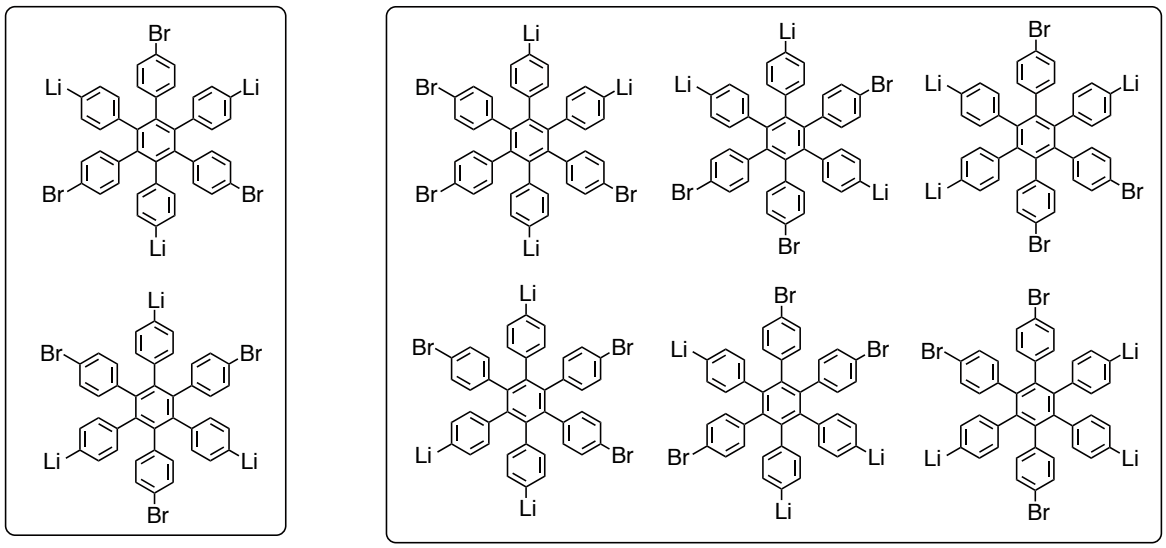

Figure 4.1 Statistical comparison of the two types of trilithiated species **29** and **70**.

4.2 Experimental study of the distribution of the lithiated species in the equilibrium mixture

To discuss the origin of the thermodynamic preference of the alternately trilithiated species, the exact composition of the equilibrium mixture is necessary. The trilithiation of compound **27** could afford 13 products in principle after proton quenching (Scheme 4.1). Unfortunately, the quantitative analysis of the obtained product by ^{1}H NMR, which was thought to be the most effective analytical method in this case, was impossible due to the severe overlapping of the signals on the ^{1}H NMR spectrum.

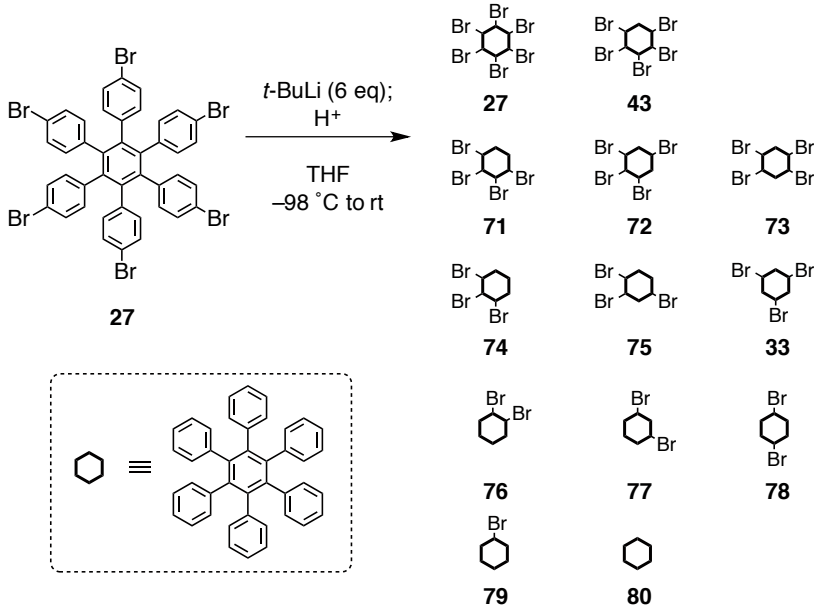

Scheme 4.1 Possible products from lithiation of compound **27** followed by proton quenching.

The author paid attention to a simpler HPB system, where the number of the possible products is restricted. Lithiation of compound **71** with 4.0 eq of *t*-BuLi should result in the mixture of starting material **71** and nine lithiated species, some of which afford the same product after protonation (Scheme 4.2). The theoretical distribution of lithiated species was calculated from the statistical viewpoint. There are eight possible HPB compounds **71** and **74**-**80** in the crude mixture. Seven of them, **71**, **74**-**76**, **78, 79** and **80** were commercially available or obtained by the reaction sequence of the double dehydrative condensation and Diels-Alder reaction without the problem of the regioselectivity. The preparation of new HPB compound **74** is shown as an example (Scheme 4.3).

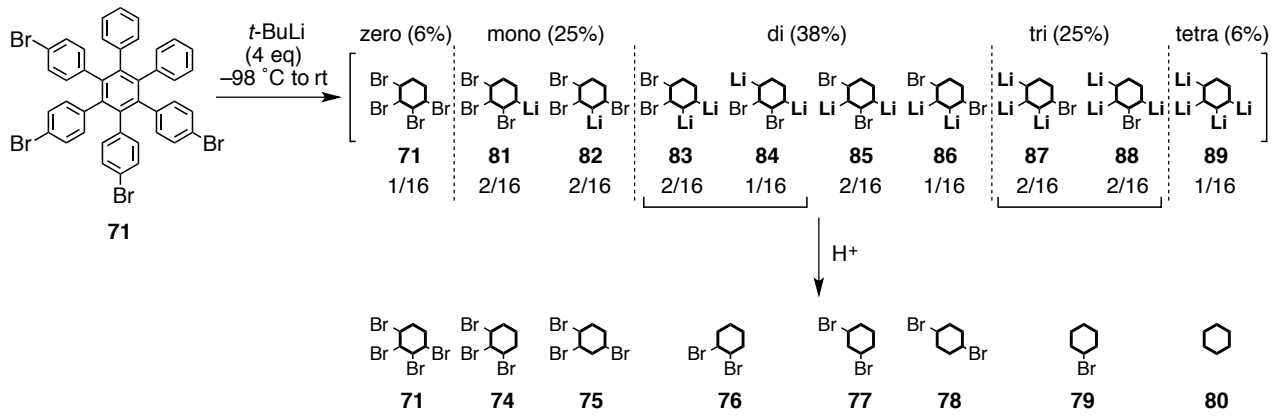

Scheme 4.2 Possible products from lithiation of compound **71** followed by proton quenching and theoretical distribution of the possible lithiated species from the statistical viewpoint with 4.0 eq of *t*-BuLi.

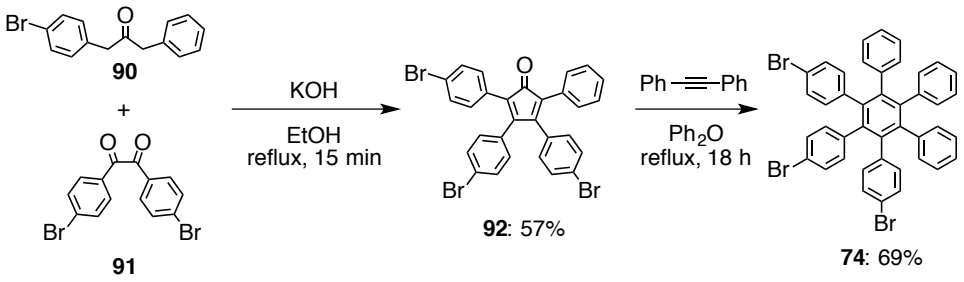

Scheme 4.3 Synthesis of compound **74**.

The other HPB compound **77** was efficiently prepared using the halogen dance protocol (Scheme 4.4). Compound **77** had been unknown probably since the selective preparation was impossible with conventional synthetic protocols. Although the selective alternate trilithiation of compound **43** followed by proton quenching afforded target compound **77** as the main product, the isolation by recrystallization was unsuccessful. Instead, the protodesilylation of compound **48**, which was obtained and isolated using the improved halogen dance protocol in Chapter 3, cleanly afforded compound **77**. Fortunately, the comparison of ^{1}H NMR spectra of pure HPB compounds **71** and **74**-**80** revealed that the quantitative analysis of the mixture of these compounds is possible by their characteristic NMR signals (Figure 4.2).

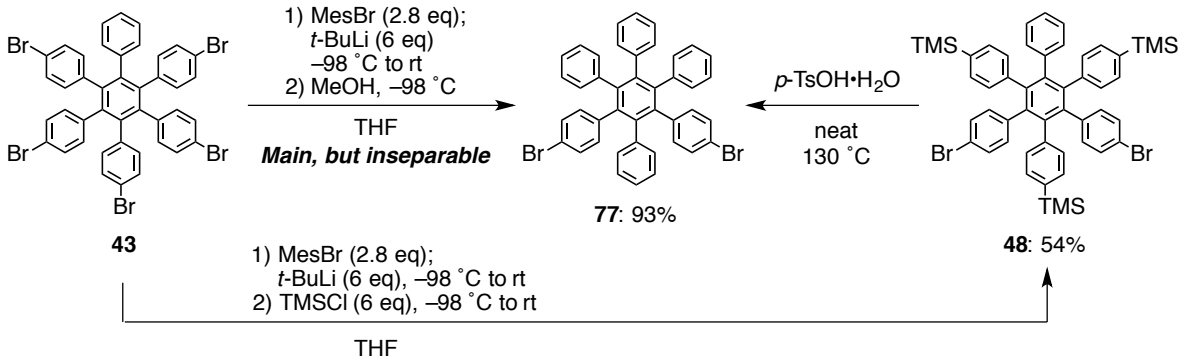

Scheme 4.4 Synthesis of compound **77**.

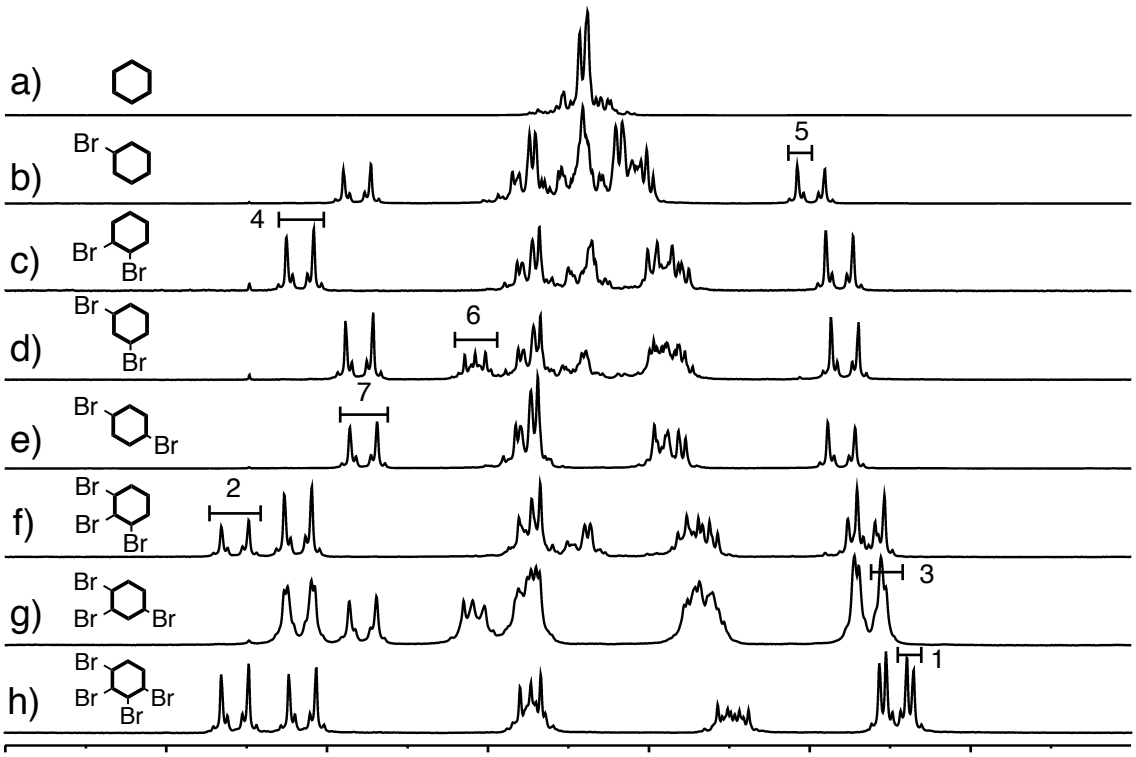

Figure 4.2 Comparison of the ^{1}H NMR spectra (500 MHz, $CDCl_3$) of HPB compounds **71**, **74**-**80**: a) **80**, b) **79**, c) **78**, d) **77**, e) **76**, f) **75**, g) **74**, h) **71**. The bars and the numbers indicate the used signals and the order for the quantitative analysis.

The author added 4.0 eq of *t*-BuLi into the suspension of **71** in THF at –98 °C, warmed it to rt to obtain a clear solution, and then quenched it with methanol at –98 °C (Scheme 4.4). The composition of the obtained crude mixture was not affected by the addition of MesBr. This result indicates that the dissolution of compound **71** is fast enough to complete the lithiation of two equivalents of the HPB framework at the initial stage of the reaction. The ^{1}H NMR spectrum of the obtained crude mixture was analyzed on the basis of the intensity of the signals with an internal standard (Figure 4.3). The distribution of the products confirmed that the lithiation of two equivalents certainly occurred in the lithiation phase. Among three possible dibrominated products **76**, **77**, and **78**, compound **78** was not generated at all. This result indicates that dilithiated species **86** does not exist in the equilibrium mixture at all before protonation and that it is much less stable than the other dilithiated species. This instability was attributed to the arrangement of Li substituents where the two lithiophenyl groups were next to each other. This instability can also explain the strong preference of dilithiated species to trilithiated species over their statistical factors (6/4). Furthermore, this instability suggests that most of compound **76**, which could be derived from dilithiated species **83** and **84**, results from dilithiated species **84**. The estimated distribution of the lithiated species in the equilibrium mixture is shown in Figure 4.4. It was found that dilithiated species **85** is much more preferred to dilithiated species **84** over their statistical factors (2/1). This preference can be phenomenologically described with the difference of the number of the bromophenyl groups or the non-substituted phenyl groups that lie next to each of the lithiophenyl groups (Figure 4.5). In the case of dilithiated species **84**, both of the lithiophenyl groups are next to one bromophenyl group and one non-substituted phenyl group. On the other hand, in the case of dilihiated species **85**, one of the lithiophenyl groups is wedged between the two bromophenyl groups and the other is next to the one bromophenyl group and the one non-substituted phenyl group. The comparison of these two dilithiated species suggests that the larger number of the bromophenyl groups or the smaller number of the non-substituted phenyl groups adjacent to each of the lithiophenyl groups is preferred in the thermodynamically stable arrangement of the substituents Li and Br.

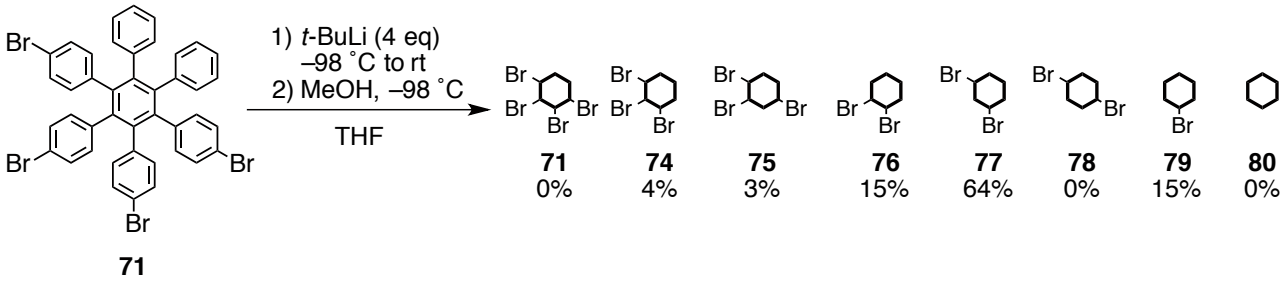

Scheme 4.4 Lithiation of compound **71** with 4.0 eq of *t*-BuLi.

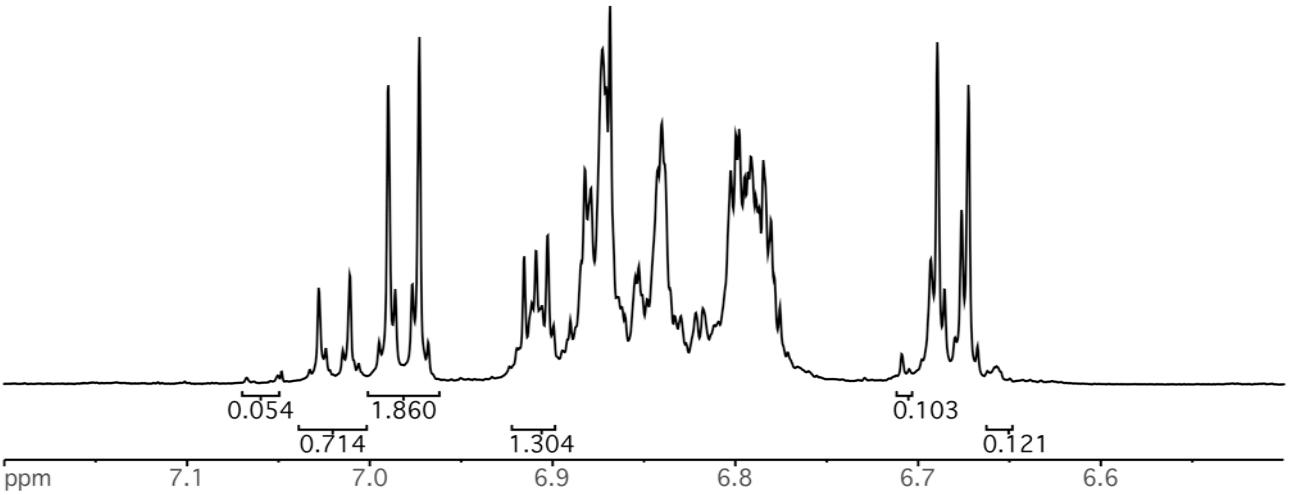

Figure 4.3 ^{1}H NMR spectrum (500 MHz, $CDCl_3$) of the obtained crude mixture in the lithiation of compound **71** with 4.0 eq of *t*-BuLi

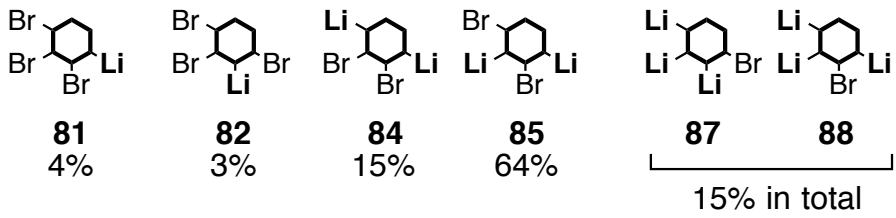

Figure 4.4 Estimated composition of the equilibrium mixture before protonation.

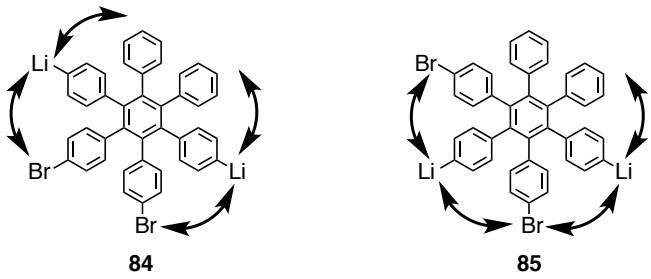

Figure 4.5 Comparison of the arrangement of the substituents of dilithiated species **84** and **85**.

In summary, the distribution of the possible lithiated species of the equilibrium mixture obtained by the lithiation of compound **71** with 4.0 eq of *t*-BuLi was described with the following rules of the arrangement of the substituents on the HPB framework: (1) the pair of the two adjacent Li substituents is highly disfavored. (2) The number of the Br substituents adjacent to the Li substituents is maximized, or (2)' the number of the H "substitutents" on the non-substituted phenyl groups adjacent to the Li substituents is minimized. The simple application of these rules to compound **27** can illustrate the much higher thermodynamic stability of the alternately trilithiated 1,3,5-type species derived from compound **27** than that of 1,2,4-type (Figure 4.6).

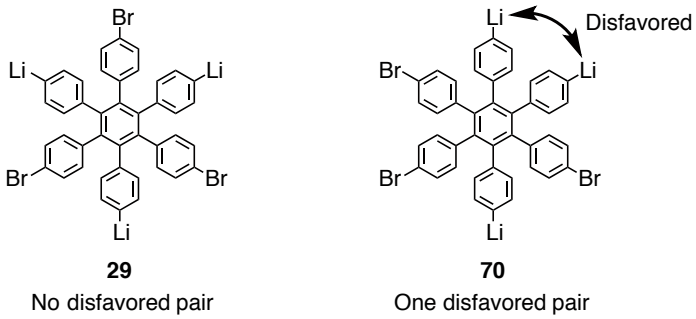

Figure 4.6 Comparison of the thermodynamic stability of 1,3,5-type and 1,2,4-type trilithiated species **29** and **70** based on the phenomenological rules of the arrangement of the substituents.

4.3 Discussion of the origin of the thermodynamic stability of the alternately lithiated species

In the previous Section, the favored and disfavored lithiated HPB species were phenomenologically described with the two rules of the arrangement of the substituents Li, Br, and H. These rules imply that the thermodynamic stability is significantly influenced by the arrangement of the substituents on the HPB framework. However, the origin of these substituent effects is not apparent since the substituents are distant and since they are distributed on the different phenyl groups, which did not communicate through effective π-conjugation.

The characteristic conformation of the HPB framework should be the most important for the discussion to rationalize the substituent effects comprehensively (Figure 4.7a). The six peripheral aryl groups are almost perpendicular to the central benzene unit owing to the steric hindrance. In this conformation, the adjacent aryl groups should experience the π-π interaction although they are not completely paralleled. The interaction should be stronger at the inner side of the framework. In particular, the *ipso*-carbons of the aryl groups are so proximal that the strong interaction between their 2p orbitals should be even possible (Figure 4.7b). The direct orbital interaction at the *ipso*-carbons of the aryl groups on the HPB framework has been studied through the oxidation behavior.[1] Compounds **93**,[2] **94**,[3] and **95**[4] exhibited the stepwise oxidation waves under electrochemical measurements, which indicated the delocalization of the hole on the six aryl groups through the strong electronic coupling between them (Figure 4.8). However, the careful consideration of this interaction is required because compounds **96**,[5] **97**,[6] and **98**[7] did not exhibit an electronic coupling behavior (Figure 4.9). This dependence on the HPB compounds was interpreted with the importance of the localization of charge on the phenyl groups on the HPB framework.[1]

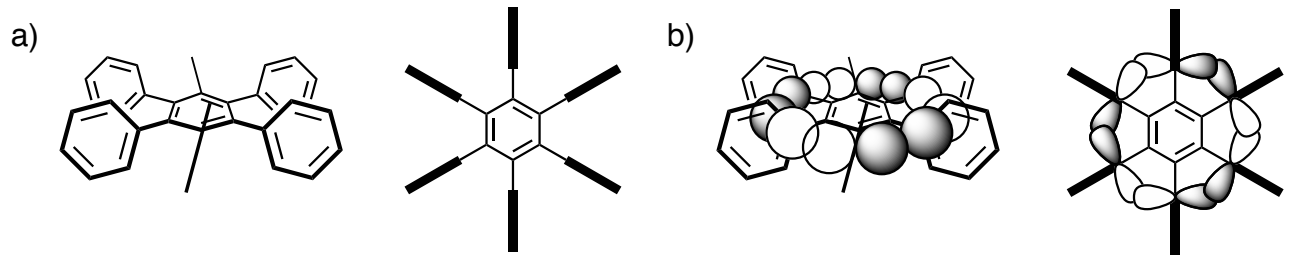

Figure 4.7 a) Characteristic conformation of the HPB framework and b) strong orbital interaction at the *ipso*-carbons of the peripheral Ph groups.

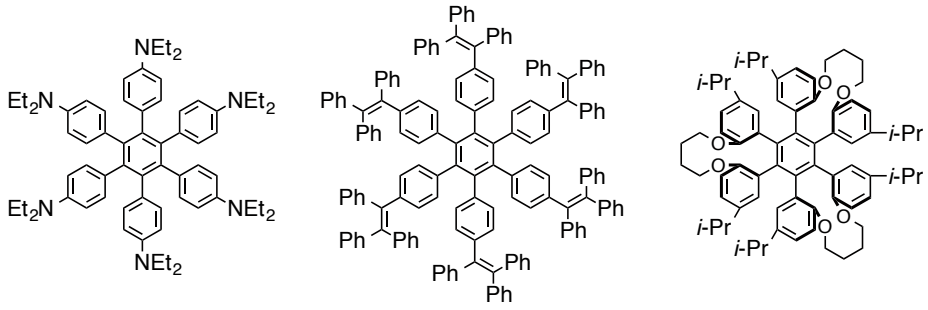

93 **94** **95**

Figure 4.8 HPB compounds **93**, **94**, and **95** exhibiting the stepwise oxidation behavior under electrochemical measurements.

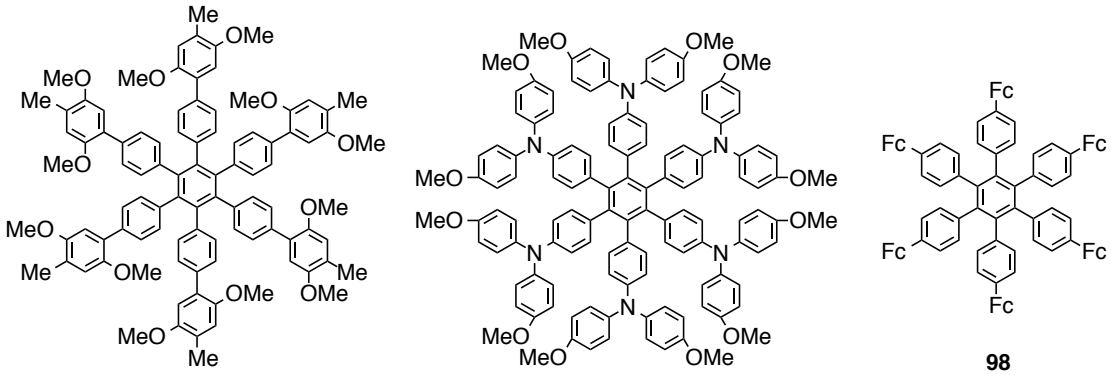

96 **97** **98**

Figure 4.9 HPB compounds **96**, **97**, and **98** not exhibiting the strong orbital interaction under electrochemical measurements.

The author supposes the two types of interaction between the adjacent aryl groups on the HPB framework (Figure 4.10). One is the direct through-space π-π interaction between the adjacent aryl groups (Figure 4.10a). Although the essence of π-π interaction is still on debate,[8] the electrostatic repulsion between the π-clouds should be one of the important contributions.[9] An electron-withdrawing substituent decreases the electron density of the π-cloud and reduces the electrostatic repulsion between the π-clouds. The benzene ring of a lithiophenyl group should be electron-rich through the polarization effects as discussed in Section 3.3. The reluctance of the lithiophenyl groups to be next to each other could be rationalized by the significant electrostatic repulsion between the electron-rich π-clouds. On the other hand, a lithiophenyl group is

expected to prefer the bromophenyl group with lower electron density as its neighboring group because this combination can minimize the electrostatic repulsion. This preference can rationalize the rule of the maximum number of the bromophenyl groups or the minimum number of the non-substituted phenyl groups adjacent to the lithiophenyl groups. This preference might be generalized that the maximum number of the more electron-withdrawing substituents adjacent to the Li substituents on the HPB framework is better. It should be noted, however, that the contribution of the other important through-space interaction such as van der Waals interaction must be considered for the strict treatment of the through-space π-π interaction.[10]

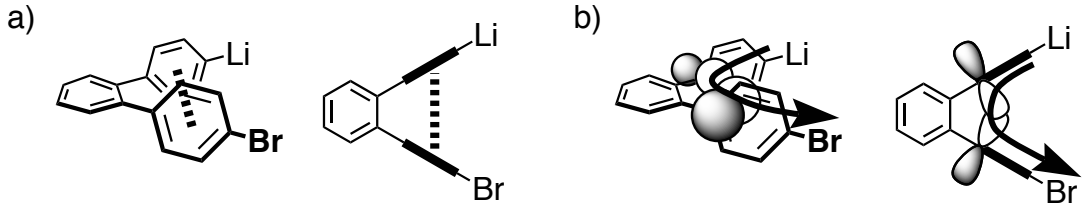

Figure 4.10 Two types of interaction between the adjacent aryl groups on the HPB framework: a) direct π-π interaction, b) σ/π polarization through the orbital overlapping at the *ipso*-carbons.

Another type of interaction is the σ/π polarization through the orbital overlapping at the *ipso*-carbons (Figure 4.10b). As discussed in Section 3.3, one of the key stabilizing effects of the substituents on aryllithiums is the distal σ/π polarization, where the increased electron density at the lithiated carbon in the σ-framework is reduced by the polarization of the π-cloud. In the case of the HPB framework, the excessive electron density on the lithiated phenyl groups could be extracted to the adjacent phenyl groups through the effective orbital overlapping at the *ipso*-carbons. Since electron-withdrawing groups have been confirmed to stabilize monocyclic aryllithiums by the σ/π polarization more effectively, it is naturally expected that the phenyl group with a more electron-withdrawing substituent also stabilizes the adjacent lithiophenyl group more effectively by the σ/π polarization through the orbital interaction at the *ipso*-carbons. This σ/π polarization through the *ipso*-carbons can also rationalize the rules of the arrangement of the substituents on the HPB framework.

It was found that the two types of possible interaction between the adjacent phenyl groups on the

HPB framework could exhibit the same tendency of the substituent effects. Therefore, the experimental distinction of these two interactions might be very difficult. The diagnostic difference of the two interactions is the existence of the flow of the electron density from a lithiophenyl group to the adjacent phenyl groups. The sophisticated theoretical approach could estimate the contribution of each interaction. At this stage, the author would like to emphasize the importance of the characteristic conformation of the HPB framework, which is essential for both of the two possible interactions that might determine the arrangement of Li and Br.

4.4 Conclusion

In this Chapter, it was clearly revealed that the distribution of the litho species in the equilibrium mixture, the goal of the halogen dance, is not statistical but biased. On the basis of the quantitative analysis of the crude mixture obtained by the lithiation of compound **71**, the distribution of the equilibrium mixture was phenomenologically described with the two rules of the arrangement of the substituents Li, Br, and H. As the origin of the significant dependence of the stability of the lithiated species on the arrangement of the substituents, the electrostatic repulsion of the π-clouds between the adjacent aryl groups and the σ/π polarization at the *ipso*-carbons were proposed. Both of these two possible interactions are based on the characteristic conformation of the HPB framework. The conformation of the HPB framework was therefore found to play one of the most crucial roles for the selective alternate trilithiation. The discussion in this Chapter has highlighted the importance of the intrinsic conformation of the framework for the late-stage selective derivatization of extended π-conjugated frameworks.

Experimental Section

Compounds **71**,[11] **75**,[12] **76**,[13] **78**,[14] **79**,[15] **90**[16] were prepared according to the literature.

Synthesis of compound 92

To the solution of compound **90** (1.02 g, 3.53 mmol) and compound **91** (1.30 g, 3.53 mmol) in ethanol (10 mL) was added the solution of KOH (0.20 g) in EtOH (2 mL). Then the mixture was refluxed for 1 h. After cooling to 0 ˚C, the resulting precipitation was filtered and washed with cold ethanol to afford compound **92** (1.25 g, 57%) as a purple solid.

^{1}H NMR (500 MHz, $CDCl_3$, 293 K): δ 7.40 (d, *J* = 8.7 Hz, 2H), 7.37 (d, *J* = 8.7 Hz, 2H), 7.34 (d, *J* = 8.7 Hz, 2H), 7.28-7.24 (m, 3H), 7.20-7.17 (m, 2H), 7.07 (d, *J* = 8.7 Hz, 2H), 6.78 (d, *J* = 8.7 Hz, 2H), 6.78 (d, *J* = 8.7 Hz, 2H); ^{13}C NMR (126 MHz, $CDCl_3$, 293 K): δ 199.30, 153.27, 152.63, 131.84, 131.73, 131.71, 131.65, 131.58, 131.50, 131.06, 130.92, 130.19, 130.15, 129.25, 128.41, 128.12, 126.25, 124.90, 123.59, 123.41, 122.43. HRMS (ASAP): Calcd for $[M+H]^+$ $C_{29}H_{18}{}^{79}Br_3O$ 618.8908, found 618.8904.

Synthesis of compound 74

The mixture of diphenylacetylene (1.12 g, 5.27 mmol) and compound **92** (2.02 g, 5.27 mmol) in Ph_2O (4.5 mL) was refluxed for 18 h. After cooling to rt, the resulting precipitation was filtered to afford a colorless solid (0.292 g). The addition of EtOH to the mother liquor resulted in another colorless solid (0.135 g), which was also collected by filtration. The combined colorless solid was recrystallized from $CHCl_3$ to afford compound **74** as a colorless solid (0.341 g, 69%).

m.p. >300 ˚C; ^{1}H NMR (500 MHz, $CDCl_3$, 293 K): δ 7.06 (d, *J* = 8.5 Hz, 2H), 7.02 (d, *J* = 8.5 Hz, 4H), 6.89-6.83 (m, 9H), 6.79-6.75 (m, 6H), 6.67 (d, *J* = 8.5 Hz, 2H), 6.66 (d, *J* = 8.5 Hz, 4H); ^{13}C NMR (126 MHz, $CDCl_3$, 293 K): δ 141.22, 140.95, 140.15, 140.02, 139.27, 139.18, 139.15, 138.84, 132.97, 132.96, 131.30, 131.29, 130.43, 130.22, 127.03, 126.83, 125.76, 125.59, 120.16, 119.96; HRMS (ASAP): Calcd for $[M]^+$ $C_{42}H_{27}{}^{79}Br_3$ 767.9663, found 767.9667.

Synthesis of compound 77

The mixture of compound **48** (0.200 g, 0.220 mmol) and *p*-toluenesulfonic acid monohydrate (2.0 g, 11 mmol) was stirred at 130 ˚C for 90 min. After the addition of water and CH_2Cl_2, the organic layer was separated, washed with aq.NaOH (10%), dried over $MgSO_4$, and filtered. Then the solvent was removed to afford compound **77** (0.141 g, 93%) as a colorless solid.

m.p. >300 ˚C; ^{1}H NMR (500 MHz, $CDCl_3$, 293 K): δ 6.98 (d, *J* = 8.6 Hz, 4H), 6.93-6.90 (m, 3H), 6.90-6.77 (m, 17H), 6.68 (d, *J* = 8.6 Hz, 4H); ^{13}C NMR (126 MHz, $CDCl_3$, 293 K): δ 140.83, 140.73, 140.33, 140.24, 140.08, 139.62, 139.29, 133.08, 131.40, 131.37, 129.97, 127.19, 126.98, 126.80, 125.85, 125.67, 125.50, 119.68 (18 signals; Two signals were not observed because of overlapping.); HRMS (ASAP): Calcd for $[M]^+$ $C_{42}H_{28}{}^{79}Br_2$ 690.0558, found 690.0581.

Lithiation of compound 71

To the suspension of compound **71** (0.150 g, 0.176 mmol) in THF (1.5 mL) was added the freshly titrated pentane solution of *t*-BuLi (1.74 M, 0.406 mL, 0.706 mmol) at –98 ˚C. After removal of the cooling bath, the reaction mixture was stirred for 40 min, and then quenched by the addition of methanol (0.3 mL) at –98 ˚C. After the addition of water and $CHCl_3$, the organic layer was analyzed by ^{1}H NMR with 1,3,5-tris(*p*-bromophenyl)benzene as an internal standard.

References

[1] Lambert, C. *Angew. Chem., Int. Ed.* **2005**, *44*, 7337.

[2] (a) Sun, D.; Rosokha, S. V.; Kochi, J. K. *Angew. Chem., Int. Ed.* **2005**, *44*, 5133. (b) Rosokha, S. V.; Neretin, I. S.; Sun, D.; Kochi, J. K. *J. Am. Chem. Soc.* **2006**, *128*, 9394.

[3] Rathore, R.; Burns, C. L.; Abdewwahed, S. A. *Org. Lett.* **2006**, *6*, 1689.

[4] Shukla, R.; Lindeman, S. V. Rathore, R. *Org. Lett.* **2007**, *9*, 1291.

[5] Rathore, R.; Burns, C. L.; Deselnicu, M. I. *Org. Lett.* **2001**, *3*, 2887.

[6] Lambert, C.; Nöll, G. *Angew. Chem., Int. Ed.* **1998**, *37*, 2107.

[7] Chebny, V. J.; Dhar, D.; Lindeman, S. V.; Rathore, R. *Org. Lett.* **2006**, *8*, 5041.

[8] Gleiter, R.; Haberhauer, G. *Aromaticity and Other Conjugation Effects*; Wiley-VCH: Weinheim, 2012.

[9] (a) Cozzi, F.; Cinquini, M.; Annunziata, R.; Siegel, J. S. *J. Am. Chem. Soc.* **1993**, *115*, 5330. (b) Cozzi, F.; Ponzini, F.; Annunziata, R.; Cinquini, M.; Siegel, J. S. *Angew. Chem., Int. Ed.* **1995**, *34*, 1019. (c) Cozzi, F.; Annunziata, R.; Benaglia, M.; Cinquini, M.; Raimondi, L.; Baldridge, K. K.; Siegel, J. S. *Org. Biomol. Chem.* **2003**, *1*, 157.

[10] Lima, F. R. A. C. C.; Rocha, M. A. A.; Gomes, L. R.; Low, J. N.; Silva, A. M. S.; Santos, L. M. N. B. F. *Chem. Eur. J.* **2012**, *18*, 8934.

[11] Yamaguchi, R.; Ito, S.; Lee, B. S.; Hiroto, S.; Kim, D.; Shinokubo, H. *Chem. Asian J.* **2013**, *8*, 178.

[12] Li, Z.; Ye, S.; Liu, Y.; Yu, G.; Wu, W.; Qin, J.; Li, Z. *J. Phys. Chem. B* **2010**, *114*, 9101.

[13] Terazono, Y.; Liddell, P. A.; Garg, V.; Kodis, G.; Brune, A.; Hambourger, M.; Moore, A. L.; Moore, T. A.; Gust, D. *J. Porphyrins Phthalocyanines* **2005**, *9*, 706.

[14] Jones, D. J.; Purushothaman, B.; Ji, S.; Holmes, A. B.; Wong, W. W. H. *Chem. Commun.* **2012**, *48*, 8066.

[15] Kübel, C.; Chen, S. L.; Müllen, K. *Macromolecules* **1998**, *31*, 6014.

[16] Arndt, K.; Godschalx, J.; Hefner, R.; Niu, Q.; Pechacek, J. Multifunctional Monomers and Their Use in Making Cross-Linked Polymers and Porous Film. U.S. Patent 20040053033, Mar. 18, 2004.

Chapter 5

Stereoselective Construction of the Triphosphatruxene Framework

5.1 Introduction

Truxene is a partial structure of fullerene and its rigid C_3-symmetric scaffold has been utilized for the development of organic functional materials (Figure 5.1).[1] The heteroanalogues of it, heterotruxenes, were also prepared such as trioxatruxene[2] and trithiatruxene.[3] In particular, triazatruxene derivatives have been exploited for a broad range of applications.[4] For example, compounds **99** and **100** exhibited high charge mobility owing to the strong intermolecular interaction between the two-dimensionally extended π-conjugated frameworks.[1e,4f] Compound **101** was found to be an efficient two-photon absorption chromophore because of its C_3-symmetric framework.[4g] The active application of truxene [5] and triazatruxene[6] should be based on the efficient synthetic protocols of them (Scheme 5.1).

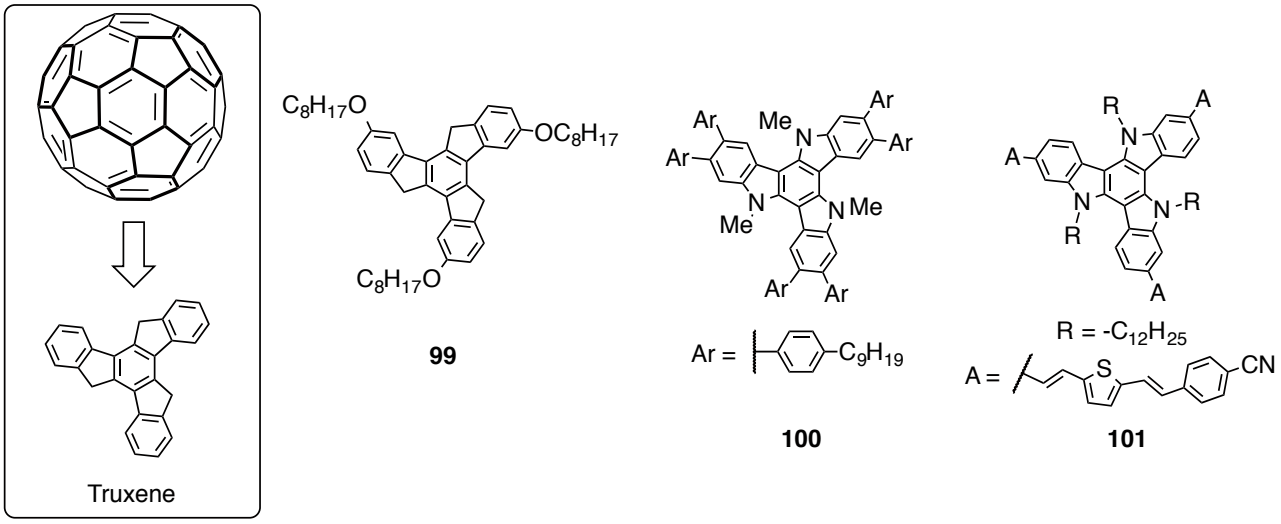

Figure 5.1 Truxene and heterotruxene derivatives.

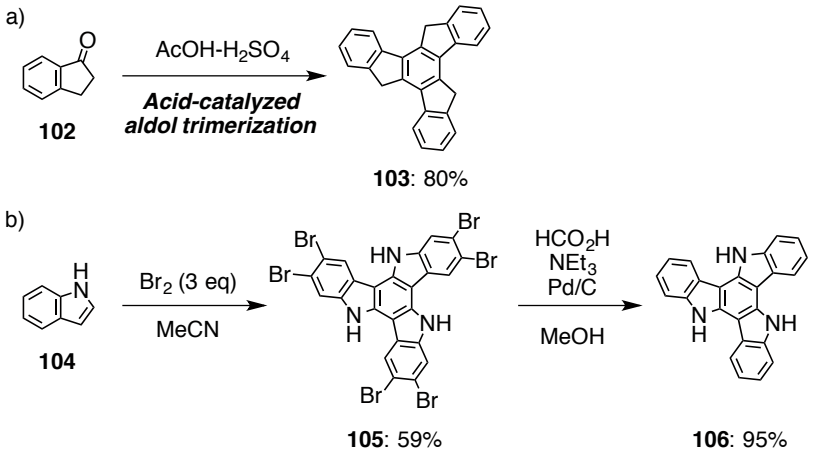

Scheme 5.1 Efficient synthetic protocol for (a) truxene and (b) triazatruxene.

However, the author found that the phosphorus analogue of truxene, triphosphatruxene (TPT), had never been reported despite the significant advances in phosphorus-containing π-conjugated materials as described in Section 1.4 (Figure 5.2). This is probably because the construction of such systems that incorporate multiple phosphorus atoms requires addressing several issues. Firstly, the suitable synthetic method for the TPT framework is still missing in spite of the recent progress of the synthetic chemistry of organophosphorous compounds. Secondly, there exist two stereoisomers, *syn*-isomer and *anti*-isomer, deriving from the relative stereochemistry of the three pyramidal phosphorus centers. The selective synthesis of one particular stereoisomer, especially, statistically unfavored *syn*-isomer, is a challenging subject. In this Chapter, the author describes a short-step preparation of TPT derivatives and the stereocontrol of the TPT framework through a simple process.

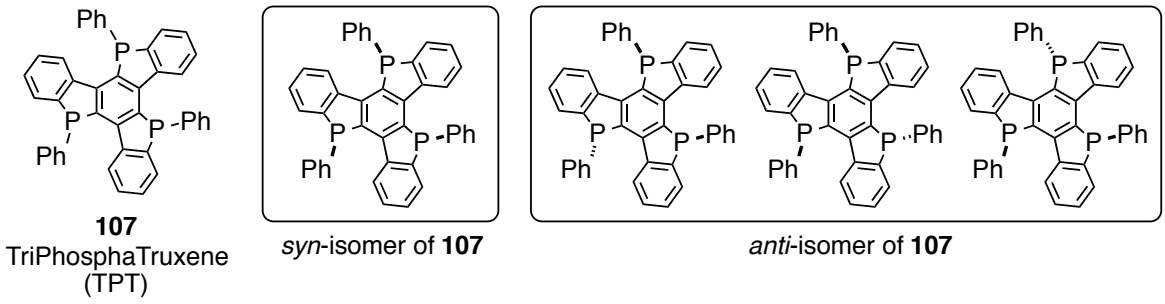

Figure 5.2 Triphosphatruxene (TPT) derivative **107** and statistical comparison of the two stereoisomers.

5.2 Synthetic strategy of a TPT framework

The reported synthetic protocols did not seem suitable for the efficient construction of a TPT framework. The most conventional synthetic method for a dibenzophosphole unit relies on the reaction of phosphorus electrophiles with dimetalated precursor **109**, which is usually derived from the corresponding brominated compound **108** (Scheme 5.2a).[7] This protocol could face the difficulty in the preparation of the polymetalated intermediate **112** (Scheme 5.2b). Furthermore, the preparation of the corresponding brominated precursor **111** could be even tedious owing to the crowding of large Br substituents. On the other hand, most of the new synthetic protocols construct a dibenzophosphole unit in two steps (Scheme 5.3a).[8] The phosphoryl group is introduced to the monometalated intermediate **114** at first. Then the transition-metal-catalyzed intramolecular cyclization reaction of precursor **115** affords a dibenzophosphole unit. These protocols can avoid the involvement of the unstable intermediate and the difficult preparation of the crowded precursor (Scheme 5.3b). However, the drawback of them is the requirement of the two synthetic steps and the expensive transition metal catalyst to form the C-P bonds. The applicability to the crowded system such as a TPT framework has also been unclear.

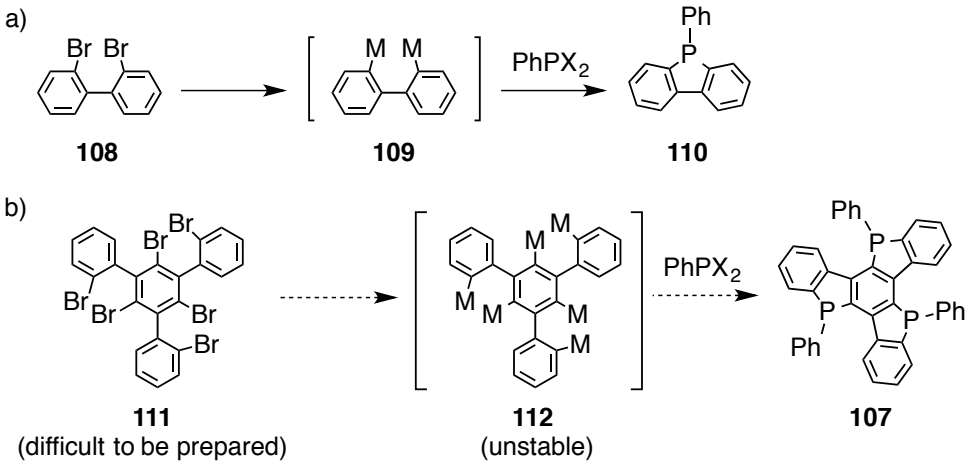

Scheme 5.2 Construction of (a) a dibenzophosphole unit and (b) a TPT framework by using polymetalation reactions.

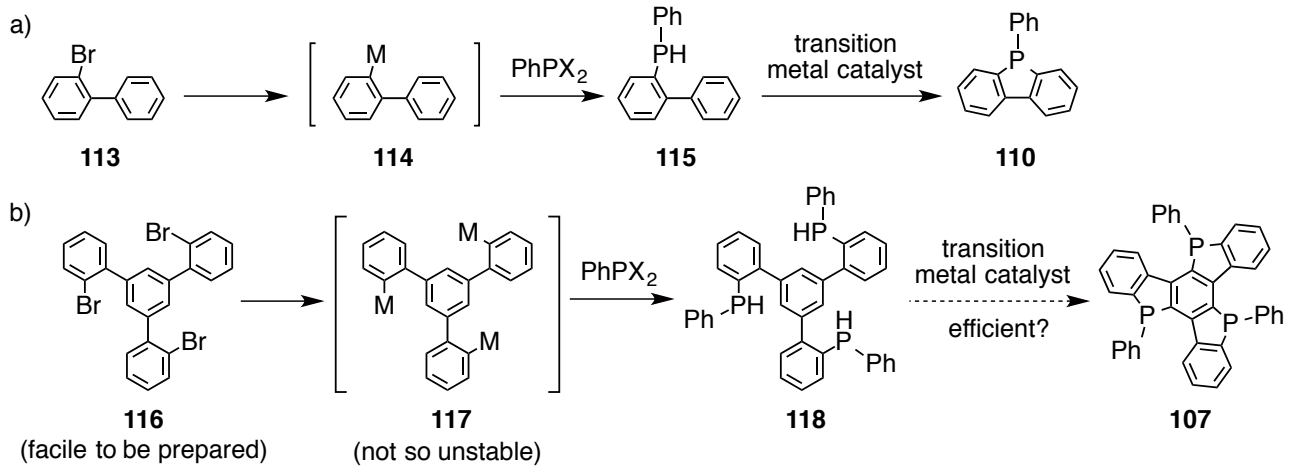

Scheme 5.3 Construction of (a) a dibenzophosphole unit and (b) a TPT framework by using transition-metal-catalyzed intramolecular cyclization reactions.

The reaction with the phosphorus reagents as a nucleophille is attractive for the more effective construction of a TPT framework. The aromatic nucleophilic substitution reaction of a primary phosphine with the corresponding fluorinated precurosor **119** could construct a dibenzophosphole unit in one step (Scheme 5.4a). Despite the high nucleophilicity of primary phosphines, which have been exploited for the synthesis of triarylphosphines,[9] a dibenzophosphole unit has never been synthesized through a simple aromatic nucleophilic substitution reaction. This protocol could construct a TPT framework only in one step without the instable intermediate (Scheme 5.4b). Furthermore, the preparation of the precursor **120** could be also facile owing to the small size of F substituents.

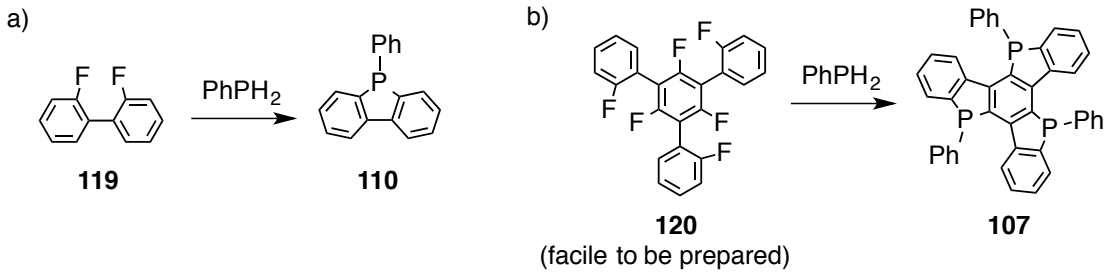

Scheme 5.4 Construction of (a) a dibenzophosphole unit and (b) a TPT framework by using aromatic nucleophilic substitution reactions.

5.3 Synthesis of TPT derivatives

The author found that sextuple aromatic nucleophilic substitution is effective for constructing a TPT framework (Scheme 5.5). The addition of phenylphosphine to fluorinated precursor **120**, which is readily available from compound **121** via triple Suzuki–Miyaura coupling, in the presence of potassium carbonate in DMSO smoothly afforded the crude product of TPT derivative **107** as an air-sensitive solid. This crude mixture exhibited three distinct singlet signals of the same strength along with one weak singlet signal as the main signals on ^{31}P NMR, which could be assigned to *anti*-isomer and *syn*-isomer of compound **107**, respectively. The *syn*/*anti* ratio was estimated by ^{1}H NMR to be 1/>15. This crude mixture was stereospecifically oxidized in dichloromethane with aqueous *t*-BuOOH at rt in 30 min,[10] and recrystallization selectively afforded crystals of *anti*-TPT trioxide (*anti*-**122**) with 43% isolated yield (from compound **120**), with *syn*/*anti* = ca. 1/2 mixture and unidentified products remaining in the mother liquor after recrystallization. The structure of *anti*-**122** was characterized by ^{1}H NMR, ^{31}P NMR, proton-and-phosphorus-decoupled ^{13}C NMR spectroscopy, elemental analysis, and MS.

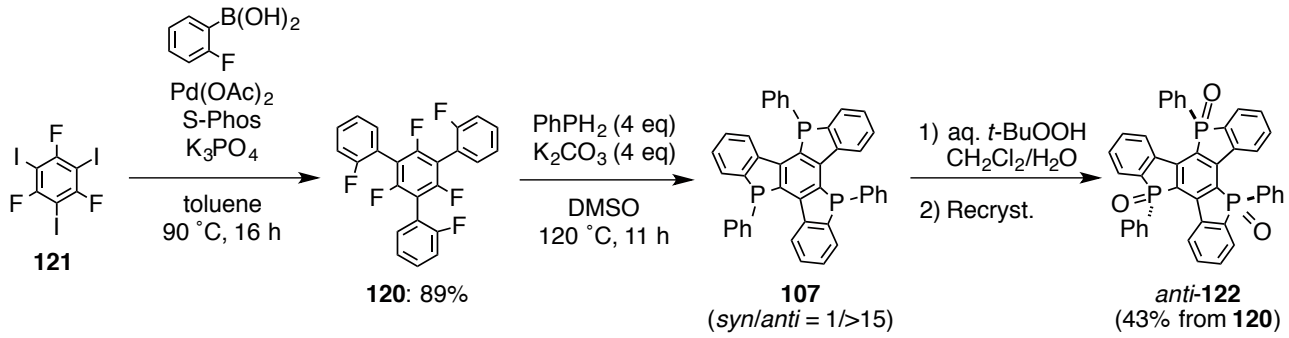

Scheme 5.5 Synthesis of TPT derivative *anti*-**122**.

5.4 Stereocontrol of the TPT framework

In the previous Section, it was found that the sextuple aromatic nucleophilic substitution proceeds with high *anti*-selectivity. However, the manipulation of the stereochemistry of the phosphorus centers is possible by the thermal inversion before oxidation. Interestingly, the author found that vacuum sublimation (290 °C/0.02 torr) of the crude mixture of **107** completely converted the *anti*-isomer into *syn*-isomer (Scheme 5.6). Subsequent oxidation of this sublimed sample afforded exclusively *syn*-**122** with 52% yield

(from compound **120**) after recrystallization. The structure of this product was unambiguously confirmed by X-ray crystallography (Figure 5.3). The ^{31}P NMR spectroscopy showed only one singlet resonance peak, consistent with its C_3-symmetric structure. The structure of *syn*-**122** was also fully characterized by multinuclear NMR and MS. The much higher yield of *syn*-**122** (ca. 6% was expected from the composition of the crude product of **107**) denied the possibilities of selective sublimation of *syn*-**107** and selective decomposition of *anti*-**107** during the sublimation process. It should be noted that this inversion during the sublimation process was reproducible in a broad range of scale from 10 mg to 3 g. By utilizing this inversion protocol, the selective preparation of both of the stereoisomers of TPT derivative **122** was achieved without the chromatographic separation of the mixture.

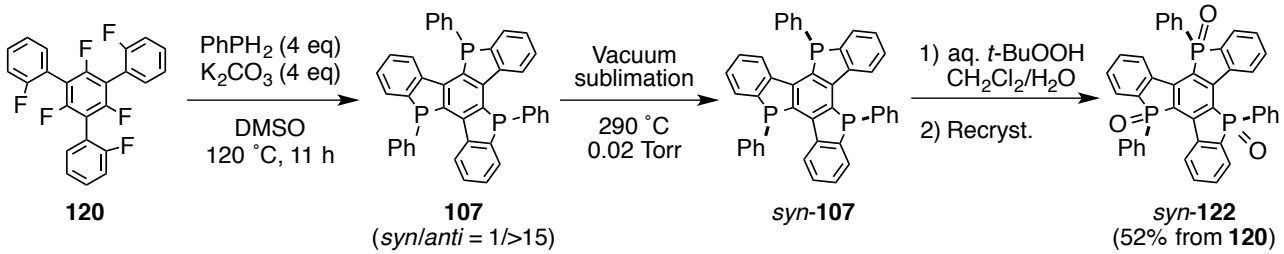

Scheme 5.6 Synthesis of TPT derivative *syn*-**122**.

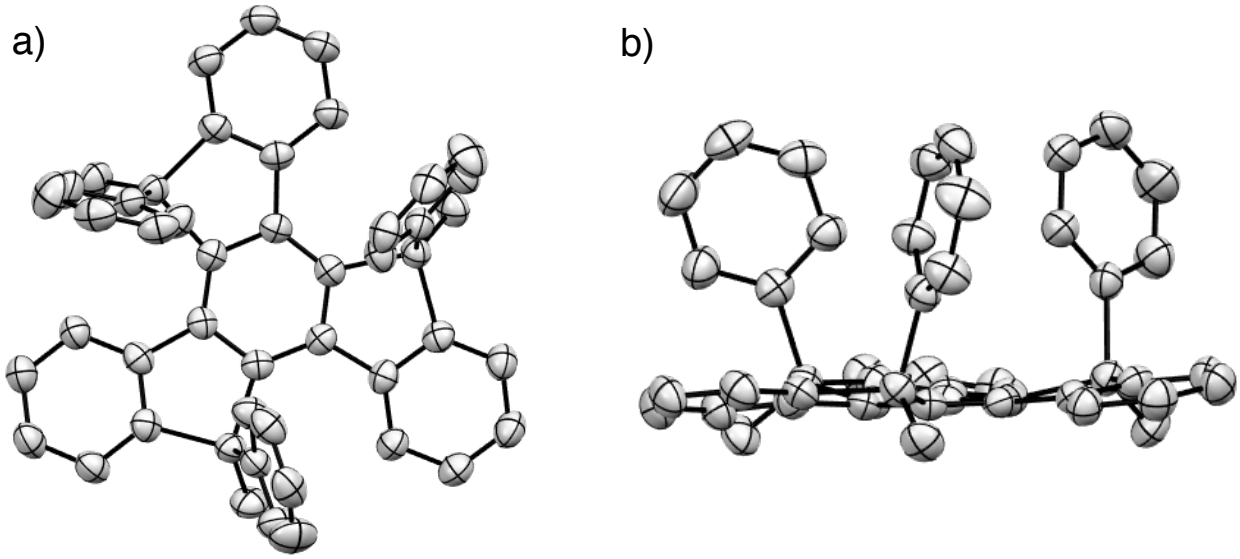

Figure 5.3 ORTEP drawings of TPT derivative *syn*-**122**: a) topview, b) sideview.

5.5 Inversion behavior of the TPT framework

To understand the selective conversion to *syn*-**107** during the sublimation process, the inversion behavior of the phosphorus centers on the TPT framework was investigated. The pure *syn*-**107** was obtained by recrystallization and vacuum sublimation of the reaction mixture before oxidation (Scheme 5.7). Recrystallization of the crude product of **107** after the sextuple aromatic nucleophilic substitution reaction afforded compound **107** (*syn*/*anti* = 1/6). The change of the ratio of the stereoisomers implied the inversion of the phosphorus centers during the recrystallization process. The vacuum sublimation of the recrystallized sample of **107** completely converted the *anti*-isomer into the *syn*-isomer. Then the conversion of pure *syn*-**107** to the equilibrium mixture of the two stereoisomers was monitored by ^{1}H NMR in $C_2D_2Cl_4$ at 80 °C. The equilibrium ratio was determined as *syn*/*anti* = 0.145, and the content of the *anti*-isomer was more than that expected from the statistical preference (3/1). The kinetic constant of the conversion of *syn*-**107** to *anti*-**107** was determined as 2.81×10^{-2} s^{-1}, and the barrier of the inversion of the phosphorus center in *syn*-**107** was calculated as $\Delta G^{\ddagger}$ = 101 kJ·mol^{-1} (353 K). This value is 5–10 kJ·mol^{-1} lower than that of the simple dibenzophosphole units (Figure 5.4).[11] As the decrease of the barrier of the inversion was previously observed for the dibenzeophosphole units bearing the simple aromatic substituents,[11b] the extended π-framework of TPT might also diminish the barrier effectively. The energetic preference of the *anti*-isomer was suggested by DFT calculation (ΔG = 8.5 kJ·mol^{-1} at B06-2X/6-31G(d) level.). Therefore, the *anti*-conformation is expected to be thermodynamically preferred in the gas phase. At this stage, the author can only argue that the selective deposition of *syn*-**107** was not under thermodynamic control in the gas phase.

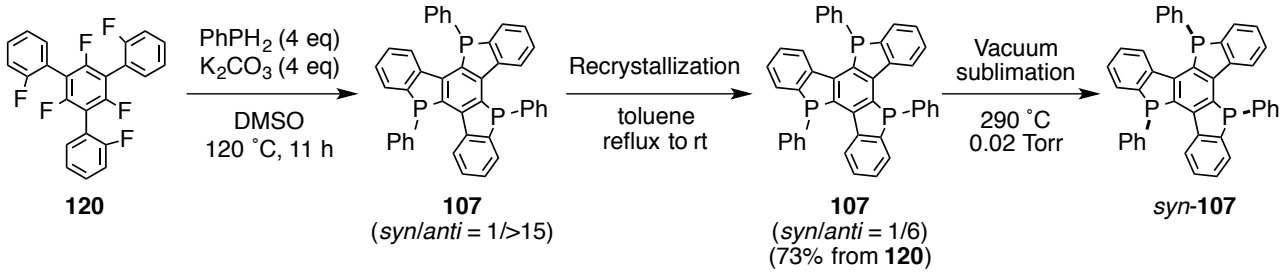

Scheme 5.7 Synthesis of TPT derivative *syn*-**107**.

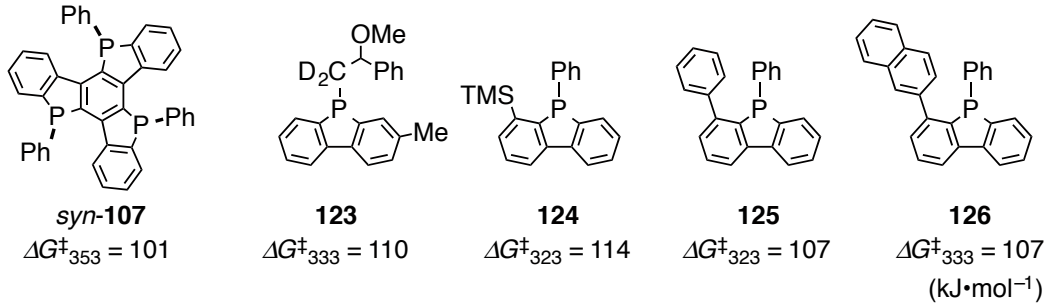

Figure 5.4 Comparison of the barrier of the inversion of the dibenzophosphole units.

5.6 Conclusion

In this Chapter, the author has developed a simple synthetic protocol to construct a TPT framework via sextuple aromatic nucleophilic substitution. While the reaction mainly afforded the *anti*-isomer, the complete conversion of the *anti*-isomer into the *syn*-isomer, which is statistically unfavored, was achieved by the sublimation process. Although the detail of this thermodynamic stability is still unclear, this result would be an important insight for the stereocontrol of the phosphorus centers in π-conjugated frameworks.

Experimental Section

General procedure for Chapter 5

All reactions dealing with air- or moisture-sensitive compounds were carried out in a dry reaction vessel under argon. Analytical thin-layer chromatography was performed on glass plates or aluminum sheets coated with 0.25 mm 230-400 mesh silica gel containing a fluorescent indicator (Merck). Flash silica gel column chromatography was performed on silica gel 60N (Kanto, spherical and neutral, 140-325 mesh). Melting points of solid materials were measured on a Mel-Temp capillary melting-point apparatus and were uncorrected. ^{1}H NMR, ^{13}C NMR, ^{19}F NMR, and ^{31}P NMR spectra were recorded with JEOL ECA-500 (500 MHz) Spectrometer, JEOL ECX-400 (400 MHz) Spectrometer, Bruker AC-500 (500 MHz) Spectrometer, or Bruker Avance-III HD 500 (500 MHz) Spectrometer. Chemical data for protons are reported in parts per million (ppm, δ scale) downfield from tetramethylsilane, and referenced internally to tetramethylsilane as a standard in $CDCl_3$ and to the residual proton in the solvent ($CDCl_3$: δ7.26, $CDCl_2CDCl_2$: δ 5.98). Chemical data for carbon are reported in parts per million (ppm, δ scale) downfield from tetramethylsilane, and are referenced to carbon resonance of the NMR solvent ($CDCl_3$: δ77.00, $CDCl_2CDCl_2$: δ 73.78). Chemical data for fluorine are reported in parts per million (ppm, δ scale) downfield and are referenced to external CF_3CO_2H (δ−77.7). Chemical data for phosphorus are reported in parts per million (ppm, δ scale) downfield and are referenced to external aq. 85% H_3PO_4. Mass spectra were acquired by JEOL JMS-700P (FAB) Spectrometer. High-resolution mass spectra were obtained with a calibration standard of polyethylene glycol (MW 600). Unless otherwise noted, materials were purchased from Tokyo Kasei Co., Aldrich Inc., and other commercial suppliers and used as received. All solvents were purified by distillation and stored over molecular sieves 4A. The following starting materials were prepared as described in the literature: phenylphosphine,[12] 1,3,5-trifluoro-2,4,6-triiodobenzene (**121**).[13]

Synthesis of 1,3,5-trifluoro-2,4,6-tris(*o*-fluorophenyl)benzene (120)

A mixture of 1,3,5-trifluoro-2,4,6-triiodobenzene (**121**) (866 mg, 1.70 mmol), *o*-fluorophenylboronic acid (1.07 g, 7.65 mmol), palladium acetate (12 mg, 51 μmol), S-Phos (42 mg, 0.10

mmol), and potassium phosphate (2.17 g, 10.2 mmol) in toluene (10 mL) was stirred at 90 ˚C under argon. After 16 h, the color of the reaction mixture turned into black. Then the resulting mixture was filtered through a short-path silica-gel column with CH_2Cl_2. After evaporation of the solvent under vacuum, the crude product was purified by silica gel chromatography ($CHCl_3$/hexane=1/10) to afford 4.76 g (88%) of compound **120** as a colorless solid. The product was the mixture of the two rotational isomers around rt (Figure 5.5). Coalescence of signals was observed on ^{19}F NMR in $CDCl_2CDCl_2$ over 90 ˚C.

^1H NMR (500 MHz, $C_2D_2Cl_4$, 393 K): δ 7.20-7.30 (m, 6H), 7.42-7.52 (m, 6H); $^{13}C\{^1H\}$ NMR (125 MHz, $C_2D_2Cl_4$, 393 K): δ 109.00-109.40 (m), 115.60 (d, J_{CF} = 21.5 Hz), 116.20 (d, J_{CF} = 16.7 Hz), 123.78 (d, J_{CF} = 3.6 Hz), 130.56 (d, J_{CF} = 8.3 Hz), 132.22 (s), 157.14 (dt, J_{CF} = 250, 9.5 Hz), 160.10 (d, J_{CF} = 248 Hz); ^{19}F NMR (470 MHz, $C_2D_2Cl_4$, 393 K) δ –116.63 (3F), –114.50 (3F). Anal. Calcd for $C_{24}H_{12}F_6$: C, 69.57; H, 2.92. Found: C, 69.27, H, 3.18.

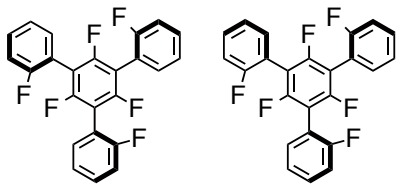

Figure 5.5 Two rotational isomers of compound **120**.

Synthesis of *anti*-TPT trioxide *anti*-122

A mixture of **120** (3.00 g, 7.24 mmol), potassium carbonate (4.01 g, 29.0 mmol) and phenylphosphine (3.19 mL, 29.0 mmol) in DMSO (30 mL) was stirred at 120 ˚C under argon. After 11 h, the mixture was poured into water. Then the resulted precipitation was collected by filtration and suspended in dichloromethane (60 mL). To the suspension was added 70% aq. *t*-BuO_2H (12 mL) at rt. The mixture was vigorously stirred for 15 min to afford a clear solution. Then the organic layer was washed with saturated aqueous solution of sodium sulfite, dried over magnesium sulfate, and filtered. After evaporation of the solvent under vacuum, the crude product was purified by recrystallization ($CHCl_3$/EtOH) to afford 2.11 g (43% from compound **120**) of compound *anti*-**122** as a colorless solid.

m.p. >300 ˚C; ^1H NMR (500 MHz, $CDCl_3$) δ 7.25-7.77 (m, 24H), 8.89 (dd, J_{HH} = 8.0 Hz, J_{PH} = 3.5 Hz, 1H),

9.07 (dd, J_{HH} = 8.0 Hz, J_{HP} = 3.0 Hz, 1H), 9.15 (dd, J_{HH} = 8.0 Hz, J_{HP} = 3.0 Hz, 1H); $^{13}C\{^{1}H\&^{31}P\}$ NMR (125 MHz, $CDCl_3$) δ 127.59, 127.70, 127.86, 128.42, 128.70, 128.82, 128.86, 128.98, 129.05, 129.16, 129.18, 129.29, 130.73, 130.77, 130.96, 131.17, 131.24, 131.26, 132.39, 132.49, 132.65, 133.01, 133.54, 133.55, 133.57, 133.62, 133.70, 138.23, 138.24, 138.55, 151.34, 151.46, 151.75 (33 signals: 3 signals were not observed because of accidental overlapping.); $^{31}P\ \{^{1}H\}$ NMR (202 MHz, $CDCl_3$) δ 34.08, 34.21, 35.02; HRMS (FAB): calcd for $C_{42}H_{27}O_3P_3$ (M^+): 672.1173; found: 672.1188. Anal. Calcd for $C_{42}H_{27}O_3P_3$: C, 75.00; H, 4.05. Found: C, 75.06, H, 3.99.

Synthesis of *syn*-TPT trioxide *syn*-122

A mixture of **120** (3.00 g, 7.24 mmol), potassium carbonate (4.01 g, 29.0 mmol) and phenylphosphine (3.19 mL, 29.0 mmol) in DMSO (30 mL) was stirred at 120 ˚C under argon. After 11 h, the mixture was poured into water. Then the resulted precipitation was collected by filtration and sublimed under vacuum (290 ˚C/0.02 Torr) to afford mild yellow solid. To the suspension of the obtained solid in dichloromethane (50 mL) was added 70% aq. *t*-BuOOH (12 mL) at rt. The mixture was vigorously stirred for 15 min and the resulted precipitation was collected by filtration. The crude product was washed with water, acetone, and dichloromethane to afford 2.55 g (52%) of compound *syn*-**122** as a colorless solid.

m.p. >300 ˚C; ^{1}H NMR (500 MHz, $CDCl_3$) δ 7.19 (td, J_{HH} = 7.5 Hz, J_{PH} = 2.9 Hz, 6H), 7.26-7.31 (m, 6H), 7.36 (t, J_{HH} = 7.5 Hz, 3H), 7.48 (td, J_{HH} = 7.5 Hz, J_{PH} = 2.9 Hz, 3H), 7.67-7.76 (m, 6H), 9.35 (dd, J_{HH} = 7.5 Hz, J_{PH} = 2.9 Hz, 3H); $^{13}C\{^{1}H\}$ NMR (125 MHz, $CDCl_3$) δ 128.31 (d, J_{CP} = 12 Hz), 128.29 (d, J_{CP} = 21 Hz), 129.36 (d, J_{CP} = 18 Hz), 129.63 (d, J_{CP} = 166 Hz), 131.01 (d, J_{CP} = 19 Hz), 131.23 (dt, J_{CP} = 154, 14 Hz), 131.41 (d, J_{CP} = 19 Hz), 132.12 (s), 132.69 (d, J_{CP} = 177 Hz), 133.93 (s), 139.52 (d, J_{CP} = 33 Hz), 151.17 (ddd, J_{CP} = 36, 12, 4 Hz) ; $^{31}P\ \{^{1}H\}$ NMR (202 MHz, $CDCl_3$) δ 33.48; HRMS (FAB): calcd for $C_{42}H_{27}O_3P_3$ (M^+): 672.1173; found: 672.1188.

Preparation of *syn*-TPT *syn*-107

A mixture of **120** (0.100 g, 0.241 mmol), potassium carbonate (0.134 g, 0.967 mmol) and

phenylphosphine (0.106 mL, 0.967 mmol) in DMSO (2 mL) was stirred at 120 ˚C under argon. After 14 h, the mixture was poured into water. Then the resulted precipitation was collected by filtration and recrystallized from hot toluene to afford compound **107** (*syn*/*anti* = 1/6, 73%) as a colorless solid. The vacuum sublimation (290 ˚C, 0.02 Torr) of the recrystallized sample afforded pure *syn*-**107**.

m.p. >300 ˚C; ^{1}H NMR (500 MHz, $CDCl_3$) δ 7.14-7.22 (m, 9H), 7.27-7.35 (m, 9H), 7.36-7.40 (m, 3H), 7.75 (broad t, J_{HH} = 6.6 Hz, 3H), 8.56 (broad t, J_{HH} = 7.3 Hz, 3H); ^{13}C{^{1}H} NMR (100 MHz, $CDCl_3$) δ 126.55 (d, J_{CP} = 24 Hz), 127.90 (d, J_{CP} = 9 Hz), 128.22 (s), 128.78 (d, J_{CP} = 8 Hz), 129.35 (s), 129.50 (d, J_{CP} = 24 Hz), 132.68 (d, J_{CP} = 19 Hz), 135.31 (d, J_{CP} = 19 Hz), 135.49 (dd, J_{CP} = 11, 5 Hz), 142.29 (s), 144.40 (s), 148.84 (dd, J_{CP} = 14, 2 Hz); ^{31}P {^{1}H} NMR (202 MHz, $CDCl_3$) δ –13.97; HRMS (FAB): calcd for $C_{42}H_{27}P_3$ (M^+): 624.1326; found: 624.1301. Anal. Calcd for $C_{42}H_{27}P_3$: C, 80.77; H, 4.36. Found: C, 80.51, H, 4.56.

Determination of the inversion barrier of *syn*-107 to *anti*-107

A solution of pure *syn*-**107** (1.3 mg) in $CDCl_2CDCl_2$ (0.50 mL) in a NMR tube under nitrogen was heated in NMR spectrometer at 353 K. The ratio of *syn*-**107** and *anti*-**107** was measured by ^{1}H NMR (500 MHz, 353 K). The equilibrium constant *K* was determined after prolonged heating. The kinetic constant and the inversion barrier were determined according to the reported protocol (Figure 5.6).[11a]

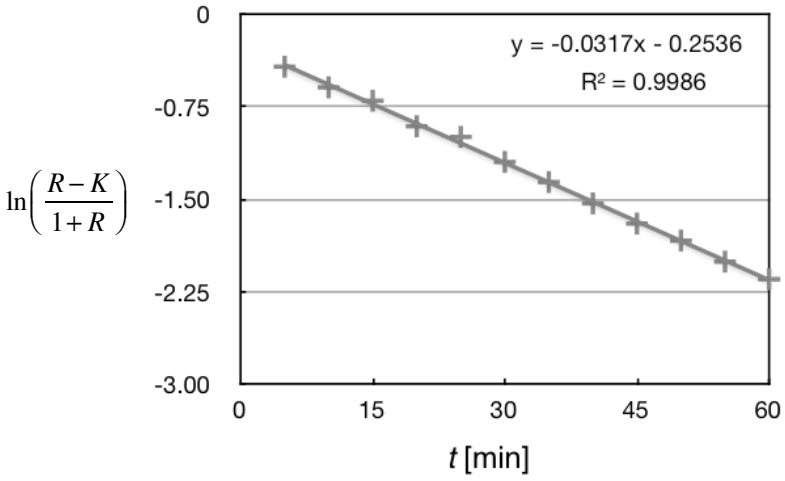

Figure 5.6 Plot of ln[(*R*-*K*)/(1+*R*)] vs *t* to determine the kinetic constant of the isomerization from *syn*-**107** to *anti*-**107**.

Single crystal X-ray diffraction analysis of *syn*-122

Single crystals of the compounds were obtained by chloroform/acetone. Measurements were performed on a RIGAKU R-AXIS RAPID II diffractometer for the others, using CuKα (graphite monochromated) radiation. Part of the solvent could not be modeled and was treated with the SQUEEZE procedure in PLATON (Spek, 2009). This solvent has not been included in the reported empirical formula, M_r, F(000), calculated density or linear absorption coefficient.

Crystal data: $C_{42}H_{27}O_3P_3$, M = 672.60, cubic, space group Pa-3 (#205), a = 19.5304(5) Å, V = 7449.6(3) Å^3, Z = 8, D_{calc} = 1.199 g/cm^3, F_{000} = 2784.0, $R1$ ($I > 2\sigma(I)$) = 0.0556, w$R2$ (all data) = 0.1444.

MO Calculation

Geometry optimizations and frequency calculations of *syn*-**107** and *anti*-**107** were performed using Gaussian 09 program[14] at the M06-2X/6-31G(d) level of theory. The Gibbs free energy of *syn*-**107** and *anti*-**107** was determined as –2639.641243 and –2639.644485 Hartree using the following output data. The *anti*-isomer was thermodynamically preferred (ΔG = 0.003242 Hartree = 2.0 kcal/mol at 298.15 K, 1 atm).

syn-**107**

Total energy = –2640.0744903

Zero-point correction =	0.502275 (Hartree/Particle)
Thermal correction to Energy =	0.540856
Thermal correction to Enthalpy =	0.541800
Thermal correction to Gibbs Free Energy =	0.433247

anti-**107**

Total energy = –2640.0710418

Zero-point correction =	0.501721 (Hartree/Particle)
Thermal correction to Energy =	0.540846
Thermal correction to Enthalpy =	0.541791
Thermal correction to Gibbs Free Energy =	0.426555

References

[1] See for examples: (a) Sun, Y.; Xiao, K.; Liu, Y.; Wang, J.; Pei, J.; Yu, G.; Zhu, D. *Adv. Funct. Mater.* **2005**, *15*, 818. (b) Luo, J.; Zhou, Y.; Niu, Z.-Q.; Zhou, Q.-F.; Ma, Y.; Pei, J. *J. Am. Chem. Soc.* **2008**, *130*, 9952. (c) Wang, J.-L.; Zhong, C.; Tang, Z.-M.; Wu, H.; Ma, Y.; Cao, Y.; Pei, J. *Chem. Asian J.* **2010**, *5*, 105. (d) Wang, J.-L.; He, Z.; Wu, H.; Cui, H.; Li, Y.; Gong, Q.; Cao, Y.; Pei, J. *Chem. Asian J.* **2010**, *5*, 1455. (e) Zhao, K.-Q.; Chen, C.; Monobe, H.; Hu, P.; Wang, B.-Q.; Shimizu, Y. *Chem. Commun.* **2011**, *47*, 6290. (f) Tsuji, H.; Ota, Y.; Furukawa, S.; Mitsui, C.; Sato, Y.; Nakamura, E. *Asian J. Org. Chem.* **2012**, *1*, 34. (g) Zong, X.; Liang, M.; Fan, C.; Tang, K.; Li, G.; Sun. Z.; Xue, S. *J. Phys. Chem. C* **2012**, *116*, 11241.

[2] Bergman, J.; Egestad, B. *Tetrahedron Lett.* **1978**, *34*, 3143.

[3] Bergman, J.; Egestad, B. *Tetrahedron* **1986**, *42*, 763.

[4] For recent examples: (a) Liu, X.; Xu, Y.; Jiang, D. *J. Am. Chem. Soc.* **2012**, *134*, 8738. (b) Lu, Z.; Li, C.; Fang, T.; Li, G.; Bo, Z. *J. Mater. Chem. A* **2013**, *1*, 7657. (c) Qian, X.; Zhy, Y.-Z.; Song, J.; Gao, X.-P.; Zheng, J.-Y. *Org. Lett.* **2013**, *15*, 6034. (d) Coya, C.; Ruiz, C.; Álvarez, Á. L.; Álvarez-García, S.; García-Frutos, E. M.; Gómez-Lor, B.; Andrés, A. d. *Org. Eletron.* **2012**, *13*, 2138. (e) Kulshreshtha, C.; Kim, G. W.; Lampande, R.; Huh, D. H.; Chae, M.; Kwon, J. H. *J. Mater. Chem. A* **2013**, *1*, 4077. (f) Benito-Hernández, A.; Pandey, U. K.; Cavero, E.; Termine, R.; García-Frutos, E. M.; Serrano, J. L.; Golemme, A.; Gómez-Lor, B. *Chem. Mater.* **2013**, *25*, 117. (g) Shao, J.; Guan, Z.; Yan, Y.; Jiao, C.; Xu, Q.-H.; Chi, C. *J. Org. Chem.* **2011**, *76*, 780.

[5] Mueller, A.; Amsharov, K. Y. *Eur. J. Org. Chem.* **2012**, 6155.

[6] (a) Robertson, N.; Parsons, S.; MacLean, E. J.; Coxall, R. A.; Mount, A. R. *J. Mater. Chem.* **2000**, *10*, 204. b) Gómez-Lor, B.; Echavarren, A. M. *Org. Lett.* **2004**, *6*, 2993.

[7] (a) Chen, R.-F.; Fan, Q.-L.; Zheng, C.; Huang, W. *Org. Lett.* **2006**, *8*, 203. (b) Geramita, K.; McBee, J.; Tilley, T. D. *J. Org. Chem.* **2009**, *74*, 820. (c) Fukazawa, A.; Kiguchi, M.; Tange, S.; Ichihashi, Y.; Zhao, Q.; Takahashi, T.; Konishi, T.; Murakoshi, K.; Tsuji, Y.; Staykov, A.; Yoshizawa, K.; Yamaguchi, S. *Chem. Lett.* **2011**, *40*, 174.

[8] (a) Kuninobu, Y.; Yoshida, T.; Takai, K. *J. Org. Chem.* **2011**, *76*, 7370. (b) Nakano, K.; Oyama, H.; Nishimura, Y.; Nakasako, S.; Nozaki, K. *Angew. Chem., Int. Ed.* **2012**, *51*, 695. (c) Baba, K.; Tobisu, M.; Chatani, N. *Angew. Chem., Int. Ed.* **2013**, *52*, 11892.

[9] (a) Herd, O.; Langhans, K. P.; Stelzer, O.; Weferling, N.; Sheldrick, W. S. *Angew. Chem., Int. Ed. Engl.* **1993**, *32*, 1058. (b) Peer, M.; Jong, C. d.; Kiefer, M.; Langer, T.; Rieck, H.; Schell, H.; Sennhenn, P.; Sprinz, J.; Steinhagen, H.; Wiese, B.; Helmchen, G. *Tetrahedron* **1996**, *52*, 7547. (c) Sudo, A.; Saigo, K. *J. Org. Chem.* **1997**, *62*, 5508. (d) Ruhland, T.; Bang, K. S.; Anderson, K. *J. Org. Chem.* **2002**, *67*, 5257. (e) Coote, S. J.; Dawson, G. J.; Frost, C. G.; Williams, J. M. J. *Synlett* **1993**, 59.

[10] Dennery, D. B.; Manifin, Jr. J. W. *Tetrahedron Lett.* **1963**, *4*, 2177.

[11] (a) Egan, W.; Tang, R.; Zon, G.; Mislow, K. *J. Am. Chem. Soc.* **1971**, *93*, 6205. (b) Widhalm, M.; Brecker, L.; Mereiter, K. *Tetrahedron: Asymmetry* **2006**, *17*, 1355.

[12] Pass, F.; Schindlbauer, H. *Monatsch. Chem.* **1959**, *90*, 148.

[13] Wenk, H. H.; Sander, W. *Eur. J. Org. Chem.* **2002**, 3927.

[14] Gaussian 09, Revision B.01, M. J. Frisch, G. W. Trucks, H. B. Schlegel, G. E. Scuseria, M. A. Robb, J. R. Cheeseman, G. Scalmani, V. Barone, B. Mennucci, G. A. Petersson, H. Nakatsuji, M. Caricato, X. Li, H. P. Hratchian, A. F. Izmaylov, J. Bloino, G. Zheng, J. L. Sonnenberg, M. Hada, M. Ehara, K. Toyota, R. Fukuda, J. Hasegawa, M. Ishida, T. Nakajima, Y. Honda, O. Kitao, H. Nakai, T. Vreven, J. A. Montgomery, Jr., J. E. Peralta, F. Ogliaro, M. Bearpark, J. J. Heyd, E. Brothers, K. N. Kudin, V. N. Staroverov, T. Keith, R. Kobayashi, J. Normand, K. Raghavachari, A. Rendell, J. C. Burant, S. S. Iyengar, J. Tomasi, M. Cossi, N. Rega, J. M. Millam, M. Klene, J. E. Knox, J. B. Cross, V. Bakken, C. Adamo, J. Jaramillo, R. Gomperts, R. E. Stratmann, O. Yazyev, A. J. Austin, R. Cammi, C. Pomelli, J. W. Ochterski, R. L. Martin, K. Morokuma, V. G. Zakrzewski, G. A. Voth, P. Salvador, J. J. Dannenberg, S. Dapprich, A. D. Daniels, O. Farkas, J. B. Foresman, J. V. Ortiz, J. Cioslowski, and D. J. Fox, Gaussian, Inc., Wallingford CT, 2010.

Chapter 6

Conclusion and Prospect

Conclusion and Prospect

In this thesis, the author described the selective construction of two C_3-symmetric extended π-conjugated frameworks: alternately functionalized hexaphenylbenzene (HPB) and *syn*-triphosphatruxene (TPT). In the construction of both of the frameworks, the key selective step was performed in the late stage of the synthetic schemes. The selective alternate derivatization of the HPB framework was achieved through a thermodynamically controlled halogen dance. The manipulation of the stereochemistry of the three phosphorus centers on the TPT framework was achieved in the simple sublimation protocol.

In Chapter 1, the difficulty and the value of the late-stage functionalization approach for the synthesis of extended π-conjugated frameworks were described. This is the most important conceptual basis of the study in this thesis. Then the utility and the synthetic problems of alternately functionalized HPB derivatives and π-conjugated compounds bearing multiple phosphorus centers were argued.

In Chapter 2, the selective alternate trilithiation of the brominated HPB derivatives was described. The reaction monitor clearly revealed that this unapparent selectivity is achieved under thermodynamic control through the reversible ArBr/ArLi exchange reaction, halogen dance. It was shown that the selective alternate trilithiation of the HPB frameworks is an effective protocol to prepare C_3-symmetric and lower-symmetric HPB derivatives, which have been difficult to obtain so far.

In Chapter 3, the improved protocol for the selective alternate trilithiation of hardly soluble HPB derivatives was developed. On the basis of the detailed discussion of the kinetics of the reaction, the use of additional bromoarenes as lithiation mediators, which juggle the two different Br/Li exchange reactions, was proposed as a new synthetic methodology. This new protocol succeeded in the selective alternate trilithiation of a broader range of HPB framework.

In Chapter 4, the origin of the thermodynamic stability of the alternately trilithiated HPB species was studied. The biased distribution of the lithiated species in the equilibrium mixture after the halogen dance was quantitatively confirmed. The observed preference of the arrangement of the substituents on the

HPB framework was discussed based on the two possible interactions between the adjacent phenyl groups on the HPB framework. The discussion in this Chapter highlighted the importance of the characteristic conformation of the HPB framework for the alternate selectivity.

The successful alternate derivatization of the HPB framework is due to the combination of the intrinsic conformation and the proper reaction. The intrinsic conformation of the HPB framework enables the adjacent phenyl groups to interact with each other strongly. This unique environment was exploited by the reversible ArBr/ArLi exchange reaction that exhibits the substantial substituent effects distinguishing the possible arrangements of the substituents energetically. The reversibility of the halogen/metal exchange reaction is peculiar to Li. The practicality of the protocol of the selective alternate trilithiation and the versatility of organolithiums and bromoarenes in organic synthesis are expected to rapidly expand the library of C_3-symmetric and lower-symmetric HPB derivatives. These derivatives will be the key building units for the bottom-up chemical synthesis of nanographenes. Furthermore, the protocol utilizing the thermodynamically controlled halogen dance could be a general methodology for the selective derivatization of extended π-conjugated frameworks. The application of this methodology to other π-conjugated frameworks is an important future subject.

In Chapter 5, the stereoselective construction of the TPT framework was described. The application of an aromatic nucleophilic substitutuion reaction with phenylphosphine effectively constructed the TPT framework, which is the first π-conjugated framework containing more than two phosphorus atoms. While this reaction proceeded in high *anti*-selectivity, vacuum sublimation completely converted the *anti*-isomer to the *syn*-isomer. The stereocontol of the phosphorus centers were efficiently achieved in a simple protocol.

The electronic perturbation of the three phosphorus moieties and the extended two-dimensional framework make TPT derivatives a promising candidate for the organic electronic material. Furthermore, the strong dipole moment derived from the synergetic effect of the three polar P=O moieties in the same direction is also promising for applications.

The author hopes that this study will contribute to the further development of the methodology for the selectivity on extended π-conjugated frameworks. In the near future, the deliberate control of the selectivity on extended π-conjugated frameworks, as is established on a benzene, should extend the realistic molecular design and stimulate the chemists to create the novel extended π-conjugated molecules.

Acknowledgement

The study presented in this thesis has been carried out under continuous help and kind assistance of many persons. The author expresses his sincerest gratitude to all of them, especially to:

Professor Eiichi Nakamura, The University of Tokyo, for his constant guidance, developing a favorable research environments, patient direction, and hearty encouragement during the course of this work.

Professor Shuichi Hiraoka, The University of Tokyo, for his constant guidance, developing a favorable research environments, valuable scientific discussion, and hearty encouragement.

Associate Professor Hayato Tsuji, The University of Tokyo, for his patient direction, valuable scientific discussion, and hearty encouragement.

Dr. Shunsuke Furukawa, The University of Tokyo, for his valuable scientific discussion, hearty encouragement, and his helping in the X-ray crystallographic analysis and the theoretical calculation.

Dr. Koji Harano, The University of Tokyo, for his hearty encouragement.

Dr. Laurean Ilies, The University of Tokyo, for his hearty encouragement.

Dr. Hideyuki Tanaka, The University of Tokyo, for his hearty encouragement.

Dr. Aiko Kamitsubo and Ms. Kimiyo Saeki, The University of Tokyo, for the elemental analysis.

Dr. Hajime Sato, Bruker BioSpin K.K., for the NMR measurement.

Dr. Mikio Yamasaki, Rigaku, for the X-ray crystallographic analysis.

The author would like to express his hearty gratitude to his parents, Mr. Masahiro Kojima and Ms. Michiyo Kojima, for their continuous encouragement and their financial support.

Finally, the author is grateful for many aspects to all members of Nakamura laboratory and Hiraoka laboratory.

January 2014

Tatsuo Kojima

List of Publications

1. "Synthesis of Triphosphatruxene via Sextuple Aromatic Nucleophilic Substitution and Simple Isolation of Stereoisomers"

   Kojima, T.; Furukawa, S.; Tsuji, H.; Nakamura, E. *Chem. Lett.* **2014**, *43*, 676-677.

2. "Selective Alternate Derivatization of the Hexaphenylbenzene Framework through a Thermodynamically Controlled Halogen Dance"

   Kojima, T.; Hiraoka, S. *Org. Lett.* **2014**, *16*, 1023-1027.